

**ANTIBACTERIAL  
POLYMETHYLMETHACRYLATE (PMMA)/  
BETA TRI CALSIUM PHOSPHATE/ ZINC OXIDE  
COMPOSITES FOR CRANIOFACIAL  
RECONSTRUCTION**

**WAN NUR FADILLA BINTI WAN HAMAD**

**UNIVERSITI SAINS MALAYSIA**

**2022**

**ANTIBACTERIAL  
POLYMETHYLMETHACRYLATE (PMMA)/  
BETA TRI CALSIUM PHOSPHATE/ ZINC OXIDE  
COMPOSITES FOR CRANIOFACIAL  
RECONSTRUCTION**

by

**WAN NUR FADILLA BINTI WAN HAMAD**

**Thesis submitted in fulfilment of the requirements  
for the degree of  
Doctor of Philosophy**

**April 2022**

## ACKNOWLEDGEMENT

First and foremost, all praises and thanks to ALLAH S.W.T, the most Merciful with endless blessing. Alhamdulillah, I have been in the last step for completing my study. I would like to express my sincere gratitude and appreciation to my main supervisor, Assoc. Prof Dr Dasmawati Mohamad for accepting me as her student, continues support, guidance, and patience throughout my research period. I am blessed to be her student. I am also indebted to my co-supervisor, Assoc. Prof Dr Asma Abdullah Mohamad for her motivation, enthusiasm and intensive knowledge in guiding me especially in biological part in order to complete my thesis. Deepest appreciation and thanks to all staffs in Dental, Craniofacial Science Laboratory at School of Dental Sciences for giving their full cooperation in helping me in my research. A special dedication to my family especially my late parents, Wan Hamad bin Wan Mahmood and Mamunah binti Daud for their endless love. I believe that their dua' was the key for what I am doing right now. To my beloved husband, Azri Jazi, I really appreciate for his endless support and understanding in the making of thesis successfully. Special thanks to my daughters Aqiesha and Aqeela for being tolerable and understanding and this thesis would not be completed without my sibling's motivation and prayers for my success. My deepest gratitude goes to my beloved colleagues Farahaini, Atikah, Najwa, Abdul Manaf, Fatimah Suhaili, Suzana, and all the postgraduate students of School of Dental Sciences for helping me in completing my thesis. Last but not least, I would like to express my sincere appreciation to the USM Bridging Grant (304/PPSG/6316131), and RUT Grant (PSG/1001/852004), for providing the funding and financial support throughout my research.

## TABLE OF CONTENTS

<b>ACKNOWLEDGEMENT</b> .....	<b>ii</b>
<b>TABLE OF CONTENTS</b> .....	<b>iii</b>
<b>LIST OF FIGURES</b> .....	<b>ix</b>
<b>LIST OF SYMBOLS</b> .....	<b>xii</b>
<b>LIST OF ABBREVIATIONS</b> .....	<b>xiii</b>
<b>LIST OF APPENDICES</b> .....	<b>xv</b>
<b>ABSTRAK</b> .....	<b>xvi</b>
<b>ABSTRACT</b> .....	<b>xviii</b>
<b>CHAPTER 1 INTRODUCTION</b> .....	<b>1</b>
1.1 Background of the study.....	1
1.2 Problem Statement .....	3
1.3 Justification of study .....	4
1.4 Objectives of study .....	6
1.4.1 General objective.....	6
1.4.2 Specific objectives.....	6
1.5 Scope of study .....	6
<b>CHAPTER 2 LITERATURE REVIEW</b> .....	<b>7</b>
2.1 Craniofacial bone replacement.....	7
2.1.1 Autograft .....	8
2.1.2 Allograft .....	9
2.1.3 Xenograft.....	9
2.1.4 Synthetic or Alloplastic .....	10
2.1.4(a) Metal .....	10
2.1.4(b) Ceramic.....	10
2.1.4(c) Polymer.....	11
2.1.4(d) Composites .....	12

2.2	Evolution of biomaterial.....	12
2.2.1	Bioinert or Biotolerant .....	13
2.2.2	Bioactive.....	14
2.2.3	Biodegradable.....	14
2.2.4	Biomimicry.....	15
2.3	Polymethylmethacrylate (PMMA).....	15
2.3.1	Properties of PMMA .....	16
2.3.2	Polymerisation of PMMA .....	17
2.3.3	Applications of PMMA.....	18
2.4	The factors that affect the filled polymer .....	19
2.4.1	Filler types.....	20
2.4.1(a)	Tricalcium Phosphate .....	21
2.4.1(b)	Zinc Oxide (ZnO) .....	24
2.4.2	Filler loading .....	26
2.4.3	Filler size .....	27
2.4.4	Filler shape .....	28
2.4.5	Filler as an antibacterial agent.....	29
2.5	Bacterial Strains .....	30
2.5.1	Staphylococcus aureus .....	30
2.5.2	Pseudomonas aeruginosa.....	33
2.6	Cytotoxicity .....	33
2.7	Implant-related infections.....	34
	<b>CHAPTER 3 MATERIALS AND METHODS .....</b>	<b>36</b>
3.1	Study Design .....	36
3.2	Sample size calculation .....	39
3.3	Materials.....	40
3.3.1	Materials for sample preparation.....	40

3.3.2	Calculation for material composition.....	40
3.3.3	Chemical and reagents for cell culture.....	40
3.3.4	Instrumentations.....	41
3.3.5	Materials used for antibacterial study.....	42
3.4	Fabrication of material.....	42
3.4.1	Silicone mold preparation.....	42
3.4.2	Polymethylmethacrylate (PMMA) composite preparation.....	43
3.5	Chemical analysis.....	44
3.5.1	Fourier Transform Infrared Spectroscopy.....	44
3.6	Physical properties evaluation.....	45
3.6.1	Surface roughness.....	45
3.5.2	Shrinkage test.....	45
3.7	Mechanical properties evaluation.....	46
3.7.1	Flexural strength.....	46
3.7.2	Tensile strength.....	47
3.7.3	Fracture toughness.....	48
	3.7.3(a) Energy-dispersive X-ray spectroscopy (EDX).....	49
3.8	Morphology Analysis.....	49
3.8.1	Field Emission Scanning Electron Microscope (FESEM).....	49
3.9	Size of samples.....	50
3.10	Cytotoxicity test.....	51
3.10.1	Aseptic technique.....	51
3.10.2	Complete media preparation.....	51
3.10.3	Culturing of hFOB cell line.....	51
3.10.4	Cell maintaining.....	52
3.10.5	Counting cell and subculture process.....	53
3.10.6	Cryopreservation of cells.....	54

3.10.7	MTT assay.....	54
3.10.8	Material extract preparation of composites.....	55
3.11	Antibacterial assays of <i>S.aureus</i> and <i>P.aeruginosa</i> .....	55
3.11.1	Preparation of the culture media .....	56
3.11.1(a)	Preparation of brain heart infusion broth.....	56
3.11.1(b)	Preparation of McFarland standard solution.....	56
3.11.2	Agar diffusion test.....	57
3.11.3	Bacterial Kinetic Growth of <i>S. aureus</i> and <i>P. aeruginosa</i> .....	57
3.11.4	SEM analysis of <i>S. aureus</i> and <i>P. aeruginosa</i> on materials.....	58
3.12	Statistical analysis .....	58
<b>CHAPTER 4 RESULTS AND DISCUSSION.....</b>		<b>59</b>
4.1	Morphology and size of fillers .....	59
4.2	FTIR analysis (Fourier Transmission Infrared).....	59
4.3	Surface roughness .....	63
4.4	Shrinkage properties.....	65
4.5	Flexural properties.....	67
4.6	Tensile properties .....	70
4.7	Fracture toughness.....	77
4.8	Cytotoxicity evaluation .....	86
4.9	Antibacterial study of <i>S.aureus</i> and <i>P.aureus</i> .....	93
4.9.1	Agar diffusion method .....	93
4.9.2	Bacteria growth study.....	95
<b>CHAPTER 5 CONCLUSION, LIMITATIONS AND RECOMMENDATIONS.....</b>		<b>106</b>
5.1	Conclusion.....	106
5.2	Recommendations .....	107
<b>REFERENCES.....</b>		<b>108</b>

## APPENDICES

APPENDIX A FLEXURAL STRENGTH

APPENDIX B TENSILE STRENGTH

APPENDIX C TENSILE MODULUS

APPENDIX D SHRINKAGE

APPENDIX E SURFACE ROUGHNESS

APPENDIX F FRACTURE TOUGHNESS 0 DAY

APPENDIX G FRACTURE TOUGHNESS 15 DAYS

APPENDIX H FRACTURE TOUGHNESS 30 DAYS

APPENDIX I FRACTURE TOUGHNESS 45 DAYS

APPENDIX J FRACTURE TOUGHNESS 60 DAYS

APPENDIX K CYTOTOXICITY 6.25mg/ml

APPENDIX L ANTIBACTERIAL STUDY OF *S. aureus*

APPENDIX M ANTIBACTERIAL STUDY OF *P.aeruginosa*

APPENDIX N CYTOTOXICITY 12.5mg/ml

APPENDIX O CYTOTOXICITY 25mg/ml

APPENDIX P CYTOTOXICITY 50mg/ml

APPENDIX Q CYTOTOXICITY 100mg/ml

LIST OF PUBLICATIONS AND PRESENTATIONS



## LIST OF TABLES

	<b>Page</b>
Table 2.1	The properties of PMMA ..... 17
Table 2.2	PMMA applications in industry sectors ..... 19
Table 3.1	Compositions of sample based on weigh percentages ..... 36
Table 3.2	Materials used for sample preparation ..... 40
Table 3.3	Compositions value of each group sample ..... 40
Table 3.4	Cell culture reagents ..... 40
Table 3.5	The list of instruments used ..... 41
Table 3.6	List of materials used for antibacterial study ..... 42
Table 4.1	FTIR for PMMA composites ..... 61
Table 4.2	Surface roughness value for PMMA composites ..... 63
Table 4.3	Shrinkage value of pure PMMA and developed composites ..... 65
Table 4.4	Flexural strength value of each sample ..... 67
Table 4.5	Tensile strength and modulus value of PMMA composites. .... 73
Table 4.6	Fracture toughness value for all sample PMMA/ $\beta$ -TCP/ZnO composites ..... 79
Table 4.7	Cell viability of PMMA composite treated with hFOB at different concentration ..... 88
Table 4.8	Zone of Inhibition (mm) of <i>S.aureus</i> and <i>P.aeruginosa</i> ..... 95
Table 4.9	Turbidity measurement of <i>S. aureus</i> treated with PMMA composites ..... 98
Table 4.10	Turbidity measurement of <i>P. aeruginosa</i> treated with PMMA composites ..... 98

## LIST OF FIGURES

	<b>Page</b>
Figure 2.1	Bone structure (Philip, 2012) ..... 7
Figure 2.2	Types of materials for bone replacement ..... 8
Figure 2.3	Addition polymerisation of PMMA initiated by a phenyl radical(Unosson, 2010) ..... 18
Figure 2.4	PMMA implant in host model (Huang <i>et al.</i> , 2015). ..... 19
Figure 2.5	(ROS) mechanism towards cell structure(Ann <i>et al.</i> , 2014b) ..... 31
Figure 2.6	Enzymatic reduction of MTT to formazan (Kuethe <i>et al.</i> , 2017) ..... 34
Figure 2.7	Osteomyelitis: bone infection (Kumari, 2016). ..... 35
Figure 3.1	Flow chart of study..... 38
Figure 3.2	Silicon mold ..... 43
Figure 3.3	Sample of PMMA composites. .... 44
Figure 3.4	Fourier Transform Infrared Spectroscopy ..... 44
Figure 3.5	Profilometer machine ..... 45
Figure 3.6	Flexural test evaluation ..... 47
Figure 3.7	Tensile test evaluation..... 47
Figure 3.8	Mould for fracture toughness sample..... 48
Figure 3.9	Field Emission Scanning Electron Microscopy ..... 49
Figure 3.10	Size of samples..... 50
Figure 3.11	Hemocytometer grid. A, B, C and D were counted areas. .... 54
Figure 3.12	SEM image of a) <i>Staphylococcus aureus</i> and b) <i>Pseudomonas aeruginosa</i> at magnification of 30000x. .... 56
Figure 3.13	Illustration of sample treatment in agar plate for inhibition zone determination..... 57

Figure 4.1	FESEM microstructure of a) Zinc oxide particles and b) $\beta$ -TCP particles at 20000x magnification. ....	59
Figure 4.2	FTIR spectra for PMMA composites .....	62
Figure 4.3	Shrinkage phenomenon .....	67
Figure 4.4	Microstructure of a) PMMA/ $\beta$ -TCP 2.5%ZnO and b) PMMA/ $\beta$ -TCP 5%ZnO.....	69
Figure 4.5	Stress strain curve for pure PMMA and PMMA composites.....	69
Figure 4.6	Tensile strength graph for pure PMMA and PMMA composites .....	72
Figure 4.7	Stress strain curves of unfilled PMMA and developed composites...	74
Figure 4.8	SEM microstructure of fractured PMMA/15 $\beta$ -TCP/2.5ZnO at a)1000x b)5000x and c)10000x magnification. ....	75
Figure 4.9	FESEM microstructure of fractured/15% $\beta$ TCP/5%ZnO at a) 10,000x and b) 50 000x magnification. ....	76
Figure 4.10	Fracture toughness value for PMMA composites at different immersion time (0,15,30,45,60) days.....	78
Figure 4.11	Schematic representation of apatite growth at surface of composite .....	80
Figure 4.12	FESEM image for fractured surface of PMMA pure at a)0 day and b)60 days at 2000x magnification .....	81
Figure 4.13	PMMA/15% $\beta$ -TCP/2.5%ZnO apatite form at a) 1000x and b)10000x magnification .....	84
Figure 4.14	SEM micrograph of PMMA/15 $\beta$ -TCP/2.5ZnO after incubating in SBF b) EDX spectrum of PMMA/15 $\beta$ -TCP/ZnO after 60 days incubation in SBF.....	84
Figure 4.15	PMMA/15% $\beta$ -TCP/2.5% ZnO a) 0 days b) after 60 days SBF soaked at 10000x magnification.....	85
Figure 4.16	Cell viability of human fetal osteoblast (hFOB) cells treated with PMMA composites using MTT. ....	89

Figure 4.17	Inhibition zone for a) Chlorhexidine b) pure PMMA c) PMMA/15%β-TCP/2.5% ZnO d)PMMA/15%β-TCP/5% ZnO against <i>S.aureus</i> .....	93
Figure 4.18	Inhibition zone for a) Chlorhexidine b) pure PMMA c) PMMA/15%β-TCP/2.5% ZnO and d) PMMA/15%β-TCP/5% ZnO against <i>P. aeruginosa</i> .....	94
Figure 4.19	OD measurement of <i>S. aureus</i> growth on PMMA composites for 12 hours incubation period.....	97
Figure 4.20	OD measurement of <i>P. aeruginosa</i> growth on PMMA composites for 12 hours incubation period. ....	99
Figure 4.21	SEM photographs of structure of <i>S.aureus</i> treated with a)PMMA pure b)PMMA/15%β-TCP/2.5%ZnO and c) PMMA/15%β-TCP/5%ZnO at magnification 30 000x.....	101
Figure 4.22	SEM photograph of a) untreated <i>P. aeruginosa</i> b) <i>P. aeruginosa</i> treated with PMMA pure under 30000x magnification. ....	103
Figure 4.23	Possible mechanism of zinc oxide on both Gram-positive and negative bacteria.....	104

## LIST OF SYMBOLS

%	Percentage
$\alpha$	Alpha
$\beta$	Beta
$\beta$ -TCP	Beta tri calcium phosphate
$\mu$ l	Microlitre
$\mu$ M	Micrometer
cm	Centimetre
cm <sup>2</sup>	Centimetre square
g	Gram
ml	Millilitre
mm	Millimetre
<sup>o</sup> C	Degree Celsius

## LIST OF ABBREVIATIONS

$\alpha$ TCP	Alpha tricalcium phosphate
AlO <sub>2</sub>	Alumina
A-MEM	Alpha minimum essential medium
Au-Pd	Gold palladium
$\beta$ -TCP	Beta tri calcium phosphate
Al	Aluminium
Ag	Silver
AgNPs	Silver nanoparticles
ATCC	American Type Cell Culture
ATP	Adenosine triphosphate
ATR	Attenuated total reflectance
BaSO <sub>4</sub>	Barium sulphate
BHI	Brain heart infusion
BPO	Bisphenol
Ca	Calcium
CaO	Calcium oxide
CFU	Colony forming unit
Cl <sup>-</sup>	Chloride ion
CO <sub>2</sub>	Carbon dioxide
DMEM	Dimethyl sulfoxide
DNA	Deoxyribonucleic acid
EDTA	Ethylenediaminetetraacetic acid
EDX	Energy dispersion Xray
FTIR	Fourier Transform Infrared
HA	Hydroxyapatite
HCO <sub>3</sub> <sup>-</sup>	Bicarbonate ion
hFOB	Human fetal osteoblast
HPO <sub>3</sub> <sup>-</sup>	Hydrogen phosphonate ion
IC	Inhibition concentration
ISO	International Organization of Standardization
IUPAC	International union pure and applied chemistry

KBr	Kalium bromide
LPS	Lipopolysaccharide
OH-	Hydroxy ion
Mg	Milligram
MgO	Magnesium oxide
MMA	Methacrylate
MTT	3-(4,5-dimethylthiazol-2-yl)-2,5-diphenyltetrazolium bromide
OD	Optical density
OH	Hydroxyl
PANI	Polyaniline
PBS	Phosphate buffer saline
PCL	Polycaprolactone
PEEK	Polyether ether ketone
PGA	Polyglycolic acid
PLA	Polylactic acid
ppm	Part per million
PMMA	Polymethylmethacrylate
<i>P.aeruginosa</i>	<i>Pseudomonas aeruginosa</i>
ROS	Reactive oxygen species
<i>S.aureus</i>	<i>Staphylococcus aureus</i>
SBF	Simulated body fluid
SD	Standard deviation
SEM	Scanning Electron Microscopy
SO <sup>4-</sup>	Sulphate ion
TiO <sub>2</sub>	Titanium oxide
UHMWPE	Ultra-high molecular weight polyethylene
V <sub>m</sub>	Volume mould
V <sub>s</sub>	Volume silicone
Zn	Zinc
ZnO	Zinc oxide

## LIST OF APPENDICES

Appendix A	Flexural strength
Appendix B	Tensile strength
Appendix C	Tensile modulus
Appendix D	Shrinkage
Appendix E	Surface roughness
Appendix F	Fracture toughness 0 day
Appendix G	Fracture toughness 15 days
Appendix H	Fracture toughness 30 days
Appendix I	Fracture toughness 45 days
Appendix J	Fracture toughness 60 days
Appendix K	<i>Staphylococcus aureus</i>
Appendix L	<i>Pseudomonas aeruginosa</i>
Appendix M	Cytotoxicity
Appendix N	Cytotoxicity 12.5mg/ml
Appendix O	Cytotoxicity 25mg/ml
Appendix P	Cytotoxicity 50mg/ml
Appendix Q	Cytotoxicity 100mg/ml



**POLIMETIKMETAKRILIK (PMMA) ANTIBAKTERIA / BETA TRI KALSIUM  
FOSFAT/ KOMPOSIT ZINK OKSIDA UNTUK PENSTRUKTURAN SEMULA  
KRANIOFASIAL**

**ABSTRAK**

Polimetilmetakrilik (PMMA) biasanya digunakan dalam pembinaan semula pergigian dan penstrukturan semula tulang kerana ia menepati ciri-ciri sifat istimewa seperti senang dipadankan secara sifat biokeserasian, tiada reaksi secara biologi dan tegar. Dalam kraniofasial, kecederaan menyebabkan trauma dan kesan ke atas otak secara fizikal. Bagaimanapun, selepas penstrukturan semula tengkorak kepala menggunakan PMMA, jangkitan kuman boleh berlaku. Oleh itu, penambahan agen antibakteria ke atas PMMA dijangkakan dapat mengurangkan jangkitan tersebut. Kehadiran Beta tricalcium phosphate ( $\beta$ -TCP) dalam komposit ini adalah salah satu alternatif untuk menggalakkan pertumbuhan sel ke tulang di sekitarnya. Dengan itu, komposit PMMA direka dengan memasukkan peratusan tertentu bagi bahan pengisi  $\beta$ -TCP dan zink oksida. Komposit ini telah dibahagikan mengikut peratusan 5%, 10%, 15%  $\beta$ -TCP. Berikutan itu, dengan menetapkan peratusan 15% $\beta$ -TCP untuk digunakan pada peringkat seterusnya, 2.5% dan 5% oksida zink pula ditambah. Saiz  $\beta$ -TCP adalah lebih kurang di dalam anggaran 1-5 $\mu$ m dan zink oksida (ZnO) pula di dalam saiz nano (256 nm). Ujian pencirian ke atas sampel dijalankan untuk sifat mekanikal, ikatan kimia, dan sifat fizikal. Mikroskop electron pengimbas (FESEM) digunakan untuk melihat struktur mikro bahagian permukaan yg retak. Kumpulan kimia yang wujud dalam komposit PMMA juga disahkan melalui analisa jelmaan Fourier Spektroskopi Inframerah (FTIR). Sifat mekanikal menunjukkan penambahbaikan kepada komposit PMMA. Perbezaan yang ketara didapati di antara PMMA tulen

dengan komposit PMMA pada sifat fizikalnya. Kesan ketoksidan disiasat menggunakan kaedah 3- (4, 5-dimethylthiazoyl) -2-5 diphenyl-tetrazolium bromide (MTT) ke atas kumpulan sel osteoblast janin manusia (hFOB). hFOB yang dikulturkan dalam 25mg/ml PMMA/15% $\beta$ -TCP/5%ZnO menunjukkan viabiliti sel yang paling tinggi (132.73%). Peratusan viabiliti sel bagi sampel 50mg/ml dan ke bawah menunjukkan tiada kesan ketoksidan kerana nilai peratusan viabiliti sel yang lebih daripada 70%. Ciri-ciri antibakteria komposit PMMA pula dijalankan menggunakan kaedah resapan agar dan ujian lengkung pertumbuhan bakteria ke atas bakteria jenis gram positif (*Staphylococcus aureus*) dan gram negatif (*Pseudomonas aeruginosa*). Tiada perbezaan yang signifikan dapat diperhatikan untuk penggabungan pengisi ZnO menggunakan kaedah resapan agar. Daripada lengkung grafik, terdapat perbezaan yang ketara ke atas komposit PMMA bagi 2.5% and 5% ZnO. Sebagai kesimpulan, komposit PMMA dengan perisian ZnO 2.5% dan 5% adalah biobahan yang sesuai diaplikasikan sebagai implant di dalam penstrukturan semula kraniofasial.

**ANTIBACTERIAL POLYMETHYLMETHACRYLATE (PMMA)  
/BETA TRI CALSIUM PHOSPHATE / ZINC OXIDE COMPOSITES FOR  
CRANIOFACIAL RECONSTRUCTION**

**ABSTRACT**

Polymethylmethacrylate (PMMA) is commonly used in dental and bone reconstruction applications due to the excellent properties such as biocompatible, biologically inert and rigid. In craniofacial, traumatic injuries will result to the defect of underlying brain. Somehow, after reconstruction of skull using PMMA, the infection may occur. Thus, incorporation of antibacterial agent such as beta tricalcium phosphate ( $\beta$ -TCP) to the PMMA is desirable to eliminate infection. Also, the presence of  $\beta$ -TCP to the composites is one of the alternatives to promote cell growth to the surrounding bone tissue. Hence, in this study, PMMA composites fabricated with specified percentages of filler content of  $\beta$ -TCP and Zinc Oxide. The composites divided into three groups of different percentages of 5, 10, 15%  $\beta$ -TCP without ZnO, and another two groups, 2.5% and 5% ZnO were added 15%  $\beta$ -TCP. The size of  $\beta$ -TCP was approximately 1-5 $\mu$ m and ZnO was in nano size (256nm). The mechanical characteristics, chemical bonding, and physical properties of the specimen were next assessed. The characterization of specimen was then evaluated for mechanical properties, chemical bonding, physical properties. Observations of the microstructure of the fracture surface were performed by Field Emission scanning electron microscopy (FESEM). Chemical groups existed were confirmed with analysis of Fourier Transmission InfraRed (FTIR). The mechanical properties showed the improvement for PMMA composites. There is significant difference detected between PMMA pure and PMMA composites in physical properties. The cytotoxicity effect

was investigated through 3-(4, 5-dimethylthiazoyl)-2-5 diphenyl-tetrazolium bromide (MTT assay), using human fetal osteoblast cell (hFOB). The hFOB cultured with 25 mg/ml PMMA filled 15%  $\beta$ TCP and 5% ZnO demonstrated the highest cell viability (132.73%). The percentages of cell viability of samples with 50 mg/ml and below showed no cytotoxicity effect due to their value of cell viability were more than 70%. The antibacterial properties of the PMMA composite were evaluated using agar diffusion and growth curve methods against Gram positive (*Staphylococcus aureus*) and gram negative (*Pseudomonas aeruginosa*). A significant difference was observed with the incorporation of ZnO filler in the agar diffusion test. The antibacterial property of PMMA composites were further evaluated with a growth curve and significant antibacterial activity was found on PMMA composites with 2.5% and 5% of ZnO filled. In conclusion, PMMA composites at 2.5% and 5% ZnO, are promising biomaterials that suit to be applied as implants in craniofacial reconstruction.

## CHAPTER 1

### INTRODUCTION

#### 1.1 Background of the study

Polymethylmethacrylate (PMMA) known in International union pure and applied chemistry (IUPAC) as poly (methyl 2-methylpropenoate), is one of important thermoplastic material used in various application include as transparent glass substitute, in medical implants, and automotive industry (lenses, daylight redirection panels, and data storage discs) (Hossain *et al.*, 2014). In dentistry, PMMA is one of the polymers that has been widely used particularly to fabricate dentures including fixed and removable dentures. The application of PMMA also has been widely used as a bone replacement in orthopedic and craniofacial reconstruction due to its biocompatibility, excellent aesthetic, lower water sorption and lack of toxicity. Usually, PMMA based materials was widely used in orthopedics to anchor joints. It acts as bone cement to achieve implant fixation. According to Soumya *et al.* (2014), PMMA has excellent toughness, stiffness, transparent to visible light, and low thermal conductivity. However, there are a few disadvantages such as high shrinkage, easily crack, mismatch stiffness between the bone and the cement, and moderate in mechanical properties reduce the performance of PMMA as implant material for bone replacement and craniofacial reconstruction (Zivic *et al.*, 2012; Karthick *et al.*, 2014).

Problems also occur when craniofacial implants using PMMA reveal an infection to the tissue surrounding the implantation. Therefore, to reduce infection, the incorporation of antibacterial agents is vital. Thus, the development of PMMA composites by incorporating fillers to overcome the limitations of pure PMMA has been investigated by many researchers (Kim *et al.*, 2004; Samad *et al.*, 2011; Velu & Singamneni, 2015; Gao *et al.*, 2019). Among the suitable fillers, zinc oxide (ZnO) was

chosen in this study due to its low cost, nontoxic and chemically stable with air and moisture. ZnO also possessed antibacterial properties as zinc ion play a role to react with bacterial cell hence combat the growth of bacterial (Sirelkhatim *et al.*, 2014). Moreover, Pasquet *et al.*, (2014) mentioned that ZnO can be efficient antimicrobial agent via several mechanisms including the production of reactive oxygen species (ROS) because of the semiconductive properties of ZnO, the destabilization of microbial membranes upon direct contact of ZnO particles to the cell walls, and the intrinsic antimicrobial properties of Zn<sup>2+</sup> ions released by ZnO in aqueous medium. Besides, the incorporation between biomaterials and ions, particles, natural and inorganic substances, antibiotic-resistant bacteria such as silver, copper or zinc are also alternative to inhibit bacteria growth (Chatzistavrou *et al.*, 2014).

Compatibility is very important for biomaterials that are being used in medical devices, whether they are permanent or biodegradable (Nazir and Mohamad, 2012). Hence,  $\beta$ -tricalcium phosphate will be used, which is a biomaterial that is widely used in dentistry and orthopedic to repair hard tissue defects. It is suitable to be used due to its nontoxic, antigenic, and noncarcinogenic biomaterial, good osteoconductive, direct bond formation with the connective tissue, and rapid bone repair within a few weeks of implantation (Alshemary *et al.*, 2015).  $\beta$ -TCP also has advantages in biodegradability. It will degrade after several periods of implantation and will be replaced with natural bone tissues.

Therefore, this study was carried out to fabricate a novel biomaterial of PMMA/ $\beta$ -TCP /ZnO. Many parameters were evaluated, compositions of all materials selected, physical and mechanical properties, biocompatibility and antibacterial activity.

## 1.2 Problem Statement

Traumatic injuries in the craniofacial areas can result in disfiguring defects and compromise the protection of the underlying brain. Hence, reconstruction is needed for the functional and aesthetic reasons. Several options of the materials are available which includes, autograft, allograft, xenograft and alloplastic. The gold standard is autograft, a patient's own bone whenever the bone is available and in good condition also able to be preserved which is safest and least complication. However, in several conditions second surgery is needed and the bone is limited also difficult to shape. Allograft, a bone taken from person carries the risk of transmitting disease. Xenograft, bones from the animal posed more transmission of disease. Alloplasts are consist of synthetic materials such as titanium, polyether ether ketone (PEEK), and PMMA.

Titanium is widely used for implantation due to the excellent strength and malleable properties. However, the cost is relatively high that it could not be bear by the patient, hence limits the usage. PEEK though started to be used, need to be fabricated through exclusive and expensive equipment such as selective laser sintering. PMMA is the commonest alloplastic material for cranial bone reconstruction due to excellent properties such as biocompatible, biologically inert and rigid (Breitbart and Ablaza, 2007). However, in contrast of that, its brittleness, shrinkage and exothermic reaction during polymerisation (as a result from polymerization to complete) may damage surrounding bone tissue. Failure of PMMA implant due to infection is current viral topic in craniomaxillofacial surgery. This is due to PMMA itself is absence of antibacterial agent. Hence, PMMA does not have antibacterial properties. Thus, modification such

as incorporation of antibacterial agent is needed to enhance the clinical properties of the material in order to suits the application.

Many researchers have studied on antibacterial activity on several materials. Infection complication to the biomaterials implants is one of the serious problems arises among orthopedic patients. Infection can lead to the obliteration of the bone and will resulted to increased rates of treatment failure (Mori *et al.*, 2019). Therefore, researchers focus on how to solve the matter including introduce antibacterial agents to the implant. Peng *et al.*, (2010) state that applying selective material to acts as an antibacterial agent is crucial since the infection occurs in implant removal and revision surgery. Magnesium oxide (MgO), calcium oxide (CaO), TiO<sub>2</sub>, ZnO are the examples of inorganic compounds that exhibited strong antibacterial activity. Among these active powders, ZnO revealed strong antibacterial activity as confirmed in many studies (Sawai, 2003; Cai *et al.*, 2015; Youssef *et al.*, 2019). To improve biocompatibility of the composites,  $\beta$ -TCP is suitable to be chosen as a bioactive filler.

### **1.3 Justification of study**

An ideal biomaterial used in implantation area should possess free of infection along with having good compatibility, durable, low in cost and better mechanical properties. However, the commonly used PMMA implant today gives side effect to patient due to the infection occurred (Ridwan-Pramana *et al.*, 2015, Actis *et al.*, 2013). To eliminate this problem, this study aimed to develop PMMA composite with having antibacterial properties. ZnO is one of the inorganic compounds and acts as antibacterial agents. Furthermore, it is nontoxic to human body (Sirelkhatim *et al.*, 2013). As stated by Gordon *et al.*,(2011), inorganic compounds present strong antibacterial activity at low concentration. This is the one of reasons to choose ZnO as a filler. Hajipour *et al.*, (2012)



investigated that antibacterial agents from organic compounds have some disadvantages like toxicity to human body. Therefore, the interest in inorganic compounds metal oxide is increasing. It could destroy bacteria without being toxic to surrounding tissues through the mechanism of antimicrobial behavior which releasing of ROS especially hydrogen peroxide, superoxide anion, hydroxyl radical, and hydroxyl ion Ann *et al.*, (2014a). Salem *et al.*, (2014) also described that metal and metal oxide (inorganic material agents) gives more advantages over organic compounds due to the stability. For instance, ZnO nanoparticles exhibits antibacterial activity and can reduce the attachment and viability of microbes on biomedical surfaces. Moreover, from studied by Ito *et al.*, (2002), the slow release of zinc into implant could stimulated the bone growth formation and recovery of patient.

The current PMMA in the market is referred as bioinert material which the material does not play a role in wound healing. However, in bioactive material, there is a response from the material to the surrounding tissue that promotes the cell growth (Bauer *et al.*, 2013). Hence, within this study,  $\beta$ -TCP a bioactive ceramic was incorporated to modify bioinert PMMA into bioactive PMMA. Hence, the combination of these two fillers could develop the PMMA composite in the craniofacial prosthesis to achieve the target of antibacterial properties. Two strains of bacteria which *S. aureus* as a representative of Gram positive and *P.aeruginosa* as Gram negative were chosen due to the early infection that related to the skin.

## **1.4 Objectives of study**

### **1.4.1 General objective**

1. To fabricate antibacterial PMMA/ $\beta$ -TCP/ZnO composite for craniofacial reconstruction.

### **1.4.2 Specific objectives**

1. To fabricate silicone mold for mechanical properties sample.
2. To investigate the effect of different  $\beta$ -TCP/ZnO composition on chemical, physical and mechanical properties of the composites.
3. To evaluate the cytotoxicity of the PMMA/ZnO/  $\beta$ -TCP composites using MTT on human fetal osteoblast cell (hFOB).
4. To evaluate the antibacterial activity of the PMMA/ZnO/  $\beta$ -TCP composites on *Staphylococcus aureus* and *Pseudomonas aeruginosa*.

## **1.5 Scope of study**

The study was divided into four stages. Firstly, fabrication of PMMA composites was prepared at different compositions of ZnO and  $\beta$ -TCP. Secondly, all the samples were characterised based on their chemical, physical and mechanical properties. Thirdly, selected samples were evaluated for their cytotoxicity on human fetal osteoblast cell (hFOB). Lastly, selected samples were evaluated for their antibacterial properties.

## CHAPTER 2

### LITERATURE REVIEW

#### 2.1 Craniofacial bone replacement

Bone mineral also known as apatite calcium phosphate consist of carbonate and small amount of sodium, magnesium and other trace component (Kenny and Buggy, 2003). Bone consists of 60% inorganic, 30% organic and 10% water (Mickiewicz, 2001). Bone consist of two kind of phases which were cortical/compact (dense and stiff) and trabecular/cancellous@ spongy bone (soft and foamed structure). Cortical bone normally found at outer part of long bones and towards density decrease to the core, trabecular was found. Foamed structure of trabecular bone filled with osseous medulla. It is surrounded by compact bone. The bone contains mineral phase and collagen part which responsible to the stiffness and flexibility respectively. Bone without mineral was easily to be twisted and bone without collagen makes it very brittle (Mano *et al.*, 2004) . Sousa *et al.* (2003) explained that bone could be assume as composite material which very complex consist of polymer matrix (collagen fibrils) and an inorganic reinforcement phase (hydroxyapatite crystal mainly). Figure 2.1 illustrated the part of the cortical and cancellous (trabecular bone).

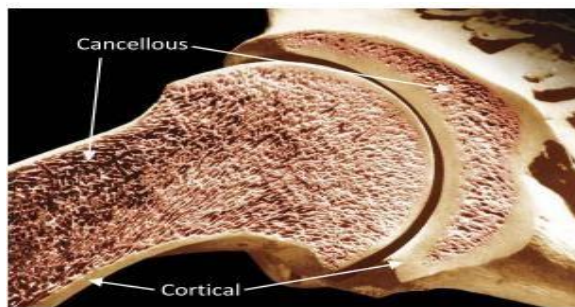


Figure 2.1 Bone structure (Philip, 2012)

Figure 2.2 shows the list of materials which could be possibly replaced bone substitution. Bone substitutes need to meet the requirements of biocompatibility, nontoxic, and resistance to deformation (Grandi *et al.*, 2011). Autograph, allograft, and xenograph bone are available to repair cranial defects (Lee *et al.*, 2009) (Pikis *et al.*, 2014).

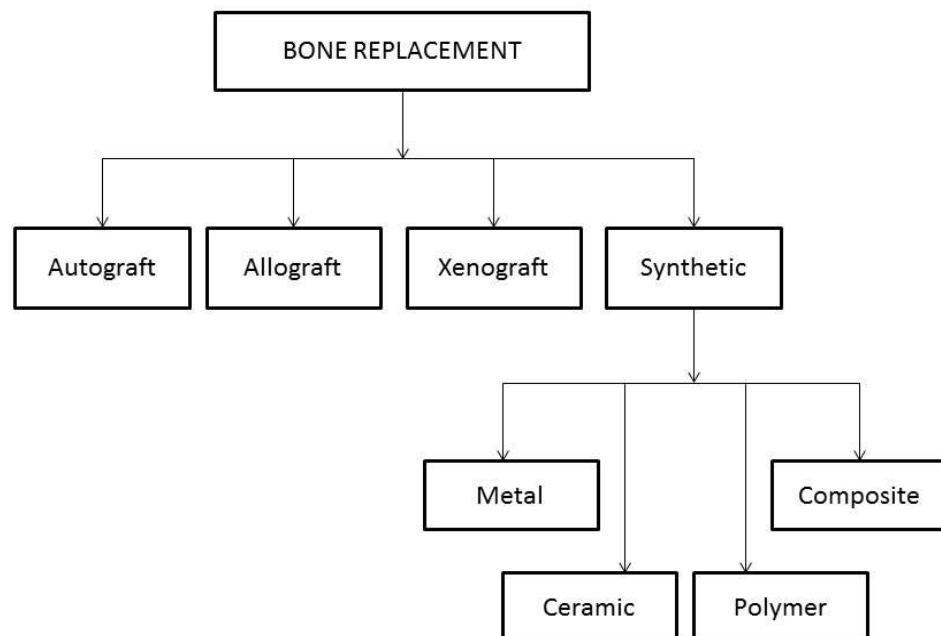


Figure 2.2 Types of materials for bone replacement

### 2.1.1 Autograft

Autograft also known as bone standard of bone regeneration (Johnson & Herschler, 2011). In other words, autograft, is a tissue obtained from patient himself/herself from near areas that are intervene. It is familiar called autologous inclusion as living tissue and do not provoke an immune reaction. In several conditions

second surgery is needed and the bone is limited difficult to shape. The drawbacks occurrence from autograft materials allowed industry to come out the new alternative through substitution allograft and xenograft, since it is wide in availability and similarity with recipient tissue. However, due to the disadvantages arises from these graft, synthetic material has been developed to overcome limitation of allo and xeno since it has similar properties of human bone tissue (Labres *et al.*, 2014). For the large defect of bone, it is not suite to use autologous bone as a sole material (Mok *et al.*, 2004).

Autograft usually obtained during initial operation. However, once autograft is not available, prosthesis may take place. The advantages are inexpensive, easy to match, no risk of disease transmission Autograft bone from other sites is less preferable due to long operating time and patient will get trauma or less comfortable experience (Lee *et al.*, 2009). Ridwan-Pramana *et al.*, (2015) stated that benefits using autograft are resistance to infection, decrease incidence of extrusion, ease to incorporate to new bone. The disadvantages are unpredictable resorption, displacement problem, prolong surgical time and donor site morbidity.

### **2.1.2 Allograft**

Allograft known as homograft, is transplanted tissue or organ between unrelated individuals of the same species (Ramakrishna *et al.*, 2001). Horch *et al.*,(2006) defined allograft, a bone taken from another person carries the risk of infection and transmitting disease.

### **2.1.3 Xenograft**

Xenograft is a material obtained from animal, non-human source that are transferred to human being (Baino & Vitale-Brovarone, 2015). The xenograph material has become a common implant material in last few decades for bone replacement in

human due to feature of good osteoconductive capacity. The limitations are associated with infection (Horch *et al.*, 2006), hence lead to disease transmissions, unpredictable resorption rate and failure of the implantation. Moreover, xenograph implant has ethical and religion issue that need be addressed (Labres *et al.*, 2014).

#### **2.1.4 Synthetic or Alloplastic**

Alloplastic or synthetic has an advantages include commercial availability, absence of donor site morbidity, and easily manipulate (Grandi *et al.*, 2011). There are several reasons of this alloplastic are preferable. Firstly, it is easily to prefabricate and secondly it is easily to modified of shape and size (Lee *et al.*, 2009). Alloplastic material used once larger defects on cranial was detected and required additional stability. Other advantage of alloplastic is unlimited availability reproducibility (Itthichaisri *et al.*, 2007). Labres *et al.*, (2014) stated that the benefits of alloplastic including not transmit disease compared to xerograph and unlimited availability. The shortcoming of alloplastic are insufficient mechanical strength and poor injectability. Titanium, PEEK, and PMMA are the example of synthetic materials.

##### **2.1.4(a) Metal**

Although metal is hard and long in durability, it would be corroded after a long period of time, that limitations was not suit to be as a scaffold for bone replacement. Moreover, metal has an adverse effect to biological response consequence to degradation by corrosion which releasing by product such as ions, chemical compound, and debris.

##### **2.1.4(b) Ceramic**

For the ceramic material, it is composed between powder, water, and clay. Ceramic could be shaped and harden in the desired form when applied to the high temperature. It is hard and resists corroding. Ceramic possess good biocompatibility

(Katti, 2004). However, ceramic suffers in brittleness and poor in fracture toughness (Katti, 2004). Ceramics play an important part in substituents of bone graft due to composition similarity with human bone (Chair *et al.*, 2017).

#### **2.1.4(c) Polymer**

Polymer is made up from long molecule or macromolecule composed of many repeated units. ‘poly’ means many and ‘mer’ means part. There are two different types of polymer for which are natural and synthetic polymer. The examples of natural polymers are rubber, protein and wood, cellulose, starch, chitin, chitosan, gelatin, dextran, alginate, pectin, guar gum, rubber, and fibrin (Zahran *et al.*, 2019). Natural polymers give advantages rather than synthetic because of nontoxicity, chemical inertness, availability, and biodegradability (Zahran *et al.*, 2019). The required implant material must have excellent properties such as inert, support antimicrobial activity, sterile, nontoxic to human, biocompatible easy handling, and rigid (Breitbart and Ablaza, 2007). Polymeric materials possess exothermic reaction which released heat, thus damage the cell and adjacent tissue of surroundings. Infection and loosening of cement at bone cement interface will occur also (Khandaker *et al.*, 2013). To date, many researchers studied on promoting the growth of osteoblast cell by modifying surface morphology of polymer. Polymer exerts low mechanical properties, however, it can be strengthening with incorporation of filler or fibre and a presence of a coupling agent to improve the bond between polymer matrix and fillers. Thus, achieved better performance of the material. Currently, polymer has been preferred as the second choice after autograph due to its durability, cheaper and ease of processing.

Mano *et al.*, 2004 also proposed that the typical kinds of polymer that suit to be used in biomedical composites such as PMMA, polysulfone (PSU), poly(etheretherketone) PEEK or epoxy resins. All that material mentioned supposedly

have characteristics including fatigue resistance, biocompatibility which additives match with the surrounding tissue, stability in dimensional, free from harmful additives and sterilization without losing their properties.

#### **2.1.4(d) Composites**

Composite is also known as the combination of two or more substituents with different properties of physical and chemical, and also the properties produced from the combination is different and stronger from the individual constituent. Composites are defined as materials that are made up of several components and generally consist of matrix of osteoconductive that will promote bone growth (Labres *et al.*, 2014). Based on Douglas *et al.* (1983), composites are mixture of resin and ceramic filler which the filler present in several phases including crystalline phase, vitreous phase, or mixture of both. Metals and ceramics known as a stiffer material and high strength than biologic hard tissue (Mano *et al.*, 2004). Currently, implants could be fabricate using stainless steel, cobalt chrome alloys, titanium and its alloy (Steflik *et al.*, 1993).

## **2.2 Evolution of biomaterial**

Heimann (2013) defined biomaterial as materials that are designed to replace human body which is safe, reliable, and aesthetically acceptable manner. Biomaterial as defined by Katti (2004) is nonviable materials used in medical devices which responses to the biological systems. Ramakrishna *et al.*,(2001) defined biomaterial as manmade materials used to replace the function of living tissue in human body (Kuemmerle *et al.*, 2005) stated that biomaterial should consider as an ideal bone substitute with requirement of chemically inert, good biocompatible, be easily contoured.

Biomaterials should have requirement of fatigue resistance, resistance to ageing in saline aqueous media, biocompatibility, dimensional stability, absence of migrating



harmful additives and being sterilisable by standard methods without loss of properties. Biocompatibility means the ability of a material to provide a favourable host response once used within the human body (Hassan *et al.*, 2019). The biocompatibility requirement should nontoxic, and no allergic reaction or inflammatory (Mano *et al.*, 2004). Bioinert, biotolerant (biocompatible) and bioactive depend on degree of interaction with living tissue potential (Heimann, 2013). Kuemmerle *et al.*, (2005) stated that biomaterial which is ideal for bone substitute need to possess properties such as chemically inert, good biocompatibility, easy to contour and dimensionally over time. The examples of polymer biomaterials are silicone, PMMA, polyesters, nylon, polyethylene, polypropylene, cyanoacrylates and polytetrafluoroethylene (Breitbart & Ablaza, 2007).

### **2.2.1 Bioinert or Biotolerant**

Bioinert or biotolerant refers to the ability of material to interact with the living tissue. Horowitz & Greenamyre, (2010) stated that biomaterial could be bioinert if it could not react with others that interfere with the function of body or it is no reaction after implantation to the function of the body. Alumina, zirconia (Yadav *et al.*, 2017) and PMMA itself is known as an bioinert material and nonbiodegradable (Gao *et al.*, 2019). Besides that, Sousa *et al.* (2003) defined bioinert polymer as a material that not changing of chemically and physically during application time. Hua *et al.*, (2019) mentioned that bioinert material gives minimum interrelation with surrounding tissue and do not provoke foreign body response. According to Heimann (2013), bioinert materials do not show positive or negative effect with living tissue. Alumina, zirconia, titania (Horowitz & Greenamyre, 2010), carbon nanotubes, diamond are the classification group of bioinert material. Ultrahigh molecular weight polyethylene (UHMWPE) also classified in this group (Omar *et al.*, 2014). Bone cement (PMMA), stainless steel, magnesium alloys are

classified as bio tolerant materials. It releases substance in larger but nontoxic concentration. This group of material could accept by body (Heimann, 2013). PMMA possess high biocompatible. It has significant in vitro use because through thermal necrosis, temperature could lead to death of surrounding tissue (Kwarcinski *et al.*, 2006). Various implant used was PMMA source due to its compatibility with human tissue. PMMA has excellent biocompatibility with the surrounding biological environment makes it suite to be applied in implant applications (Radha *et al.* (2017).

### **2.2.2 Bioactive**

Hua *et al.*, (2019) defined bioactive material as materials that interact with the surrounding biological system. Examples of bioactive fillers are bioactive glass, hydroxyapatite,  $\beta$ -TCP, and metal oxides (Mano *et al.*, 2004). Bioactive compounds have actions in the body that may promote rapid bone repair within a few weeks of implantation (Alshemary *et al.*, 2015).

### **2.2.3 Biodegradable**

Biodegradable materials could be defined as materials that break down because of macromolecules degradation. It can be attacked by biological elements so that the system is affected and degrade by product (Woodruff and Hutmacher, 2010). Optional material for implants included tricalcium phosphate, polycaprolactone (PCL) (Park *et al.*, 2014), biodegradable polyglycolic acid (PGA), polydioxanone (Mok *et al.*, 2004). In orthopaedic area, the examples of biodegradable polymers are the PLA and the PGA, which commonly used in pins, screws, bone fixation plates and in tissue engineering scaffolds (Sousa *et al.*, 2003). PLA and PGA were strongest biodegradable polymers applied in medical applications, possess tensile strength and Young Modulus up to 72 MPa for PLLA, 57 MPa for PGA and 4 GPa for PLLA and 6.5 GPa for PGA (Daniels *et*

*al.*, 1990) respectively. However, the cortical bone still has higher mechanical properties compared to them and reinforcement needs to back up it.

#### **2.2.4 Biomimicry**

Biomimicry or biomimetic is interdisciplinary field which allows imitation of models, systems and element of nature that have functions mimicking biological process for the reasons to overcome human problems. In cranial field, biomimetic considers fabricating synthetic bone grafts that mimic to biological apatite (Barba *et al.*, 2019).

#### **2.3 Polymethylmethacrylate (PMMA)**

PMMA also known as acrylic which is a transparent thermoplastic. It is an alternative to glass and polycarbonate whenever extreme strength is not desired. PMMA is a strong and lightweight material (Pawar *et al.*, 2016). It is colourless and odourless polymer of acrylic acid. PMMA widely used for replacement of bone. In some cases, PMMA was utilized with antibacterial agent to treat infection from implantation (Ding *et al.*, 2018). PMMA is completely dissolved in chloroform, di and trichloroethane. Thus, it is not recommended used with chlorinated or aromatic hydrocarbons, esters or ketones. PMMA not dissolved by detergents, cleaner, dilute inorganic aids, alkalis and aliphatic hydrocarbons.

PMMA is one of the bioinert (Kwarcinski *et al.*, 2006) and not biodegradable (Gao *et al.*, 2019). Various filler has been used the polymer matrix to enhanced their biocompatibility and resulted to long term attachment to the local bone tissue.  $\beta$ -TCP used as bone substitution in orthopaedic surgery because of possessing characteristics in good resorption rate or ability to regenerate bone. Matteis *et al.*, (2019) stated that PMMA has properties of high biocompatibility low cost, and ease of manufacture. The concentration of ions released from PMMA was very low and it was not considered toxic

to human cells. PMMA has drawbacks such as none bonding capability (Puska *et al.*, 2016) low mechanical strength (Zafar, 2020), greater heat generation during polymerization (Puska *et al.*, 2016), (Daglilar and Erkan, 2007).

### **2.3.1 Properties of PMMA**

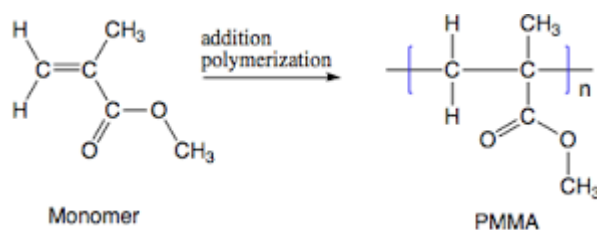
PMMA has superior properties such as processing ease, accurate fit, stability in oral environment, good colour stability, superior aesthetics and use with inexpensive equipment (Ladha and Shah, 2011). PMMA has been observed as an alternative material for polycarbonate due to low cost, moderate properties and easy of handling and processing. One of unique properties of PMMA was transparency. These features allow only trace of UV light to be absorbed and less molecule of polymer attacked by the light hence the level damaged of the polymer was lower makes them suitable for application that need to weather resistance. PMMA is low cost but easily manipulate, hence it is widely used in craniofacial reconstruction. However, PMMA has some disadvantages including a lack of bone bonding capacity, low mechanical strength, excessive shrinkage, and significant heat generation during polymerisation (Samad *et al.*, 2011; Pikis *et al.*, 2014). In comparison to the host bone, it has a strong exothermic response, low mechanical strength, and poor radiopacity and osteointegration (Khandaker *et al.*, 2013). Nonbioabsorbable, is one of the problem of PMMA which could inhibit tendon to bone healing and may prone to problems in surgery (Oshtory *et al.*, 2010). There are several ways that could improve mechanical properties of PMMA which were introducing other alternative other than PMMA such as rubber modified acrylic polymer, chemically modified it, and reinforcing PMMA with another materials (Vojdani *et al.*, 2012). Table 2.1 referred the details physical properties of PMMA.

Table 2.1 The properties of PMMA

Properties	Value
Shrinkage (%)	0.3-0.6
Water sorption (%)	0.3
Density(g/cm <sup>3</sup> )	1.18
Melting point(°C)	220-240
Refractive index	1.490
Glass transition temperature (°C)	100-130

### 2.3.2 Polymerisation of PMMA

PMMA was produced via free radical addition polymerisation. It involves of free radicals propagates with monomer. As stated by Silikas, Al-Kheraif and Watts, (2005), there are three activation types of acrylic which are heat curing, self-curing and light curing. Heat curing illustrated that polymerisation is initiated by free radical from bisphenol (BPO). Whereas self-curing described the polymerisation reaction of methacrylate monomer is initiated by the activation reaction of BPO with an amine accelerator at room temperature which give free radicals for addition to monomer molecules. Light curing referred to the photo initiator that irradiated with blue light to produce free radicals in the presence of amine and monomer. PMMA was produced from addition reaction polymerisation with the presence of benzoyl peroxide as initiator, and dimethyl-p-toluidine as chemical activator in the reaction (Hassan *et al.*, 2019) as illustrated in Figure 2.3.



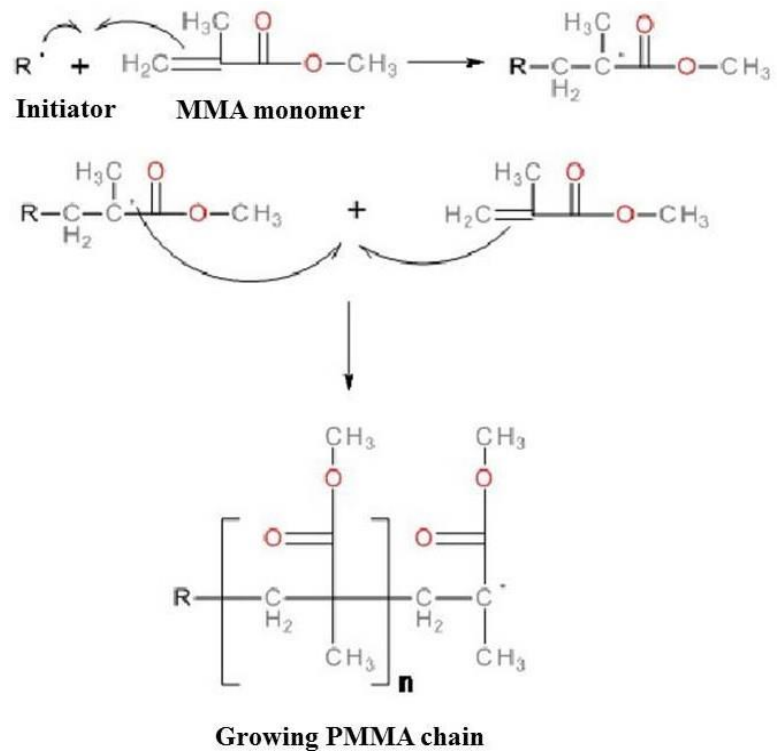


Figure 2.3 Addition polymerisation of PMMA initiated by a phenyl radical(Unosson, 2010)

### 2.3.3 Applications of PMMA

PMMA is a versatile material, this polymer has widely used in many fields and application. PMMA filled satisfaction in aerospace, machinery, medical and architecture industries (Ma *et al.*, 2015), construction, automotive and transportation, automotive glazing, lighting and in medical health (Pawar *et al.*, 2016). Table 2.2 summarizes the application of PMMA as reported in the literatures.

Table 2.2 PMMA applications in industry sectors

Findings (year)	Applications
Hamizah <i>et al.</i> (2011)	In dentistry: filling and orthopaedic surgery for fixation of prostheses.
Ma <i>et al.</i> (2015)	Filled the gap of aerospace, machinery, medical and architecture industries.
Pawar <i>et al.</i> (2016)	Architecture and construction, automotive and transportation, automotive glazing, lighting and in medical health
Radha <i>et al.</i> (2017)	In dentistry for different applications, such as denture basis, orthodontic appliances, and provisional restorations

In medical applications, PMMA is mostly used in craniofacial reconstruction specifically on skull as shown in Figure 2.4 (Huang *et al.*,2015). Low *et al.*, (2019) applied PMMA to eleven patients' skull and no adverse effects were reported after 3 months of implantation.



Figure 2.4 PMMA implant in host model (Huang *et al.*, 2015).

#### 2.4 The factors that affect the filled polymer

Factors that affect filled polymer should be considered in the preparation of the composites, such as filler type, filler loading, and filler size in order to get better

performance of the composites. Jones & Rizkalla, (1996), stated that the strength of the composite also influenced by volume, types of filler loading and type of resin system. The important parameter has been discussed in previous literature. Liang (2013), investigated the factors that influence the mechanical properties of polymer composites filled particulate fillers including the compatibility between filler and composites, their shape, size, surface morphology, and concentration. The value of modulus strength found for composites with silane treated filler was significantly higher than nonsilane treated filler. Mickiewicz, (2001) stated that mechanical properties depend on the adhesion of polymer and filler, which mechanical suffers when polymer and filler have poor adhesion. This is due to the polymer surface in hydrophobic nature hence poor wetting of hydrophilic filler, thus resulted in low adhesive force between polymer matrix and filler.

#### **2.4.1 Filler types**

Polymer suffers low in stiffness and strength. The addition of inorganic particulate such as glass, aluminium oxide, calcium carbonate, carbon nanotube are believed could improve the limitations of polymer (Fu *et al.*, 2008). They found that the addition of rigid particles which are commonly associate to the inorganic filler (Friedrich *et al.*, 2005) could enhance modulus with increasing particle loading, and composite modulus also increasing. Aluminium reinforcement decrease impact and tensile strength of PMMA due to the poor adhesion of polymer and weaken stress concentration around metal (Gad *et al.*, 2017). Chou *et al.*, 2010 investigated the occurrence of two types of filler in same amount which is 16% of HA and titania to the composite give in mechanical properties effect to the composites.

Many organic fillers have a great potential to be a combination to the matrix in order to enhance their mechanical properties as well as others properties. Usually, this



kind of fillers comes from natural base like sawdust, rice husk (Noushad *et al.*, 2014), cellulose and others. They are lower in price since it commonly is a side product that no longer use after their production. Hence, it is useful to be customized rather thrown it without use. The features of the fillers that have to be care were in an aspect of low surface size of filler. The tendency of water uptake was lower and take time to fillers/matrix interface to degrade. The shape of the fillers also important since the spherical shape could lead to better dispersion in matrix due to the free entanglement compared to the irregular filler particles. Besides, the spherical shape is valuable to exhibit lower in shrinkage. This phenomenon was attributed from the movement of dispersed phase within the matrix and relax stress which was increased.

Recently, studies have focused on ceramic based biomaterial as antibacterial agent to control bacteria. They have advantages including durability, stability, and safety. The most widely studied inorganic nanomaterials for biomedical applications include hydroxyapatite nanoparticles (HA) and zinc oxide (ZnO) nanomaterial (Ding *et al.*, 2018). Inorganic fillers also hard and dense make them important to improve mechanical and wear properties (Moszner and Klapdohr, 2004). Commonly, the fillers combined with PMMA were zirconium oxide, barium sulphate, zinc oxide, calcium phosphate and magnesium oxide (Chang, 1981). ZrO, BaSO<sub>4</sub> and ZnO commonly useful as radiopaque fillers while CaPO<sub>3</sub> and ZnO as bioactive fillers that could improve biocompatibility. Fouda and Al-harbi, (2017) found that the addition of metal oxide on PMMA improve physical and mechanical properties. They suggested that addition of filler and fibres to PMMA could enhance mechanical properties and physical also.

#### **2.4.1(a) Tricalcium Phosphate**

Calcium phosphate classified into two classes which are apatite cement and brushite cement (metastable phase under physiologic condition). However, in

craniofacial application, apatite cement has been focused (Kuemmerle *et al.*, 2005). It has excellent bioresorbability. TCP subjected to three polymorphs ( $\alpha$ -,  $\beta$ ,  $\alpha'$ ) according to their thermal stability (Alshemary *et al.*, 2015).  $\beta$ -TCP divided by three types  $\beta\alpha\alpha$  based on their thermal stability. Al-sanabani *et al.* (2013), mentioned that only two polymorphs phases used as biomaterial ( $\alpha\beta$ ).

Carrodeguas & De Aza, (2011) stated that the difference of polymorphs which is differ in terms of temperature:  $\beta$  TCP-the low temperature,  $\alpha$ -,  $\alpha'$  -high temperature forms.  $\beta$ -TCP is used mainly for preparing biodegradable bio ceramics shaped as dense and macro-porous granules and blocks, whereas the more soluble and reactive  $\alpha$ -TCP is used mainly as a fine powder in the preparation of calcium phosphate cements, although some commercial bio ceramic granules and blocks made of  $\alpha$ -TCP may be found on the market. Both  $\beta$ - and  $\alpha$ -TCP materials are used in clinics for bone repair and remodelling applications. Radin & Ducheyne, (1993) stated that  $\alpha$ -TCP is very reactive and degrades rapidly in vitro, so it is not used as bone graft material.

Generally, the high mechanical properties can be achieved by addition of different additives such as titanium dioxide ( $\text{TiO}_2$ ), silica ( $\text{SiO}_2$ ), hydroxyapatite (HA), tricalcium phosphate (TCP), alumina ( $\text{Al}_2\text{O}_3$ ), and fibre in the polymer base. Among with these additive, HA and TCP are more interesting than others, because of close matching to natural bone units and high mechanical properties. According to Zebarjad (2011), biocompatibility and mechanical properties could be enhanced by addition of HA due to features of HA itself in having biocompatibility properties and osteoconductivity. Materials like TCP are osteoconductive because osteoblast adhere to them and deposit bony tissue on their surface (Horowitz and Greenamyre, 2010). Osteoconductive could be describe which has features to support proliferation or attachment of new osteoblast

(Heimann, 2013).  $\beta$ -TCP is one of the bioceramic which is used in clinical fields due to the close composition to the bone ( Park *et al.*, 2012; Al-sanabani *et al.*, 2013).

Besides that, the properties of biocompatible and biodegradable of  $\beta$ -TCP make it interesting characteristics as a bone substitute (Park *et al.*, 2012).Combes and Rey, (2010) stated that  $\beta$ -TCP is applied in coatings on inert bone implants due to osteoconductive, bioresorbable and bone bonding ability. Alshemary *et al.*,(2015) stated that tricalcium phosphate applied in replacement or repair of mammalian hard tissue defects.

$\beta$ -TCP is nontoxicity, antigenic, and noncarcinogenic biomaterials, good osteoconductivity, direct bond formation, and rapid bone repair within short time of implantation (Alshemary *et al.*, 2015). Kwarcinski *et al.* (2006) stated that calcium phosphate bone cement classified as method for cranial reconstruction due to strong biocompatibility and osteoconductive nature. From Al-Sanabani *et al.* (2013), one of the reason using  $\beta$ -TCP widely used over HA because of the resorbable properties. It allows positive interaction with living tissue towards bone cells which enhances strong bonding osteogenesis. Park *et al.*, (2012) stated that among other bioceramics,  $\beta$ -TCP has been chosen due to properties of biocompatible and biodegradable. Daglilar & Erkan (2007) found in their study that the incorporation of  $\beta$ -TCP up to 2.5% only could give increment on flexural strength value. Above 2.5%, the value of mechanical strength was drop. Lopez-heredia *et al.*, (2012) mentioned that CaP has tendency to produce new bone after resorption process. Because of that, it suggested to be a candidate to combine with PMMA. As we know, ceramic has an ability to bond directly to bone through apatite layer. Besides, the incorporation of bioactive glass ceramic to PMMA bone cement could reduce the amount of added monomer, hence exothermic polymerization was decreased as well as shrinkage polymerization and will enhance the mechanical properties. Chair

*et al.*, (2017) mentioned that TCP exist in four forms.  $\alpha$  is stable between 1120-1470°C and metastable at room temperature. The  $\alpha$  stable above 1470°C. The  $\beta$  form is stable below 1120°C. The  $\gamma$  form obtained under high pressure. In our study,  $\beta$  form was chosen. It produced by heating amorphous CP (ACP) between 800-1000°C. It is also obtained by calcination at 900°C of apatitic tricalcium phosphate or amorphous TCP.  $\beta$  form has C/P ratio 1.5 more soluble than HA and more subjected to degradation.  $\beta$  form produced ceramic granules usable as bone substitute and it is bioactive thus could allowing the interaction occur between cells and body fluid hence perform good bone integration. Monchau *et al.*, (2013) stated that  $\beta$ -TCP is resorbable which has ability to adapt with living tissue that important to bone replacement which induce and improve self-healing capacity of bone. From their studied, calcite prone to stronger degradation, hence the quality of cell adhesion obtained from SEM result was decreased hence the cell proliferation rate also decreased.

The improvement of  $\beta$ -TCP should be concerned since the mechanical properties of  $\beta$ -TCP approximately low in range of 3-5MPa. Hence, the introduction of bioinert metal oxide is needed because it will cover the poor mechanical properties of  $\beta$ -TCP due to the metal oxide possess bio inertness, excellent tribology properties, high wear resistance, fracture toughness and strength (Pignatello, 2013). Grandi *et al.*, (2011) expressed that calcium phosphate are resorbed due to osteoclastic activity forming bone tissue between bone cement interface.

#### **2.4.1(b) Zinc Oxide (ZnO)**

Metal oxides, calcium phosphate and glass ceramics are in the bioceramic classes. Bioceramic possess excellent biocompatibility and bioactivity. ZnO is one of the metal oxides groups and considered as bioinert in biological environment. Whereas, calcium phosphate and glass ceramics have the ability to bond with the bone at the bony site after

implanted. Due to that, bioceramics were commonly used in the replacement of hard tissue. Hydroxyapatite and tricalcium phosphate are classified in calcium phosphate classes, while  $\text{Al}_2\text{O}_3$  and  $\text{MgO}$  (Black,1981) are classified in metal oxides group and bio glass (Hench *et al.*, 1971; Kokubo, 1996) was under glass ceramic.

Zinc oxide possess excellent properties in physical, chemical, biological (Ding *et al.*, 2018) as well as low in cost, environmental friendly and biocompatible (Botsi *et al.*, 2019). More importantly,  $\text{ZnO}$  has antibacterial properties besides of biocompatible and biodegradable (Gordon *et al.*, 2011, Kasraei *et al.*, 2014, Ann *et al.*, 2014a) Sirelkhatim *et al.*, 2015, Vimbela *et al.*, 2017). Zinc is necessary for cell growth, development and differentiation. Yamaguchi, Oishi and Suketa (1987), advocated that zinc may be restricted largely in the osteoblasts of bone and can boost bone formation, make it important role as an activator in bone metabolism. Ito *et al.*, (2002) mentioned that the incorporation of zinc to the implant could enhance growth of bone formation around the implant and accelerate recovery of a patient.

According to Gordon *et al.*, (2011),  $\text{ZnO}$  is one of the metal oxide powders, that reveal growth inhibition of a broad spectrum. Catalysis of formation of reactive oxygen species (ROS) from water and oxygen is described for the mechanism for antibacterial activity of  $\text{ZnO}$ . ROS will disrupt the activity of membrane bacterial. Moreover, antibacterial activity is stronger once the particles possess high surface area. Based on Kasraei *et al.*, (2014), they found that when  $\text{ZnO}$  and Ag converted to nanoparticles (surface to volume ratio increases), they demonstrated better antibacterial activity.

Ann *et al.*, (2014a) reported that particles of  $\text{ZnO}$ ,  $\text{CaO}$  and  $\text{MgO}$  demonstrated antibacterial properties without the presence of light. The benefits from utilized inorganic materials where they contain mineral element that vital to human body as well as

exhibited high antibacterial properties. Furthermore, Ann *et al.*, (2014b) found that ZnO particles are the best choice among other metal oxides due to their excellent properties and extensive applications.

A previous study reported that ZnO has stronger antibacterial activity even at neutral pH, besides being biocompatible and nontoxic to human beings (Pulit-Prociak *et al.*, 2016). Sirelkhatim *et al.*, (2015) found that nanosized ZnO could interact with bacterial surfaces and easily enter cell, thus exhibiting significant antimicrobial activity. Among other metal oxide including Al<sub>2</sub>O<sub>3</sub> and TiO<sub>2</sub>, ZnO is easy to dispersed and have almost no surface water (Wacharawichanant, 2010). 3% wt of ZnO incorporated with biocomposite was found effective amount to inhibit *S. aureus* at 6<sup>th</sup> day (Marra *et al.*, 2016). ZnO concentration at 3 mM to 10 mM was found to inhibit bacteria growth (Sirelkhatim *et al.*, 2015). Marra *et al.*, (2016) also stated that the efficiency of antibacterial activity of ZnO more effective when the particles in micron size rather than nano size. Ann *et al.*, (2015) stated that ZnO with smaller particles size are prone to have higher toxicity rather than larger particles size.

#### **2.4.2 Filler loading**

Filler loading in polymer composites play an important role to enhance mechanical properties of the composites such as flexural strength, modulus, microhardness and fracture toughness. Colombini, (2004) found that increasing particle loading will reduce composite strength for particles at and larger than 80nm. However, this trend reversely for particles composites of 10nm. In the studied by Bose and Mahanwar *et al.*, (2004) the increment of tensile strength value achieved once filler loading was added up to 40%. Kim *et al.*, (2004), in their study also describe that the increment of filler loading will cause increase of fracture toughness because of by adding

more filler tend to crack branching, hence increase in crack surface areas and resultant fracture energy.

### **2.4.3 Filler size**

The size of particle will influence its mechanical properties, such as stiffness and toughness. The smaller the size of particles especially nanosize, the more efficient the material will be for many applications (Friedrich *et al.*, 2005). Colombini, 2004 found that mechanical enhancement achieved from contribution of smaller size of hard particles. Mahanwar *et al.* (2004) studied the influence of using filler of mica particles with decreased on particle size lead to the increment of mechanical strength and dielectric also thermal properties. The size used is microscopic filler as agreement with studied by Abdullah (2015), they used microscopic filler HA at loading 5% to 15% as a filler inclusion to acrylic resin and this study showed that 5% HA addition is the ideal value to show the improvement of mechanical properties. Ann *et al.*, (2015) mentioned that one of the unique features of nanoparticle size is in their high surface to volume ratio compared to macro sized material. It offers large surface adsorption Ann *et al.*, (2015) stated that ZnO with smaller particles size are prone to have higher toxicity rather than larger particles size.

Commonly, hydroxyapatite (HA) is one of the fillers that has been used in dentistry since it is easily mixed with dental resin to obtain desired product. Tham *et al.*, (2010) in their study found 5% HA added to PMMA give improvement in fracture toughness,  $K_{IC}$ .

Even in a very little amount of nanoparticle size present in a polymer composite will transform the property of polymer host (Chatterjee, 2010). Nano ZnO incorporate with polypropylene showed excellent in antibacterial properties against *Staphylococcus*

*aureus* and *Klebsiella pneumoniae* makes it important in food packaging application (Chandramouleeswaran, *et al.*, 2007). The advantages of nanofiller also proved by studied of Lin and Mahmud, (2009) in term of improving mechanical performance which increment of tensile modulus and strength are detected in their study. Yamamoto, (2001) also found that the antibacterial efficiency was increasing with decreasing the particle size and increment of powder concentration. Particle size used to range from 0.1 to 0.8 $\mu$ m. Marra *et al.*, (2016) also stated that the efficiency of antibacterial activity of ZnO more effective when the particles in micron size rather than nano size. However, ZnO nanoparticle possess strong antimicrobial activity due to the nanoparticle could enter the cell wall of microbes via ions channel or protein carrier hence bind with organelles therefore disturbing metabolic process as a result of production of ROS (Sharma *et al.*, 2010). Colombini (2004) mentioned that larger surface area of filled particles is a factor to increase strength since mechanism of stress transfer undergo efficiently. The stress transfer is inefficient for poorly bonded particles. Hence, a strong particles /matrix interface loading will give higher strength. Kong *et al.*, (2008), stated that nanosize particles will attack a loose cell wall from Gram- positive *S.aureus*. Hence, the released silver nanoparticles could pass through *S.aureus* cell wall and bind with DNA, resulting DNA denaturation.

#### **2.4.4 Filler shape**

There are three types of particles which were sphere, sheet (block), needle (column) particles. Inorganic particles contribute to the strength and rigidity of the composites. Usually inorganic sheet (block particles is one of the common filler types used in polymer industry. The examples are mica, talcum powder and clay.



#### **2.4.5 Filler as an antibacterial agent.**

Antibacterial agents are needed in prevent infection of implantation procedure in medical and dentistry field. Antibacterial agents come with two types which obtained from organic and inorganic compounds. As mentioned by Zahran *et al.*, (2019), antimicrobial properties could be improved by combination of natural polymer and inorganic filler.

Marra *et al.*, 2016 stated that antibacterial action could be effective with incorporation metal particles, metal oxide, carbon nanotube and organic compound to the polymer. These compounds could develop antimicrobial activity. Kasraei *et al.*, (2014) proved that introduction of antibacterial agent to nano level size could enhance their antibacterial activity since their surface to volume ratio increases. The examples of organic compounds usually used as a fillers such as chitosan (Pandiselvi and Thambidurai, 2015) and coumarin (Rahman *et al.*, 2016). However, this kind of compound related to give several disadvantages including sensitive to high temperature and pressure also toxic to human body. Such problem occurs in many industrial processes. That is the reason to used inorganic compound such as metal oxides (Gordon *et al.*, 2011).

Inorganic materials have widely used in physical, biomedical, biological and pharmaceutical (Ann *et al.*, 2014b). According to Gordon *et al.* (2011), inorganic materials exhibited stronger antibacterial activity at low concentration. Advantages from using inorganic compound was stated to be stable in extreme conditions, also considered as nontoxic and contain mineral element that gives benefits to human body. Other than that, Raj *et al.*,(2018) mentioned that advantages from using antimicrobial inorganic are robustness, stability, and long shelf life. Padmavathy and Vijayaraghavan, (2008) also stated that inorganic oxides contain mineral element to human body but the usage is in

small amounts. Besides that, the superior properties are durability, less toxicity and greater selectivity and heat resistance. As reported by Pasquet *et al.* (2015), the antibacterial activity of ZnO involved mechanism i) ROS generated from photochemical reaction of semiconductor properties which could damage cell membrane of microorganism. ii) cytotoxic effect of Zn<sup>2+</sup> release in water from partial dissolution of ZnO particles iii) destabilization of microbial cell membrane from adsorption of ZnO particles. Other than that, Zahran *et al.*, (2019) reported the same conclusion on action of ROS which the presence of ROS will enhance the presence of oxide protein in mitochondria and will affect the lipid as well as DNA thus damage the cell membrane and mitochondria function.

Interest of studying inorganic compounds has risen due to their stability, long shelf life, and safety. Pandiselvi and Thambidurai, (2015) also investigated the incorporation of chitosan/ZnO/Polyaniline (PANI) against two pathogenic bacteria, *S. aureus* and *P.aeruginosa*. They found that the composites showed remarkable strong antimicrobial and biofilm activity in vitro compared to chitosan (CS) and PANI individually. Four factors that influence the antibacterial efficiency of ceramic powders are cations eluted from the powder, the active oxygen generated from powder, the pH, and mechanical destruction of cell membrane (Yamamoto, 2001).

## **2.5 Bacterial Strains**

### **2.5.1 Staphylococcus aureus**

*S. aureus* is one of pathogenic skin bacteria which could cause skin infections such as impetigo, ecthyma, and cellulitis. *S. aureus* comprise grape-like cocci in clusters. It appears around 0.8µm in average. The habitat is on the human skin. It grows aerobically as yellow or gold colonies on blood agar. Antibiotics that familiar against

*S.aureus* are penicillin, flucloxacillin, erythromycin, fusidic acid (for skin infection) and vancomycin. *S.aureus* also is the source of infection in any surgical procedure.

Ann *et al.*, (2014a), found that ZnO could not damage cells at a concentration of 5 mM. The release of ROS from ZnO inhibited cell damage. UVA photo activation increases bacterial inhibition of ZnO against *S. aureus* by producing  $O_2^-$  and  $\cdot OH$  from UVA light, which activates bacteria  $O_2$  species and damages active enzyme, DNA, and protein. Hence, these species of  $O_2^-$ ,  $\cdot OH$ , and  $H_2O_2$  play an important element in the inhibition of bacterial growth. Figure 2.5 summarises the possible formation of ROS.

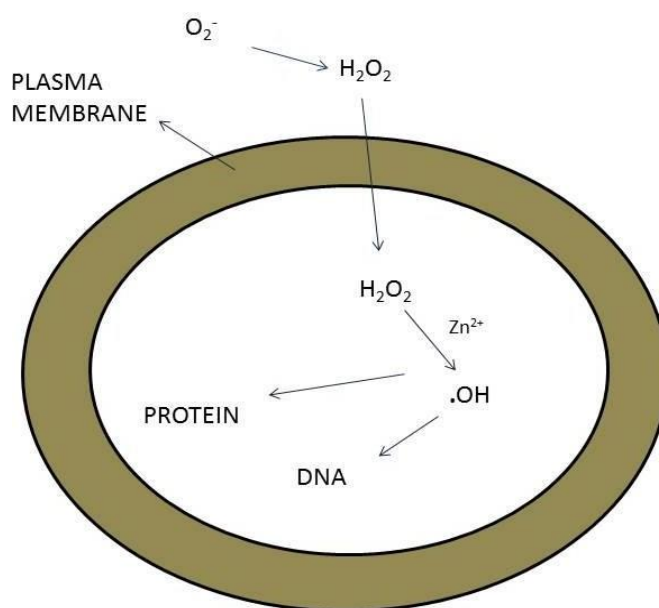


Figure 2.5 (ROS) mechanism towards cell structure(Ann *et al.*, 2014b)

Figure 2.5 also could be understood via equation below:



$\text{H}_2\text{O}_2$  produced from reaction of two  $\text{O}^{2-}$  and two hydrogen ions through Fenton reaction,  $\text{H}_2\text{O}_2$  reacts with  $\text{Zn}^{2+}$  producing hydrogen radical ( $\cdot\text{OH}$ ).  $\text{H}_2\text{O}_2$  could penetrate the cell wall of bacterial (Saito, 1988). ROS is important since it could damage DNA, protein and lipids (Ann *et al.*, 2014a). Concentration of  $\text{H}_2\text{O}_2$  will effect to the antibacterial activity. Decreasing particles size will generated more  $\text{H}_2\text{O}_2$  from surface of ZnO.  $\text{H}_2\text{O}_2$  could penetrate the wall of bacteria.

Gram-positive bacteria, for example, *S. aureus* and *Staphylococcus epidermidis*, are the main pathogens causing implant-related infections. These bacteria enter the patient's body during joint replacement surgery and subsequently adhere to the implant surface and surrounding body tissues. The bacteria continue to proliferate and form a biofilm, which in turn causes an infection. The biofilm formed will also greatly enhance the antibiotic resistance, anti-immune response, and drug resistance of the bacterial communities. *S. aureus* are a typical hydrophobic bacterium with a surface contact angle of approximately  $72.2^\circ$ . The wettability of the bacteria and the sample surface also has an important effect on the adhesion process. As the surface roughness decreases, the surface gradually changes from hydrophobic to hydrophilic, thus effectively inhibiting the adhesion of hydrophobic *S. aureus*. From Ann *et al.*(2015), they mentioned that similar type of human pathogenic bacteria from Gram-positive are *Basillus*, *Enterococcus*, *Listeria*, *Strepcococcus* and *Klebsielle pneumoniae*.

### 2.5.2 *Pseudomonas aeruginosa*

*P. aeruginosa* is one of the pathogenic skin bacteria instead of *S.aureus* and streptococcus pyogenes. *P. aeruginosa* is rod shaped Gram-negative bacterium of 0.4um in diameter and 1.2 um long. Similar type of Gram-negative are acinetobactes, Escherichia, and salmonella. It is an aerobic, gram negative rods, motile by means of polar flagella. It grows over a very wide temperature range including room temperature. It also has characteristics of 'fishy' aroma. Samarayanake, (2006) reported that *P. aeruginosa* also involved in infections to moist skin area such as groin, axillae and perineum. *P. aeruginosa* is a flexible organism. Its properties depend with the changes in the environment. *P. aeruginosa* has arisen as a main pathogen during the past two decades. Most cases between 10% and 20% of infections form *P. aeruginosa* has been traced in most hospitals. *Pseudomonas* infection is especially predominant among patients with burn wounds, cystic fibrosis, acute leukemia, organ transplants, and intravenous-drug addiction. Malignant external otitis, endophthalmitis, endocarditis, meningitis, pneumonia, and septicaemia are such the most infections occur. Many new drugs with antipseudomonal activity, including penicillins, cephalosporins, and other  $\beta$ -lactams, have been introduced in recent years and offer the potential for new approaches to therapy for these infections (Bodey *et al.*, 1983). Hazra *et al.*, (2014) stated that cell wall of *P. aeruginosa* made up thin membrane of peptidoglycan and outer membrane (lipopolysaccharide, lipoprotein and phospholipid) which less prone to the attack of nanoparticles.

### 2.6 Cytotoxicity

In cytotoxicity, MTT (3-(4, 5-dimethylazolyl)-2-5-diphenylte- trazolium bromide) and MTS (3-(4,5-dimethylthiazol-2-yl)-5-(3-caebozomethoxyphenyl)-(4sulfophenyl)-2H-tetrazolium) assay are two types of assays that involved in measuring

cell viability *in vitro*. The MTT assay is easy, accurate and provided reproducible results (Murugavel *et al.*, 2019). MTT reagent is cheaper than MTS and MTT assay has an additional step to solubilize formazon crystal but MTS does not. MTT involved the enzymatic reduction of yellow coloured of tetrazolium salt to its formazan crystal of purple colour through mitochondrial dehydrogenase activity. This mechanism is the same as MTS assay. Another evaluation for cytotoxicity is Alamar Blue. The reagent of Alamar blue is resazurin (blue indicator dye) and nontoxic to cells. However, this reagent is high in cost. Hence, in this study, MTT assay was chosen to evaluated cell viability. Figure 2.6 shown the mechanism for MTT assay.

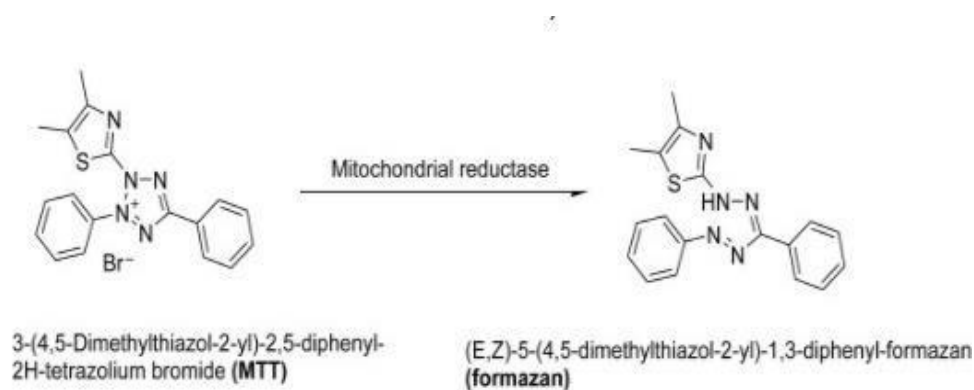


Figure 2.6 Enzymatic reduction of MTT to formazan (Kuetze *et al.*, 2017)

## 2.7 Implant-related infections

Craniofacial defects due to the trauma or injuries need to be reconstructed by implantation of several types implant material. The commonest material used is alloplastic PMMA as has been explained earlier prone to infection after the implantation. The infection is associated with the presence of bacterial adhere to biomaterial with the ability of microorganism to form biofilm (Nam, 2014) and thus lead to implant failure. PMMA implantation related to the occurrence of osteomyelitis (Olson and Horswill, 2013) which a bacterial infection to the bone commonly caused by *S.aureus*.

*P.aeruginosa* are also related to the skin infection as found in studied of Bodey *et al.*, (1983; Gottenbos *et al.*, 2000; Blyth *et al.*, 2011; Khullar *et al.*, 2016). Figure 2.7 showed osteomyelitis bone infection.

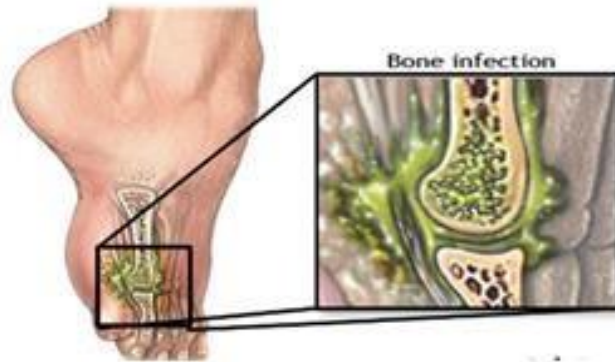


Figure 2.7 Osteomyelitis: bone infection (Kumari, 2016)

## CHAPTER 3

### MATERIALS AND METHODS

#### 3.1 Study Design

This was an experimental study which was conducted at the Dental Laboratory, and Craniofacial Science Laboratory, School of Dental Sciences to fabricate PMMA composite with the addition of two inorganic fillers, beta tricalcium phosphate( $\beta$ -TCP) and zinc oxide. This study was divided into five parts:

**Part I:** Mold preparation using silicone mold. To fabricate silicone mold, silicone liquid was used.

**Part II:** Material selection and classifying the composition for each material for several systems by using process polymerization of heat curing achieved by mixing PMMA + ZnO +  $\beta$ -TCP. This process was conducted in fume cupboard Dental Laboratory, School of Dental Sciences using pressure pot to cure the sample. There are five different compositions used in this study as shown in Table 3.1.

Table 3.1 Compositions of sample based on weigh percentages

Sample	Type of samples	Composition Ratio
Control	Pure PMMA	100:0
1	PMMA: $\beta$ -TCP	95: 5
2	PMMA: $\beta$ -TCP	90: 10
3	PMMA: $\beta$ -TCP	85:15
4	PMMA: $\beta$ -TCP: ZnO	82.5:15:2.5
5	PMMA: $\beta$ -TCP: ZnO	80:15:5

**Part III:** Characterisation of the sample. All the samples were characterised for mechanical testing in Dental Laboratory School of Dental Science using



Universal Testing Machine, Shimadzu to run flexural and tensile testing. While physical testing was performed in multidisciplinary (MDL) laboratory.

**Part IV:** The biocompatibility testing was performed in cell culture room at Craniofacial Science Laboratory, School of Dental Science.

**Part V:** Antibacterial evaluation was carried out in Microbiology Unit, Craniofacial Science Laboratory, School of Dental Sciences, USM. The strains involved were *Staphylococcus aureus* (Gram-positive) and *Pseudomonas aeruginosa* (Gram-negative).

The summary of the study is illustrated in Figure 3.1.

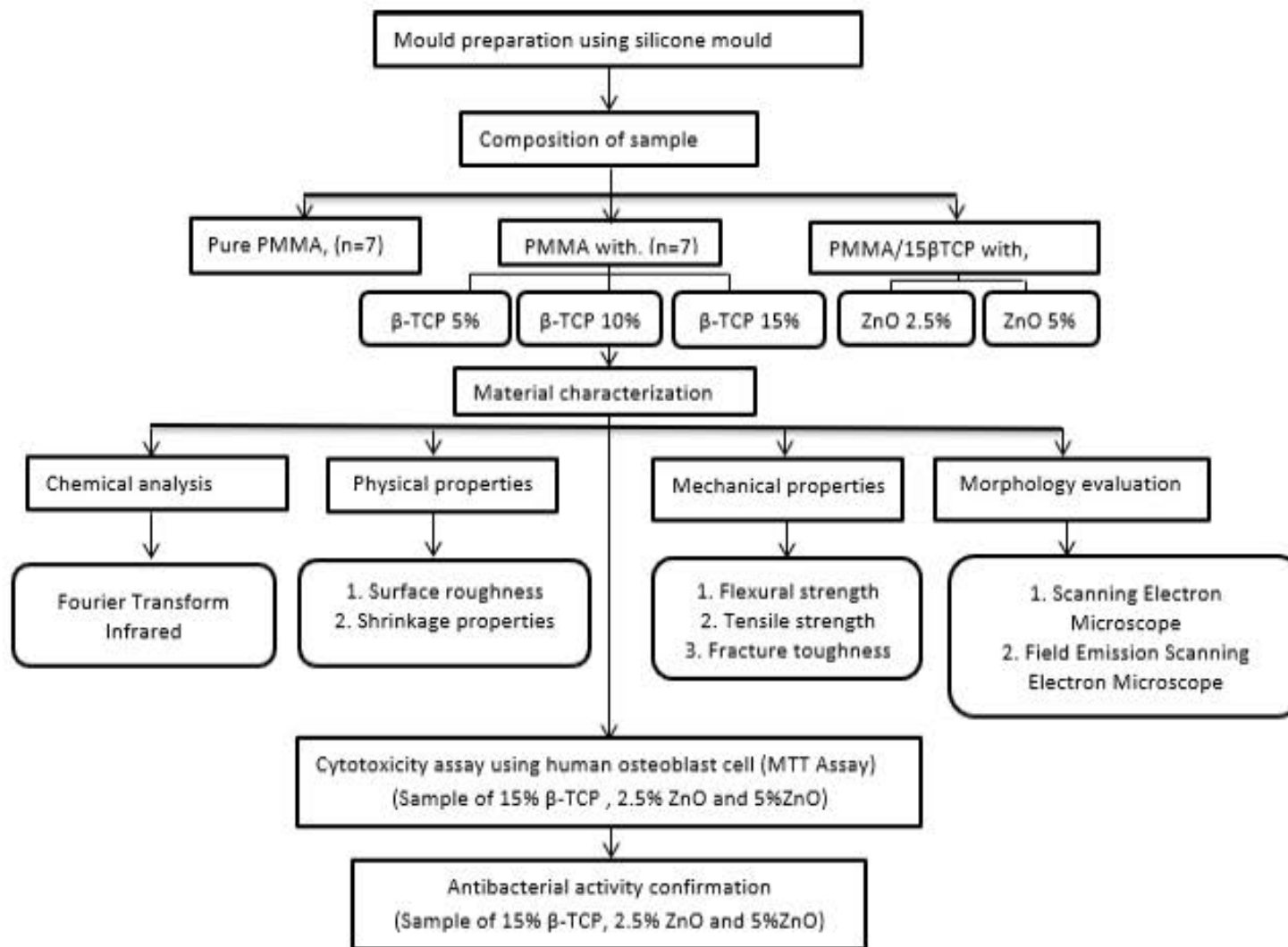


Figure 3.1 Flow chart of study

### 3.2 Sample size calculation

The sample size was calculated using PS software (version 3.80) (Dupont & Plummer Jr, 1998).

For objective 2, to evaluate the physical properties of PMMA composites based on detection of difference of  $0.03\mu\text{m}$  with power of 0.8 and standard deviation of 0.02(Choi *et al.*, 2020), the estimated sample size for surface roughness were 5 sample in a group. For mechanical properties of PMMA composite to evaluate flexural properties of PMMA composite in order to detect the difference of 117.2 MPa with power of 0.8 and standard deviation of 37.80 (Soygun *et al.*, 2013) the estimated sample size were 5 samples in the group. Hence, to anticipate 20% of failure, for all mechanical properties within this study the sample size was used  $n=7$ . For fracture toughness, in order to detect the difference of 6.14MPa, with power of 0.8 and standard deviation of 1.7(Lee *et al.*, 2009), the estimated sample size were 3 samples in a group.

For objective 3, the study of cytotoxicity based on detection difference of 78.2%cell viability with power of 0.8 and standard deviation of 6.44(Yamada *et al.*, 2009) the estimated samples size were 3 for each group. For objective 4, the study of antibacterial activity based on detection difference of growth curve 0.27 % with power of 0.8 and standard deviation of 0.06 (Perni *et al.*, 2015) the estimated samples were 3 for each sample.

### 3.3 Materials

#### 3.3.1 Materials for sample preparation

The PMMA composite fabrication are listed in Table 3.2.

Table 3.2 Materials used for sample preparation

Name	Manufacturer
Beta Tricalcium Phosphate	Sigma Aldrich, USA
Zinc Oxide (ZnO)	Nacalai Tesque, Japan
PMMA (Acrylic vertex Castavaria powder + liquid)	Sigma Aldrich, USA

#### 3.3.2 Calculation for material composition

The weight (g) of each group sample in Table 3.3 below was calculated based on the ratio of 1ml liquid PMMA required for 1.7 g powder MMA.

Table 3.3 Compositions value of each group sample

Types of sample	Weight (%)	Weight (g)
PMMA	100	20:0
PMMA: $\beta$ TCP	95: 5	19:1
	90:10	18:2
	85:15	17:3
PMMA: $\beta$ TCP: ZnO	82.5:15:2.5	16.5:3:0.5
	80:15:5	16:3:1

#### 3.3.3 Chemical and reagents for cell culture

The commercial cell line and reagents used for cytotoxicity study are listed in Table 3.4.

Table 3.4 Cell culture reagents

Name	Manufacturer
Normal Human Osteoblast Cell Line (NHOst)	Lonza, Switzerland
DMEM/Hem'F-12 with L-Gln, Sodium Pyruvate and HEPES with phenol Red	Gibco, USA

$\alpha$ MEM with L-Gln, Ribonucleosides and Deoxyribonucleosides	Gibco, USA
Dimethyl Sulfoxide (DMSO)	Sigma Aldrich, USA
Fetal Bovine Serum (FBS)	Gibco, USA
Phosphate Buffer Saline (PBS)	Sigma Aldrich, USA
Trypan Blue Stain	Gibco, USA
3-(4,5-dimethylthiazolyl-2)-2,5-diphenyltetrazolium bromide (MTT)	Gibco, USA
PenStrep/penicillin streptomycin	Gibco, USA

### 3.3.4 Instrumentations

All the instrument used in this study are listed in Table 3.5.

Instruments	Manufacturer
Autoclave	Hirayama, Japan
Biomedical medcool freezer (-20°C)	Sanyo, Japan
Biosafety cabinet	Lablenco, USA
Carl Zeiss inverted microscopy	Zeiss, Germany
CO <sub>2</sub> incubator IR2424	Shel lab, USA
Field Emission Scanning electron microscope (FESEM)	Quanta FEG 450, Netherland
Fourier Transform Infrared (FTIR)	Bruker, USA
Freezer (-80°C)	Eppendorf, Germany
Microplate reader	Molecular devices, USA
Shimadzu Machine	Instron, USA
Sunrise Elisa Plate Reader	Tecan, Switzerland
Surface Profilometer	Accretech, Japan
Universal 32 R centrifuge	Hettich zentrifugen, Germany
Vortex Genie 2	Scientific industries, USA
Water bath TW8	Julabo, Germany

### 3.3.5 Materials used for antibacterial study

The materials for antibacterial analysis are list in Table 3.6.

Name	Company
<i>Staphylococcus aureus</i>	American Type Culture Collection (ATCC 25923), USA
<i>Pseudomonas aeruginosa</i>	American Type Culture Collection (ATCC 27853), USA
Mueller Hilton Blood Agar	Oxoid Ltd., England
Brain Heart Infusion (BHI)	Oxoid Ltd., England
Colombia Sheep Blood Agar	Oxoid Ltd., England

### 3.4 Fabrication of material

#### 3.4.1 Silicone mold preparation

PMMA composites were created by firstly, PMMA powder was mixed with the appropriate fillers. The liquid monomer was applied to the powder portion and mixed for 20 seconds until the paste was homogeneous. The liquid to powder ratio was 1.7g/1ml, which was in compliance with the manufacturer's recommendations. After that, the paste was poured into the dumbbell and bar shape mold and allowed to harden for 8 minutes. To achieve a flat form of specimen, the mold was first coated with an upper layer of silicone mold, then covered with gypsum green stone as a clamp (Figure 3.2). Finally, the mold was placed in a pressure pot for 30 minutes at 2 bars to complete the polymerisation process. The process was completed when no heat release anymore/cooled down.



Figure 3.2 Silicon mold

### 3.4.2 Polymethylmethacrylate (PMMA) composite preparation

Firstly, the powder of PMMA with ZnO and  $\beta$ -TCP were mixed and measured according to composition specified as shown in Table 3.1. Then, liquid monomer MMA was poured with the mixture in ratio (powder: liquid of 1.7g: 1ml) according to the manufacturer recommendation. They were stirred for 30 seconds until homogenous paste state is ready. Vaseline was applied to the silicone mold before pouring the dough into the mold. The paste was then casted in silicon rubber mold to prepare the PMMA composite sample. Then, the gypsum green stone type III was covered on the silicone mold to make it tight. The paste was put in pressure pot with hot water for 30 minutes (2 bars). The composites already cured. The finish sample was polished in order to get smooth surface. These following steps referred from manufacturer sheet. Figure 3.3 showed the example of sample preparation for flexural testing.

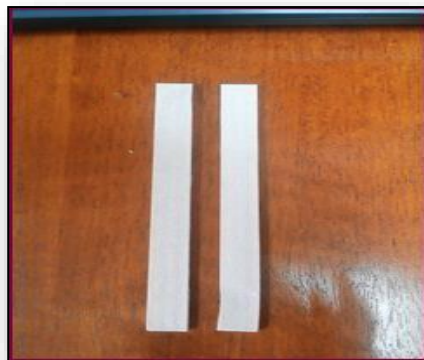


Figure 3.3 Sample of PMMA composites.

### 3.5 Chemical analysis

#### 3.5.1 Fourier Transform Infrared Spectroscopy

FTIR-ATR (Attenuated Total Reflectance) of PMMA composites were performed at School of Health Science, USM using Model Tensor 27 (Bruker, USA) (Figure 3.4) for verification of chemical compounds. All the samples were analysed in the range of  $4000$  to  $500\text{cm}^{-1}$ .

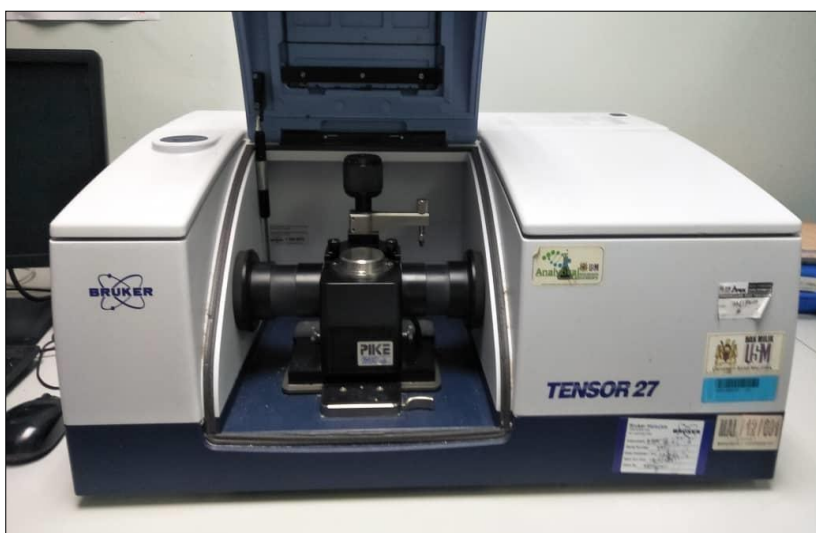


Figure 3.4 Fourier Transform Infrared Spectroscopy



### 3.6 Physical properties evaluation

#### 3.6.1 Surface roughness

Surface roughness was measured by Profilometer using a Mitu-loyo SURFTEST 301, Accretech, Japan as shown in Figure 3.5. All seven samples from each composition were subjected to surface roughness testing. The sample used was taken from flexural specimens. Measured speed was set at 0.3mm/sec.  $R_a$  value taken as an average of three reading. Statistically significant difference in the  $R_a$  values was determined by ANOVA statistical analysis. Differences were considered significant if  $p \leq (0.05)$ .

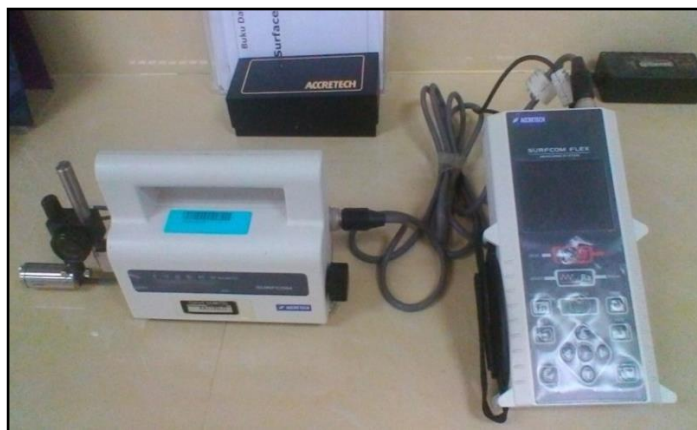


Figure 3.5 Profilometer machine

#### 3.5.2 Shrinkage test

Shrinkage of the composites was calculated according to formula of  $(V_m - V_s)/V_m \times 100\%$  where  $V_m$ = volume mold and  $V_s$ = volume specimen. The calculation was based on measurement of length and width of the samples and also the mold.

### 3.7 Mechanical properties evaluation

#### 3.7.1 Flexural strength

A flexural test was performed to examine the mechanical properties of the prepared samples by using Universal Testing Machine, Shimadzu (USA) (Figure 3.6). The samples were cut into bars of rectangular cross-sections with dimensions of 3.2mm x 12.7mm x 125 mm, as recommended by ASTM 790 (Standard for Thermoplastic). The test was conducted at a cross-head speed of 5 mm/ min at room temperature, and the support length was set to 50 mm. For each sample, seventh specimens (n=7) were tested. The sample size of the specimen for each characterization was determined via PS software. Modulus and flexural strength were calculated from the load versus the displacement curve.

Results were computed using the following standard formulas:

$$\text{Young's modulus, } E = \frac{L^3 M}{4bd^3} \quad \text{Equation 3.1}$$

$$\text{Flexural strength, } S_{\max} = \frac{3PL}{2bd^3} \quad \text{Equation 3.2}$$

Where L is the distance between the supports (m), P is a load at a given point on the load deflection curve. M is the gradient of the initial straight-line portion of the load deflection curve (N/m), b represents the width of the specimen (m), d represents denotes the thickness of the specimens (m).

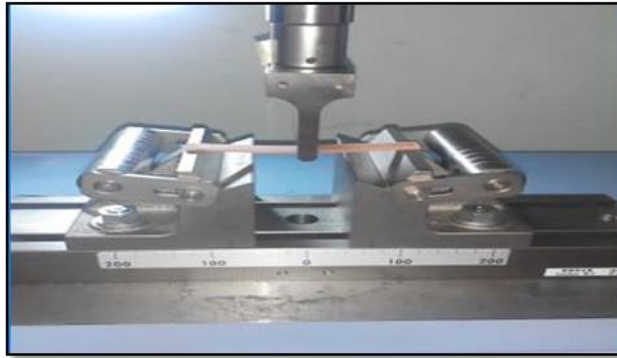


Figure 3.6 Flexural test evaluation

### 3.7.2 Tensile strength

A tensile test was performed to examine the mechanical properties of the prepared samples by utilizing Universal Testing Machine, Shimadzu (USA) as shown in Figure 3.7. The tensile properties of PMMA biomaterial were evaluated according to ASTM D638 (Type IV) with dimension of 3.2mm x 12.7mm x 125 mm. Seven of specimens (n=7) were tested for each sample. Dumbbell-shaped specimens of 50 mm gauge length were tested under crosshead speed of 20 mm/min. The tensile strength, tensile modulus, and elongation at break for each composite were tabulated and analysed.

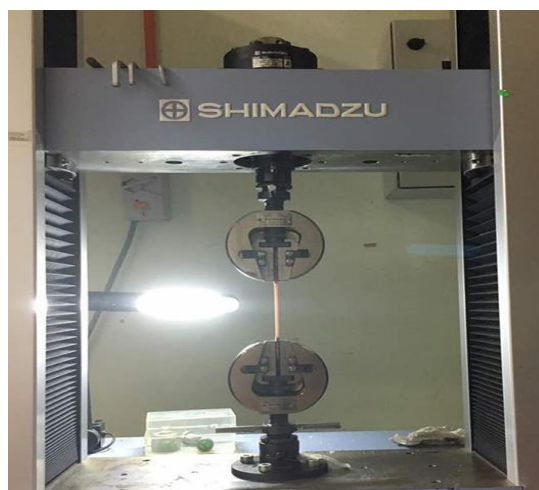


Figure 3.7 Tensile test evaluation

### 3.7.3 Fracture toughness

The single-edge-notched-beam test was carried out using the Universal Testing Machine, Shimadzu (USA) to measure the fracture toughness of the craniofacial implant cement samples. The sample was immersed on simulated body fluid (SBF), for interval time of 0,15, 30, 45 and 60 days. The dimensions of the test specimen were 74 x12.5x 3 mm<sup>3</sup> as recommended by ASTM D5045. Three specimens were prepared for each type of sample. For each specimen, a notch of 5.6 mm in depth was created on one side using a band saw. A support span length of 51 mm was used with a cross-head speed of 1.00 mm/min. The specimens in SBF was taken out for fracture toughness evaluation at 0, 15,30,45, and 60 days. The value of fracture toughness ( $K_{IC}$ ) of each specimen was calculated via equation:

$$K_{IC} = \frac{3PSa^{1/2}y}{2tw^2} \quad \text{Equation 3.3}$$

where  $K_{IC}$  = plain-strain fracture toughness of the test specimen, (MPa m<sup>1/2</sup>), P = the load at peak, S =the support span length, a = the notch length, t = the specimen thickness, w = the specimen width, and y = the geometrical correction factor. Figure 3.8 showed the mold used for fabrication of fracture toughness sample.



Figure 3.8 Mould for fracture toughness sample

### **3.7.3(a) Energy-dispersive X-ray spectroscopy (EDX)**

EDX spectroscopy was performed using FESEM to analyse the chemical composition of the PMMA composite.

## **3.8 Morphology Analysis**

### **3.8.1 Field Emission Scanning Electron Microscope (FESEM)**

The morphology of bacteria at a fracture surfaces of the composites were observed using Zeiss Supra 35VP Field Emission Scanning Electron Microscope (FESEM) as shown in Figure 3.9. All the samples were coated with gold-palladium (Au-Pd) in a sputter coater chamber before analysis. The morphology was observed at magnification between 400x and 20000x with 5 KV accelerating voltage of SEM (Quanta 450 FEG, Fei, Netherland).

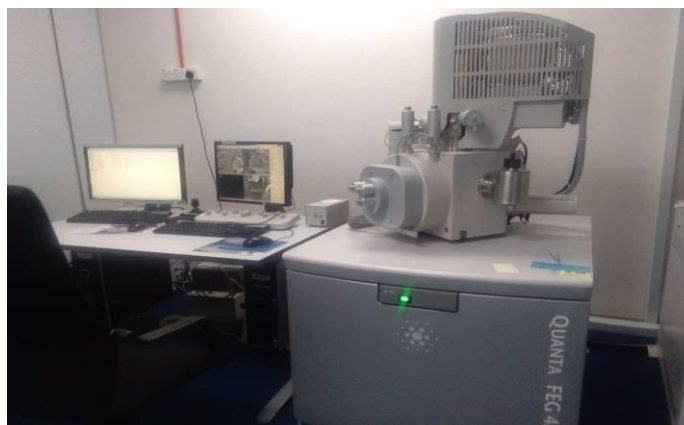


Figure 3.9 Field Emission Scanning Electron Microscopy

There are few general preparations of bacteria for morphology evaluation through scanning electron microscope. Firstly, the bacteria solution with sample was resuspended and the supernatant was discarded and the sample was resuspended with the chemical of Mc dowel trump fixative (40°C) for 2 hours. After that, the sample was

washed with PBS buffer 0.1M 2 times. Secondary fixation was done by using 1% osmium tetroxide for 1 hour, then washing step with distilled water 2 times. Next, the dehydration step was done using acetone 50%, 75% and 95%, 100% about 10 minutes for each percentage 2 times. Proceed with 100% HDMS for 10 minutes repeated two times. After that, the sample was dried air overnight. Next, the sample was mount onto sample stub, the sample was coating with gold before viewing the sample. All centrifuge procedure was set up for 10 minutes for each processing. The setting for the Hettich micro 120 centrifuges is 4560rpm.

### 3.9 Size of samples

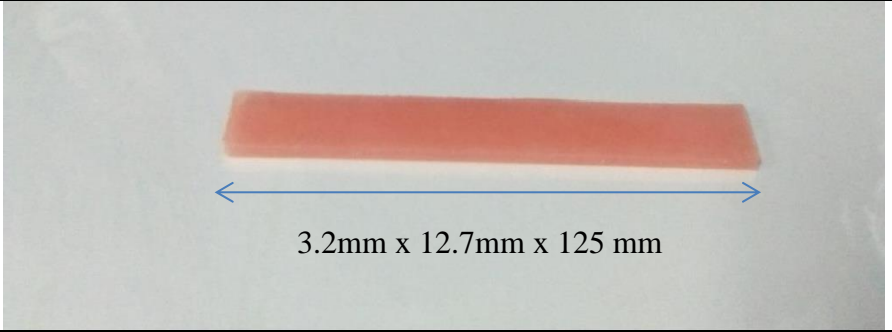
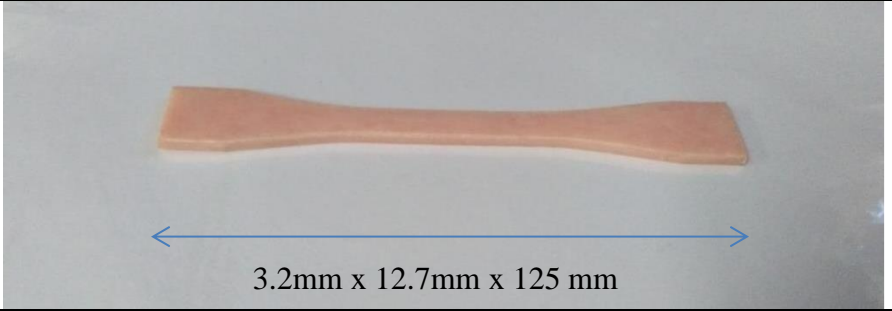
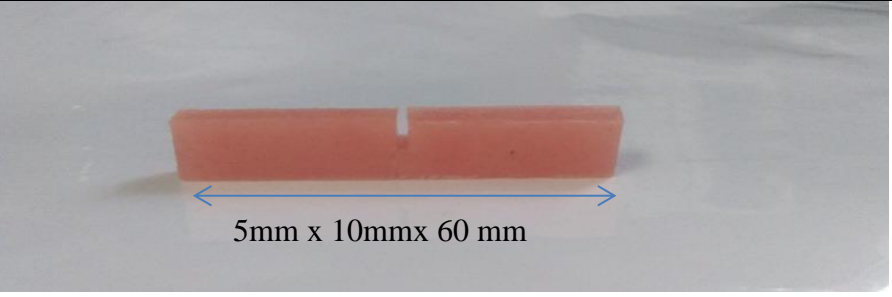
Testing	Specimen size
Flexural strength	 <p>3.2mm x 12.7mm x 125 mm</p>
Tensile strength	 <p>3.2mm x 12.7mm x 125 mm</p>
Fracture toughness	 <p>5mm x 10mm x 60 mm</p>

Figure 3.10 Size of samples

### **3.10 Cytotoxicity test**

Human Fetal osteoblasts cell was chosen as a model for in vitro biocompatibility assay. In vitro testing for cytotoxicity was performed according to ISO 10993. The proliferation of cells on the materials were investigated by in vitro cytotoxicity test using MTT assay.

#### **3.10.1 Aseptic technique**

Aseptic technique is important to prevent the cell cultures from contamination. Hence, it is important to make sure proper aseptic technique applied when performing cell culture. All experiments which involved cell culture was performed in biosafety cabinet class II (Delta series, Lab Conco, USA).

#### **3.10.2 Complete media preparation**

Complete media for hFOB culture was prepared by adding 10% FBS (50 ml) and 10% penicillin/streptomycin (5ml) into 445 ml of Dulbecco's Modified Eagle Medium (DMEM) media. The sterile complete media was then stirred to make it homogeneous and ready to be used or stored at 4°C.

#### **3.10.3 Culturing of hFOB cell line**

Human fetal osteoblast cell (hFOB) obtained from Lonza, in a standard CO<sub>2</sub> incubator at 37°C. The cells from passages 5 to 10 were used in this study. The cells were thawed in warm water in a 37°C water bath right away. The produced complete media was also thawed in a 37°C water bath at the same time. Once the cells reconstituted, the cells were transferred into the 15ml centrifuge tube 5ml of complete

media to the cell suspension. After that, the suspension was centrifuged at 800 x g for 5 minutes. The supernatant was discarded and the pellet was dissolved with 1 ml of complete medium. The cells were suspended several times to get homogeneous before cell counting performed. Then, the cell suspension was transferred into 25ml<sup>2</sup> culture flask. The culture flask was then put in incubator with 5% CO<sub>2</sub> at 37°C. The media was changed every 3 days.

#### **3.10.4 Cell maintaining**

Using inverted phase contrast microscope (Nikon, Japan), the morphology of cells was observed. After several days of incubation, the structure of cells could be seen clearly. When observing the cells, the condition in medium should be examine properly to make sure it is free from contaminants which may cause deterioration to the cells. Once the cells become confluent, sub-culture process will be performed. To perform sub-culture, the medium in culture flask must be removed and replaced by 1 ml of buffer saline solution, swirled and discard. This method was repeated 3 times to confirm elimination of unwanted particles from the flask. Following washing, 2ml of trypsin/EDTA was added into the flask to tyrosinase the cells from the flask's surface. Then, the flask was transferred into the incubator for 4 minutes at 37°C. This step was performed to ensure the detachment of cells before adding the neutralizing solution. Then, the cells suspension was resuspended and rinsed to ensure all cells were detached from the flask. Then, the cells were transferred into a 15ml centrifuge tube to obtain cell pellet. Following centrifugation, 1ml of complete media was then added to the pellet, resuspended before cell counting performed. Finally, the calculated cells were transferred to 25 cm<sup>2</sup> culture flask for culturing process.



### 3.10.5 Counting cell and subculture process

Trypan blue stain was used for cell counting procedure. Using parafilm, trypan blue stain (10µl) was pipetted on the film. After resuspending the cells, 10 ul of cells were pipetted and mixed with the Trypan blue stain solution. Then, the stained cells were transferred onto hemocytometer by touching the surface of coverslip with the pipette tip. Once transferred, the hemocytometer was observed under inverted phase contrast microscope. A grid of 9 square was seen at magnification of 100x using only 4 parts, which were A, B, C and D calculated as showed in figure below. The cells stained in blue were indicated as dead cells. The colorless cells indicated as live cells and counted under the inverted microscope.

The concentration of cells was calculated by using the formula below:

$$C = A \times 2^* \times 10^2 \quad [4]$$

Where: C= cell concentration

A=average of counted cells

2\*=dilution factor

The required number of culture flask was based on calculation below:

$$\text{Number of culture flask} = \frac{\text{cell concentration}}{\text{total density} \times \text{area of the culture flask}} \quad [5]$$

Two types of culture flask used were 25cm<sup>2</sup> and 75cm<sup>2</sup>.

The density for hFOB cell is 3500 cells/cm.

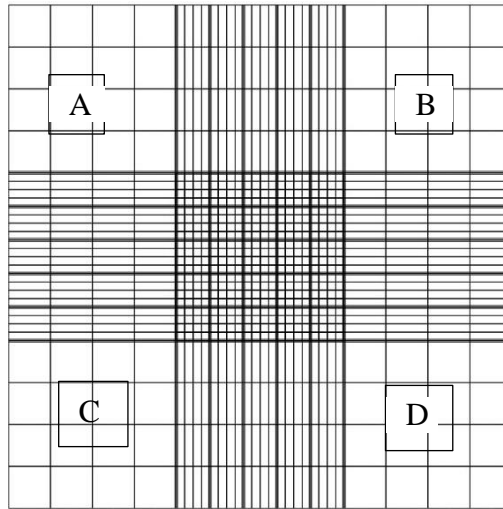


Figure 3.11 Hemacytometer grid. A, B, C and D were counted areas.

### 3.10.6 Cryopreservation of cells

The cryopreservation of cells is performed to make cell stock for future analyses. To preserve the cells, the harvested cells were mixed with complete medium and resuspend in 15 ml of centrifuge tube. Then, the cells suspension was transferred into cryovial and slowly added with 10% or 250  $\mu$ l dimethyl sulfoxide (DMSO). The total volume of cryopreserved cells was 1 ml. To keeps it safe, the cells were firstly refrigerated at  $-4^{\circ}\text{C}$  for 30 minutes then frozen at  $-20^{\circ}\text{C}$  for 1 hour. After that, second frozen was done at  $-80^{\circ}\text{C}$  for overnight and lastly at  $-196^{\circ}\text{C}$  in liquid nitrogen.

### 3.10.7 MTT assay

3-(4, 5-dimethylthiazoyl)-2-5 diphenyl-tetrazolium bromide), MTT assay is used to evaluate the toxic characteristics of a material or substance. In this study, yellow tetrazolium salt (MTT) is reduced in metabolically active cells to form insoluble purple Formazan crystals which are solubilized by the addition of a solvent (dimethyl

sulfoxide). Cell viability is quantified by colorimetric enumeration whereby a low OD reading corresponds to low cell viability associated with a loss in mitochondrial dehydrogenase activity. The MTT solution was prepared by dissolving 5g of MTT powder in 1 ml of PBS, and then filtering 100µl onto 96 wells. The suspension solution was left for four hours. After that, the solution was discarded and DMSO was added 100µl ELISA reader was utilized to calculate the result.

### **3.10.8 Material extract preparation of composites.**

The PMMA composites sample from each group measured about 0.3g (300mg) were sterilized in an autoclave at 120°C for 20 minutes and three replicates were tested for each sample, n=3. After sterilization, the samples were immersed in DMEM medium for 72 hours at 37°C. According to ISO standard the ratio between the sample weight and the volume of extracts solution was 100 mg/ml. The dilution of the stock solution was then prepared 100mg/ml, 50 mg/ml, 25 mg/ml, 12.5 mg/ml and 6.25mg/ml.

### **3.11 Antibacterial assays of *S.aureus* and *P.aeruginosa***

Two common bacteria were chosen: Gram-positive *S. aureus* (ATCC 25923) and Gram-negative *P. aeruginosa* (ATCC 27853) (Figure 3.12). In order to preserve the sterility of the environment and prevent contamination, proper handling of bacteria culture and treatment were performed in a biosafety cabinet class II (Heraeus, German).

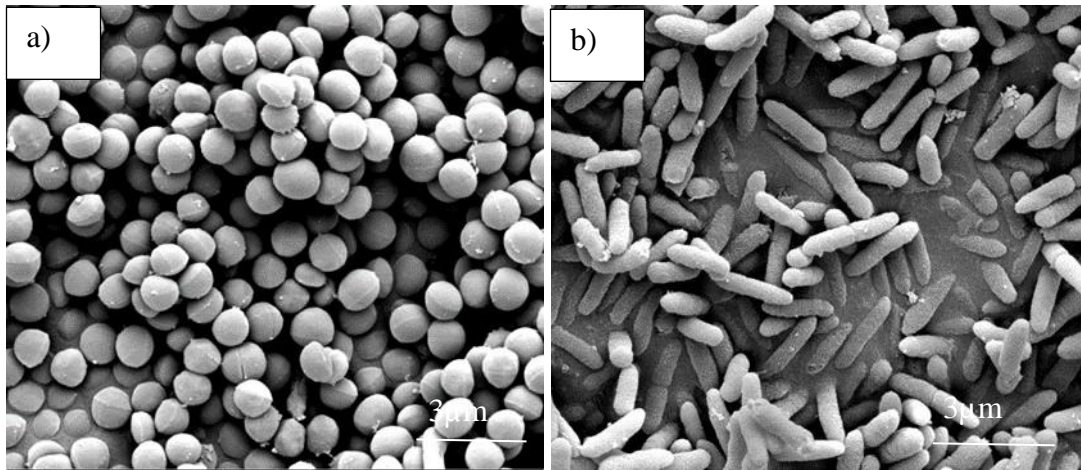


Figure 3.12 SEM image of a) *Staphylococcus aureus* and b) *Pseudomonas aeruginosa* at magnification of 30000x.

### 3.11.1 Preparation of the culture media

In this study, the media used for culturing were Mueller Hilton blood agar, Colombia sheep blood agar and brain heart infusion broth which both are commercially brought from Oxoid Ltd., England.

#### 3.11.1(a) Preparation of brain heart infusion broth

To prepare BHI broth, 18.5gm of BHI was dissolved in 500ml of distilled water in a sterile Scotts bottle. After that, the suspension was stirred to dissolve the medium and autoclaved at 121°C for 15 minutes.

#### 3.11.1(b) Preparation of McFarland standard solution

The standard method to estimate density of microorganism is by using McFarland standard. McFarland Standards are used to standardize the approximate number of bacteria in a liquid suspension by comparing the turbidity of the test suspension with that of McFarland Standard. The standard most commonly used in clinical microbiology laboratory is the 0.5 McFarland Standard, which is prescribed for

antimicrobial susceptibility testing. McFarland value was measured using McFarland Densitometer.

### 3.11.2 Agar diffusion test

The method was carried out to investigate the antibacterial activity of PMMA composites against *S. aureus* and *P. aeruginosa*. The bacterial suspension was made, adjusted to 0.5 McFarland ( $1.0 \times 10^8$  CFU/ml) and diluted to 1:150 ( $1.0 \times 10^6$  CFU/ml), followed by seeding on an agar plate. The 8 mm diameter wells were created aseptically with a sterile cork borer. The PMMA composite samples were then placed in the wells. The bacterial inhibition zone was measured after 24 hours using a digital caliper. The experiments were done in triplicates. PMMA pure serves as a negative control, whereas chlorhexidine serves as a positive control. The illustration is depicted in Figure 3.13.

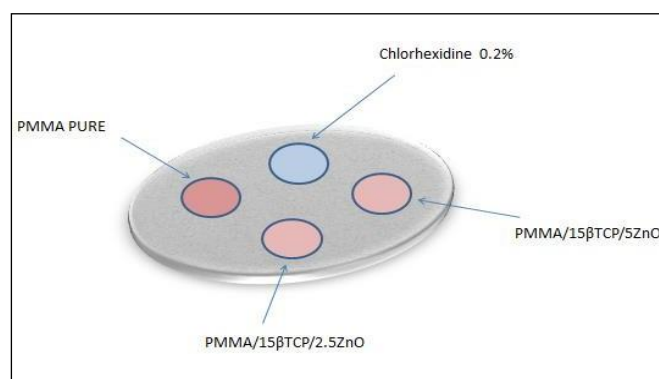


Figure 3.13 Illustration of sample treatment in agar plate for inhibition zone determination

### 3.11.3 Bacterial Kinetic Growth of *S. aureus* and *P. aeruginosa*

For the kinetic growth, the material extracts were prepared as described in Section 3.10.8. The bacteria culture was prepared by transferring a colony of bacteria using a wire loop into the BHI broth and incubated at 37°C overnight. The bacteria were then cultured on an agar plate. A bacteria suspension of 0.5 McFarland was prepared

and added into the extraction solution. A kinetic growth test was then performed after 24 hours. The data was then measured hourly at an OD of 570–600 nm wavelength. The growth curve was plotted for up to 12 hours.

#### **3.11.4 SEM analysis of *S. aureus* and *P. aeruginosa* on materials**

The bacteria suspensions were prepared by adding 14.9ml BHI and 100 $\mu$ l 0.5McFarland bacterial suspension. Then, 3 ml of the mixture was added to each sample to achieve a concentration of 50 mg/ml, as used in the cell culture procedure. The solution was then stored at 4°C overnight for 12 hours before being examined under a SEM. The SEM analysis was carried out similar as described in section 3.8.1.

#### **3.12 Statistical analysis**

The data obtained were analyzed using SPSS software, version 24.0. The observation of normality and homogeneity test were initially performed and confirmed. The data were statistically evaluated by parametric test of one-way analysis of variance (ANOVA) and post hoc Tukey's multiple comparison test at 95% confidence interval to analyse physical and mechanical properties. Meanwhile, non-parametric test of Kruskal-Walis were performed to assess the differences in biological performance of composites. The significant difference ( $p > 0.05$ ) was observed between group means.

## CHAPTER 4

### RESULTS AND DISCUSSION

#### 4.1 Morphology and size of fillers

ZnO particles were in nanosize of less than 260nm, whereas  $\beta$ -TCP particles were in 1-5  $\mu\text{m}$  sizes. Figure 4.1 depicts the microstructure of ZnO and  $\beta$ -TCP at a magnification of 20000x.

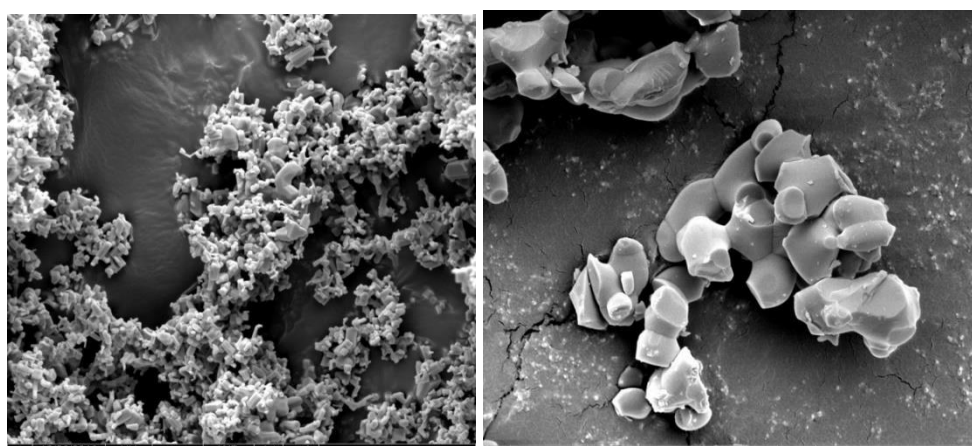


Figure 4.1 FESEM microstructure of a) Zinc oxide particles and b)  $\beta$ -TCP particles at 20000x magnification.

#### 4.2 FTIR analysis (Fourier Transmission Infrared)

The FTIR spectra of zinc oxide, pure  $\beta$ -TCP, pure PMMA and PMMA /  $\beta$ -TCP /ZnO samples are shown in Figure 4.2. Spectrum of ZnO was seen in the range of 400 to 480  $\text{cm}^{-1}$ . From studied by Yadav & Kumar (2020), supported that the peaks in the range of 490–550  $\text{cm}^{-1}$  indicated the presence of metal oxide stretching vibration, which was belonged to ZnO stretching vibration. Pulit-Prociak *et al.* (2016) observed that at wavelength of 500 $\text{cm}^{-1}$ , ZnO bond occurred. There is also a peak around 3300  $\text{cm}^{-1}$  indicating that the stretching vibration band of the OH groups existed in water molecules (Pulit-Prociak *et al.*, 2016). Wavelength of 1383 $\text{cm}^{-1}$  represents O-H alcohol

group associated with original functionality of PMMA. C-H stretching was observed at  $2991\text{ cm}^{-1}$  as agreement with study of Ramesh *et al.* (2007). The characteristic bands for PMMA was observed at 2993, 1730, and  $1420\text{ cm}^{-1}$ . For pure PMMA, absorption bands were seen at 2993, 1730, and  $1420\text{ cm}^{-1}$  as the value near to the result obtained from studied by Chatterjee *et al.* (2010). The existence peak of  $2850\text{ to }2950\text{ cm}^{-1}$  owing to transition between unsaturated alkenes to saturated alkene as polymerization of MMA to PMMA occurred (Ayre *et al.*, 2014). The band at  $2995\text{ cm}^{-1}$  could be allocated to the stretching vibration of  $\beta\text{-TCP-OH}$  where O-H formed by the C=O of PMMA. The addition of  $\beta\text{-TCP}$  in PMMA did not change the functional characteristics of the composite as no new absorption bands were observed. This was due to PMMA and  $\beta\text{-TCP}$  were physically mixed, thereby, no changes detected in the chemical structures of the composites. Additionally, the peak of  $2162\text{ cm}^{-1}$  in PMMA composites with 5% $\beta\text{-TCP}$  was not clear due to the low concentration of  $\beta\text{-TCP}$ . The characterisation of C-O-C and C-O stretching vibration is at the peak from PMMA at 1014, 1116, and  $1722\text{ cm}^{-1}$ . A similar phenomenon was observed from studied of Chakraborty *et al.* (2013). Peak in range  $1260\text{-}1040\text{ cm}^{-1}$  indicate C-O-C single bond.  $\text{CH}_3$  band at  $1441\text{ cm}^{-1}$  and  $\text{CH}_3$  asymmetric stretching band at  $2953\text{ cm}^{-1}$ . The introduction of  $\beta\text{-TCP}$  is confirmed by appearance characteristic vibration band at  $603\text{ cm}^{-1}$ . However, unclear peak of  $\beta\text{-TCP}$  at  $1000\text{ cm}^{-1}$  was detected in PMMA resin and PMMA composites probably due to the low concentration of microparticles. The characteristics of  $1722\text{ cm}^{-1}$  in spectrum of PMMA is attributed to C=O stretchy vibration of acrylate carboxyl group (Chew and Tan, 2011). Once the  $\beta\text{-TCP}$  added to PMMA the bonding of at  $2147\text{ cm}^{-1}$  peak was disappear and shifted to  $2359\text{ cm}^{-1}$ .  $\beta\text{-TCP}$  at  $1014\text{ cm}^{-1}$  for  $\text{PO}_4^{3-}$  ions was shifted to  $1386\text{ cm}^{-1}$  in PMMA/ $\beta\text{-TCP}$  blend. The introduction of 10% and 15% of fillers at a peak of  $2842\text{ to }2924\text{ cm}^{-1}$  start to intensify. However, the peak at this wavelength was not



clearly intensifying once amount of filler up to 15%. Table 4.1 summarize the wavelength existed for compound appeared in FTIR.

Table 4.1 FTIR for PMMA composites

Description of vibration	Wavelength( $\text{cm}^{-1}$ )
$\text{CH}_3$	1446
CH stretching	2951
$\text{PO}_4^{3-}$	603-722, 1014-1116
C=O	1238, 1722-1733
C-H <sub>2</sub> asymmetric stretch mode	2842-2942
O-H	1383

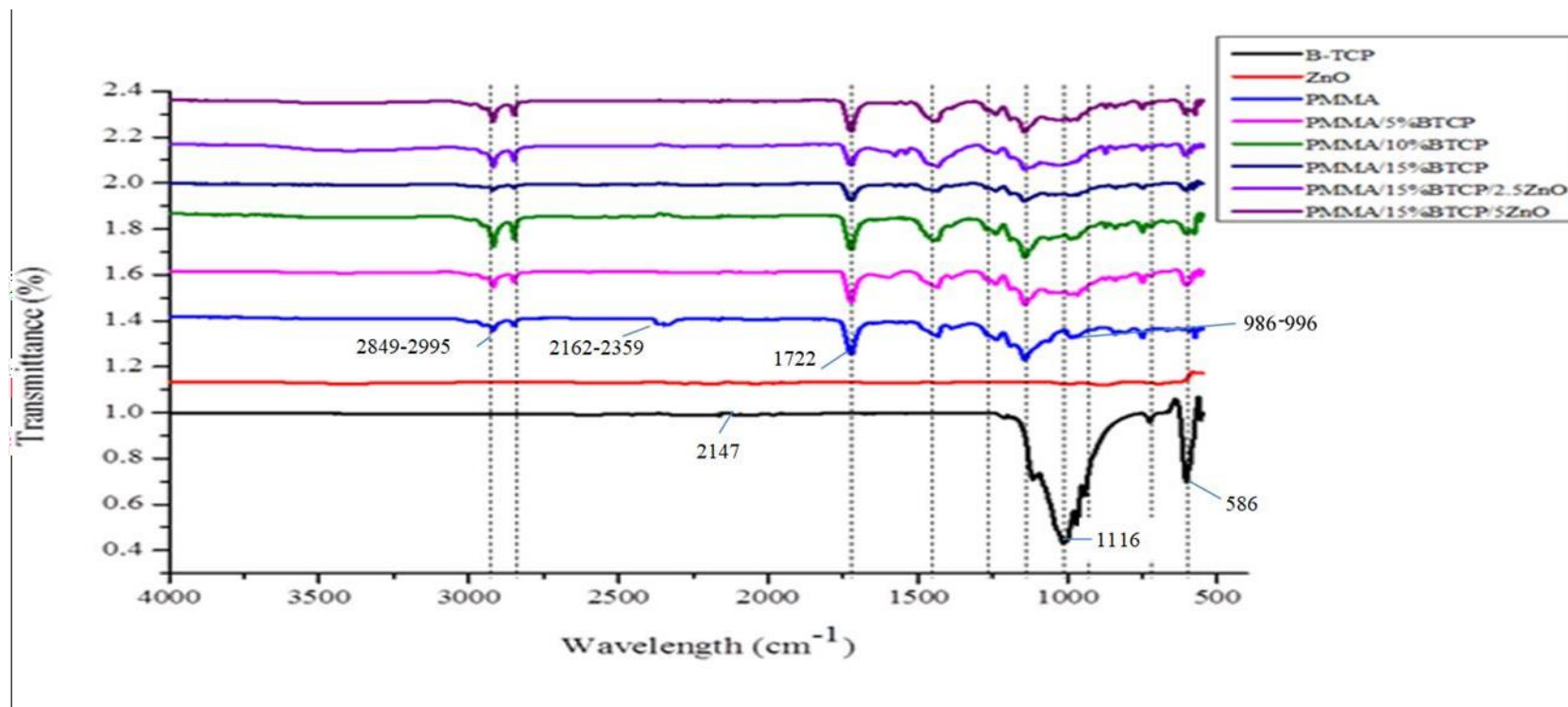


Figure 4.2 FTIR spectra for PMMA composites

### 4.3 Surface roughness

From Table 4.2, the surface roughness was reduced after addition of fillers to the polymer matrix.

Table 4.2 Surface roughness value for PMMA composites

Sample	Surface roughness ( $\mu\text{m}$ )
Pure PMMA	2.45(0.30) <sup>b</sup>
PMMA /5% $\beta$ -TCP	1.83(0.33) <sup>a</sup>
PMMA/ 10% $\beta$ -TCP	1.94(0.48) <sup>a</sup>
PMMA /15% $\beta$ -TCP	1.64(0.29) <sup>a</sup>
PMMA/15% $\beta$ -TCP/2.5%ZnO	1.47(0.27) <sup>a</sup>
PMMA/15% $\beta$ -TCP/5%ZnO	1.56(0.17) <sup>a</sup>

*Mean values and standard deviation in parentheses. Different small letters in the same column are statistically significant according to pairwise comparison test for surface roughness.*

$\beta$ -TCP filler occupied the vacant space between polymer molecules, resulted in a lower surface roughness (1.64  $\mu\text{m}$ ) for 15% loading. Remaining vacant space between polymer molecules was later filled by the addition of 2.5% ZnO, which led to a decrease in surface roughness value (1.47  $\mu\text{m}$ ). However, 5% ZnO addition led to an increase in surface roughness (1.56  $\mu\text{m}$ ). It was possibly due to ZnO aggregation, which formed a cluster of ZnO. It should be noted that more than 4% ZnO loading was reported to induce an aggregation of ZnO particles (Wacharawichanant, 2010).

On microbial adhesion versus surface roughness, pure PMMA has higher value in surface roughness (2.453 $\mu\text{m}$ ) which is near to 2.2 $\mu\text{m}$ , a value found colonization of bacteria easy to attach. (Vojdani *et al.*, 2012). An overall reduction in surface roughness of composites could possibly lead to a lower risk of microbial colonisation (Santos *et al.*, 2013). The result of studied from Lu *et al.*, (2009) found that with an increase in surface roughness, the number of adherent bacteria increase too. With that, incorporation of filler gives advantages in term of reducing infection after implantation.

In contrast, high surface roughness is preferable for cell attachment. The development of osteoblast proliferation seems to be aided by rough surfaces (Meretoja *et al.*, 2010). Therefore, an optimisation of surface roughness needs to be defined in order to prevent microbial colonisation and at the same time provide a conducive topography for cell attachment. In statistical analysis showed that there were significant differences between PMMA composites and pure PMMA. However, no significant differences in surface roughness value among PMMA composites. It is clearly stated that the surface roughness was significantly improved with the addition of both fillers. Marghalani, (2010) expressed that the smoothness of surface in many composites depending on their filler components including type of inorganic particles, size of filler and extent of filler loading. They also mentioned that the higher surface roughness attributed to the larger filler particles because they tended to protrude from the surface resulted in high surface roughness. The spherical particles seem to deboned easily in the matrix rather than irregular fillers. Similar to the result in Table 4.2 showed that with the addition of  $\beta$ -TCP fillers, the value of surface roughness tends to be higher than PMMA with addition of zinc oxide due to the size of  $\beta$ -TCP which is in micron size whereas zinc oxide is in nano size.

In this application, the lowest of surface roughness value is needed and this study accomplish to produce the PMMA composites with this lower value of surface roughness. Shalabi *et al.* (2006) stated that optimal surface for bone integration is between  $R_a$  value of 1 and  $1.5\mu\text{m}$ . It was proved that the surface roughness value of the fabricated PMMA composites with the addition of zinc oxide is suitable to bone implantation.

In addition, Jiao *et al.*, (2015) found in study that  $R_a$  value below than  $0.75\mu\text{m}$  was assumed as a smooth surface correspond to study the  $R_a$  achieve from PMMA

containing N-acetyl cysteine(NAC) 0.15% was 0.6 $\mu$ m. Moreover, this value was near the surface roughness threshold which is 0.2  $\mu$ m which could minimize accumulation of plaque (Busscher *et al.*, 1984)(Quirynen *et al.*, 1990). There are two parameters that affect the deposition of microorganisms on surface of PMMA such as the roughness and the nature of hydrophobic and hydrophilic of the surface. The property of biofilm is reduced with the increase of hydrophilic nature of surface (Ciarech *et al.*, 2019).

#### 4.4 Shrinkage properties

From the Table 4.3, the shrinkage percentage is reduced with the addition of fillers of  $\beta$ -TCP. However, it increased once ZnO was added to the composites but still lower from pure PMMA. There is significant difference only between pure PMMA and developed composites of PMMA/15% $\beta$ -TCP/5%ZnO in shrinkage percentages value.

Table 4.3 Shrinkage value of pure PMMA and developed composites

Samples	Shrinkage percentage (%)
Pure PMMA	8.29 (3.81) <sup>a</sup>
PMMA+ 5% $\beta$ -TCP	7.55 (1.47) <sup>ab</sup>
PMMA+10% $\beta$ -TCP	6.63 (1.89) <sup>ab</sup>
PMMA +15% $\beta$ -TCP	5.51 (0.74) <sup>ab</sup>
PMMA+ $\beta$ -TCP 15%+ZnO 2.5%	6.09 (1.23) <sup>ab</sup>
PMMA+ $\beta$ -TCP 15%+ZnO 5%	4.80 (0.55) <sup>b</sup>

*Mean values and standard deviation in parentheses. Different small letters a and b in the same column are statistically significant according to pairwise comparison test for shrinkage.*

Polymerisation shrinkage happen when the contraction and expansion started. It started immediately upon initiation of the polymerisation and continues along with the curing. Conversion of van de Waals distances to covalent bond will result to contraction effect. In addition, after polymerisation, thermal expansion and conversion of double bond to single bond occurred as a result of expansion effect. This is due to the bonding of van der Waals strengthen the compound bond, thus reduce void and shrinkage value

is low. Other than that, shrinkage of polymer occurred when there is an internal rearrangement of the structural elements within stretched sample (Pefferkorn, 2012).

Polymerisation shrinkage could lead to poor tissue/cement interaction. The weak bond between tissue and the cement interface provides a barrier to direct fracture healing (Dalby *et al.*, 2002). It also showed that the lowest value of the shrinkage percentages is at higher filler loading, which is for sample PMMA/15% $\beta$ -TCP/5%ZnO. In agreement with Lai (1993), the study found that with a high molecular weight monomer and high filler loading, the polymer will exhibit less shrinkage. Besides, Pefferkorn (2012), stated that with the incorporation of organic and inorganic fillers into the polymer composite, polymerisation contraction will be reduced. Similarly, Marghalani (2010) also stated that the incorporation of nano fill resin could reduce polymerisation shrinkage.

This study focused on volumetric shrinkage to calculate the shrinkage properties. Agreement with study from Baroudi *et al.*, (2007), mentioned that temperature is one of the factors influence the shrinkage value. The shrinkage strain increased when the temperature increase up to 37°C due to increasing of network conversion of resin monomer. Gilbert *et al.*, (2000), mentioned that density change is one of the factors that prone to shrinkage phenomenon. It is a result of changing from lower density of liquid monomer to higher density of polymer form. Figure 4.3 below showed the phenomenon of shrinkage occurred.

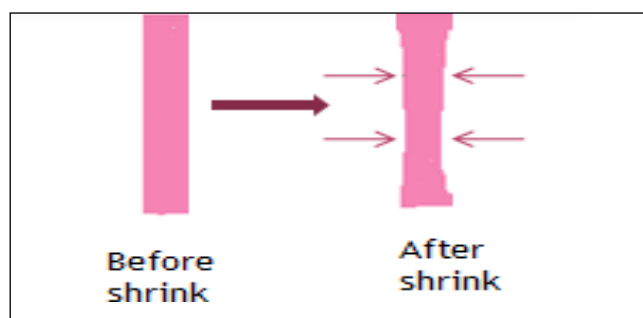


Figure 4.3 Shrinkage phenomenon

#### 4.5 Flexural properties

The value of flexural strength of pure PMMA and PMMA composites are summarised in Table 4.4. The flexural strength of PMMA composites was lower as compared to pure PMMA. The flexural strength between the PMMA composites showed no significant differences. Incorporation of fillers has reduced the flexural strength of the composites.

Table 4.4 Flexural strength value of each sample

Sample Name	Flexural strength (MPa)
Pure PMMA	60.79(8.00) <sup>b</sup>
PMMA + 5% $\beta$ -TCP	40.49(6.67) <sup>a</sup>
PMMA +10% $\beta$ -TCP	45.77(9.99) <sup>a</sup>
PMMA +15% $\beta$ -TCP	46.74(7.29) <sup>a</sup>
PMMA +15% $\beta$ -TCP+2.5%ZnO	38.72(6.69) <sup>a</sup>
PMMA +15% $\beta$ -TCP +5%ZnO	41.49(9.30) <sup>a</sup>

*Mean values and standard deviation in parentheses. Different small letters a and b in the same column are statistically different according to Post hoc Tukey test  $p < (0.05)$ .*

Significant reduction in flexural properties of the composites were possibly due to the stress concentration owing by filler agglomeration, void formation as well as air entrapment during mixing process (Wacharawichanant, 2010). The addition of fillers interrupted the arrangement of polymer molecules, hence reduced the ability of the composites to withstand the given load which resulted to a reduction in flexural strength. In addition, other researchers found that the incorporation of calcium phosphate based materials such as hydroxyapatite (HA) for 10% to 15% were found to

decrease the mechanical strength of PMMA composites due to the deficiency of interfacial bonding between fillers and polymer matrix (Kul *et al.*, 2016),(Abdullah, 2015). The flexural strength of PMMA/15% $\beta$ -TCP/5%ZnO was higher than PMMA/15% $\beta$ -TCP/2.5%ZnO due to particles of zinc oxide filled the space in matrix hence reduced void content and revealed a better mechanical strength as shown in Figure 4.4. It is a fact that the presence of void in composites affected the original structure of the polymer matrix resulted to a lower mechanical property. The results showed that flexural strength was decreased by the incorporation of  $\beta$ -TCP. This may be due to the agglomeration of  $\beta$ -TCP particles in PMMA matrix. Also, the trend could be related to incompatibility between PMMA and  $\beta$ -TCP (Chow *et al.*, 2008).

The presence of matrix particle interfacial defects also was the reasons to the decreasing of flexural strength (Chow *et al.*, 2008)(Pereira *et al.*, 2003). Alhareb and Ahmad, (2011) found that the value of PMMA flexural and modulus were 88.1 MPa and 2GPa respectively. Flexural modulus was increased when added  $\text{AlO}_3/\text{ZrO}_2$  fillers. It was concluded that different ratio of these fillers affected the flexural strength and flexural modulus of the composites. The microstructure of the specimen after load force has been applied could be observed in Figure 4.4.

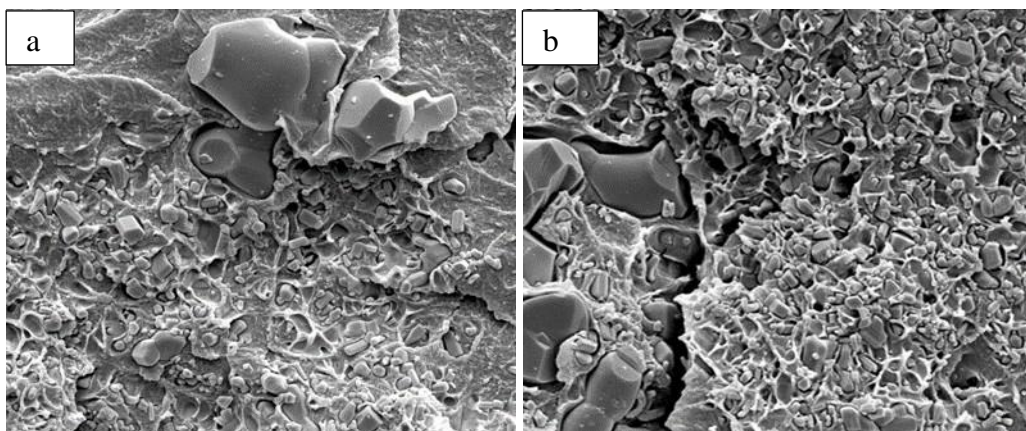




Figure 4.4 Microstructure of a) PMMA/ $\beta$ -TCP 2.5%ZnO and b) PMMA/ $\beta$ -TCP 5%ZnO.

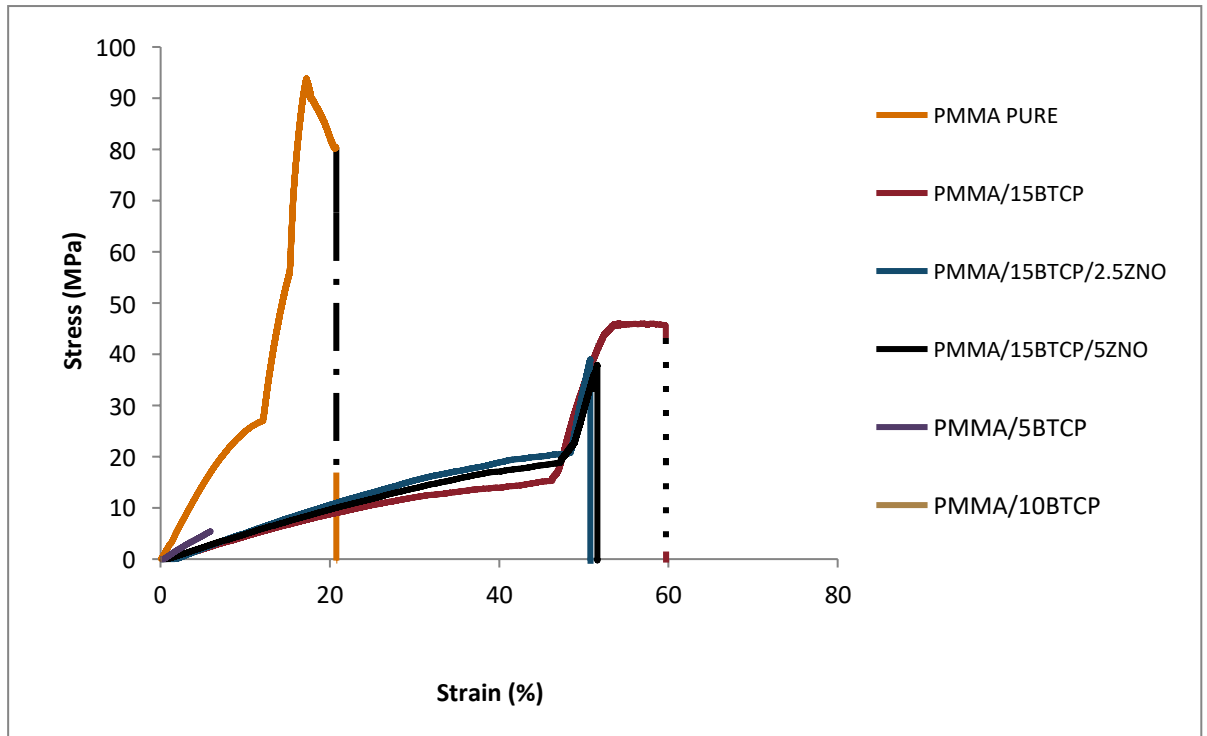


Figure 4.5 Stress strain curve for pure PMMA and PMMA composites

Figure 4.5 showed the stress strain behaviour of pure PMMA and PMMA composites. The pure PMMA showed a brittle behaviour. As opposed to the pure PMMA, the composites showed a ductile behaviour with an incorporation of  $\beta$ -TCP. After incorporation of ZnO, the percentage of strain has reduced sufficiently. PMMA specimen behaves in a ductile manner (strain hardening), whereas the material shows a brittle failure (strain softening) at high strain rate. There were significant reduction in flexural strength of the composites with the addition of zinc oxide as compared to pure PMMA. Gao *et al.*, (2019) support the result of PMMA above cements were stronger than  $\beta$ -TCP PMMA composite cement. Moreover, PMMA was hydrophobic and  $\beta$ -TCP

is hydrophilic because of that features, PMMA has a poor compatibility with  $\beta$ -TCP. Once mixing together, they will not be mixed homogeneously hence resulted to non-uniform morphology and become brittle.

Figure 4.5 plot the corresponding values of stress and strain. Elastic modulus achieved from the slope of the stress strain curve in the straight-line portion. The elastic modulus could measure the stiffness of the material. The flexural value is low due to the presence of voids or porosities that could contribute to the micro cracks formation (Qasim *et al.*, 2012). Degree of conversion also affected to the value of flexural strength. For instance, the degree of conversion could be increased from the attribution of curing for both sides for denture application. Similar to studied from Tham *et al.* (2011), confirm that the presence of HA improved the modulus but reduced the strength. Among the incorporated fillers, the flexural strength of PMMA/15% $\beta$ -TCP is the highest compared to 5% and 10% of  $\beta$ -TCP. Therefore, it is chosen for the next composition incorporated with ZnO.

#### **4.6 Tensile properties**

The value of tensile strength of pure PMMA and PMMA composites are summarized in Table 4.5. The tensile strength of PMMA composites was lower as compared to pure PMMA. The tensile strength between the PMMA composites showed no significant differences. Baroudi *et al.*, 2007 said that tensile properties are very crucial for bone cement due to the effect of stabilisation of the implant in the bone bed. Pure PMMA has a highest tensile strength value as shown in Table 4.5. The addition of filler  $\beta$ -TCP to the composite revealed the reduction of the tensile strength value. However, incorporation of 2.5% ZnO increased the value of tensile strength but reducing the strength after addition of 5% ZnO. The increment of tensile strength value

for addition of 2.5% ZnO is due to the better uniform dispersion of zinc oxide particle and strong interfacial interaction in the polymer matrix. For the higher loading of 5% ZnO, the value of tensile strength could reduce due to the agglomeration of ZnO particles and non-uniform distribution consequence. This will result in a weak point there, lowering the tensile strength (Poddar *et al.*, 2016).

When there is interfacial contact in the polymer matrix, a defect will form because the tensile strength value will be reduced due to the higher loading of particles. Besides that, cracks will propagate due to the stress field around the aggregation of ZnO, which will cause failure and reveal to lower value of tensile strength. The reduction of tensile strength with addition of zinc oxide could be explained from the features of ZnO itself. ZnO is hydrophilic in nature and the interfacial bonding of ZnO and PMMA was difficult to achieved hence stress transfer highly required to achieve strengthening effect. The bonding between polymer matrix and ZnO filler was incompatible thus weakened the bonding between molecules. Smaller forces are needed to break the bond as compared to pure PMMA(Omar et al., 2014). Tensile strength was significantly reduced in the presence of a bio ceramic component, according to Velu and Singamneni (2015). They also found Young modulus was reduced for 5%  $\beta$ -TCP and increased back once adding 10 and 15%  $\beta$ -TCP. The increment of  $\beta$ -TCP content will lead to more porosity and larger pore size. The values of tensile modulus of pure PMMA and PMMA composites are summarised in Table 4.6. The tensile modulus of PMMA composites was lower as compared to pure PMMA. There are increments of tensile modulus value since the addition of filler to the composites.

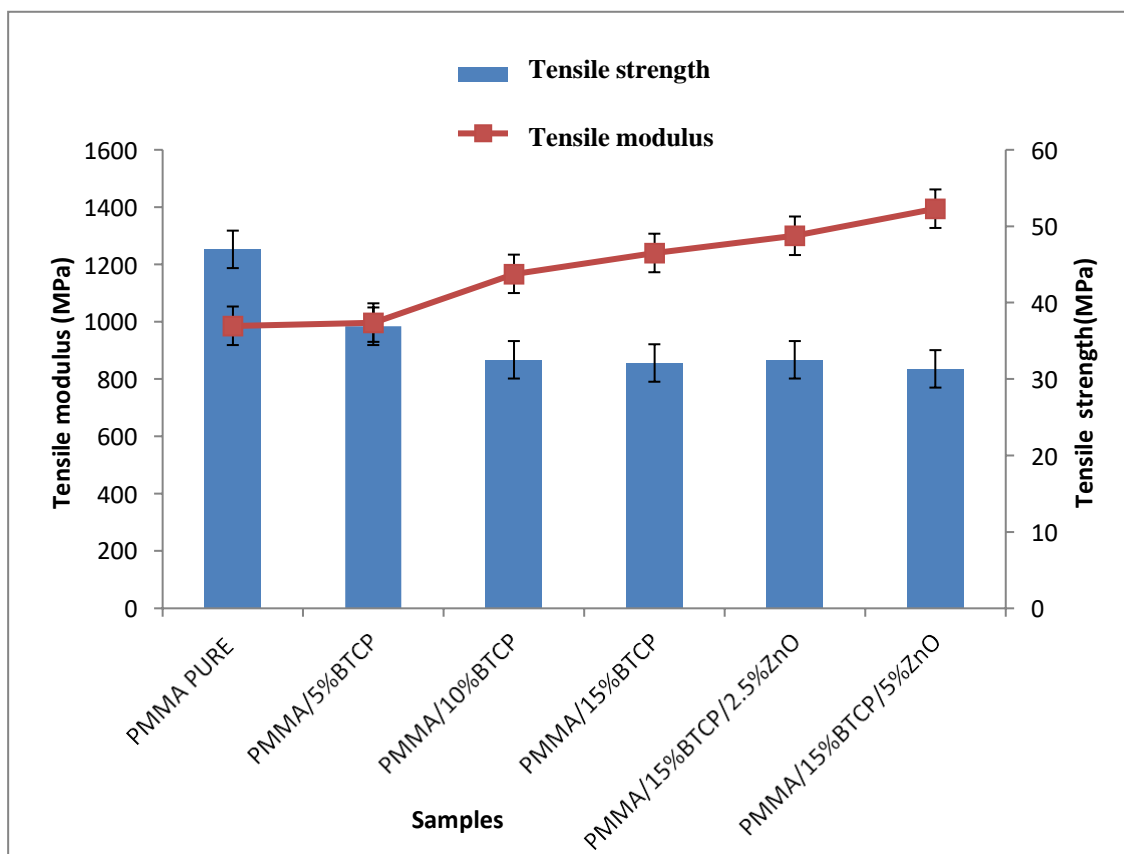


Figure 4.6 Tensile strength graph for pure PMMA and PMMA composites

Wacharawichanant (2010) found that Young Modulus was increased once adding ZnO powder and tensile was reduced. Young modulus showed decreased as higher loading of zinc was used at 2,4, and 5 wt%. Cao *et al.*, (2006) showed from SEM observation, the aggregation of ZnO were reduced once ZnO were grafted with PMMA. They addressed that the aggregation of ZnO was reduced once ZnO nanoparticles introduced to PMMA. As observed by (Omar et al., 2014) in their study, the composites with 10% ZnO loading showed normal distribution in matrix but with addition of ZnO to 30% ZnO start to agglomerate which caused the formation of holes due to poor stress transfer from matrix to filler. Hence the manner will be attributed to decrement of tensile strength. This observation was consistent with the tensile strength trend in Figure 4.6. The PMMA composite with 2.5% ZnO reduced elongation at break

indicating a little bit loss of ductility. The increment of tensile modulus was accompanied with reduction of elongation at break for PMMA composites as illustrated in Figure 4.7. Omar *et al.* (2014) stated that the presence of rigid filler ZnO to the composite could enhance the stiffness of the composites thus improve the modulus value. Such a finding was in agreement to this study because the modulus was increased with the addition of number content to the polymer matrix as illustrated in Figure 4.6. The result of mechanical properties was not greatly improved as mentioned by Chang *et al.*, (2011), that the priority of ZnO is act as an antibacterial agent. This filler not give strength properties compared to alumina, SIC and CF.

Table 4.5 Tensile strength and modulus value of PMMA composites.

Sample Name	Tensile strength (MPa)	Tensile modulus (MPa)
Pure PMMA	46.98 (6.02) <sup>a</sup>	985.71 (370.94) <sup>a</sup>
PMMA/5%β-TCP	36.92 (13.25) <sup>ab</sup>	996.93 (167.92) <sup>a</sup>
PMMA/10%β-TCP	32.52 (9.80) <sup>b</sup>	1166.99 (386.15) <sup>a</sup>
PMMA/15%β-TCP	32.11 (7.51) <sup>b</sup>	1239.71(327.07) <sup>a</sup>
PMMA/15%β-TCP /2.5%ZnO	32.52 (7.24) <sup>b</sup>	1299.99(262.07) <sup>a</sup>
PMMA/15%β-TCP /5%ZnO	31.34 (5.91) <sup>b</sup>	1394.49(191.59) <sup>a</sup>

*Mean values and standard deviation in parentheses. Different small letters in the same column are statistically significant according to pairwise and t-test comparison for tensile strength.*

The value of tensile properties of pure PMMA and PMMA composites are summarized in Table 4. 5. Pure PMMA has a highest tensile strength value. The addition of filler β-TCP to the composite reveals the reduction of the tensile strength value. However, incorporation of 2.5% ZnO increased the value of tensile strength but reducing the strength after addition of 5% ZnO. The tensile strength between the PMMA composites showed no significant differences ( $p>0.05$ ). However, the significant differences were detected only between pure PMMA ( $p= 0.028$ ) and developed composites ( $p>0.05$ ). Meanwhile, the tensile modulus of PMMA composites was higher as compared to pure PMMA. There are increments of tensile modulus value

since the addition of  $\beta$ -TCP to the composites. However, the reduction was detected slightly with incorporation of 2.5% ZnO but increase with incorporation of 5% ZnO. Dalby *et al.*, (2002) found that the addition of HA up to 15% could increase in flexural modulus and addition up to 40% HA to cement could increase the fracture toughness.

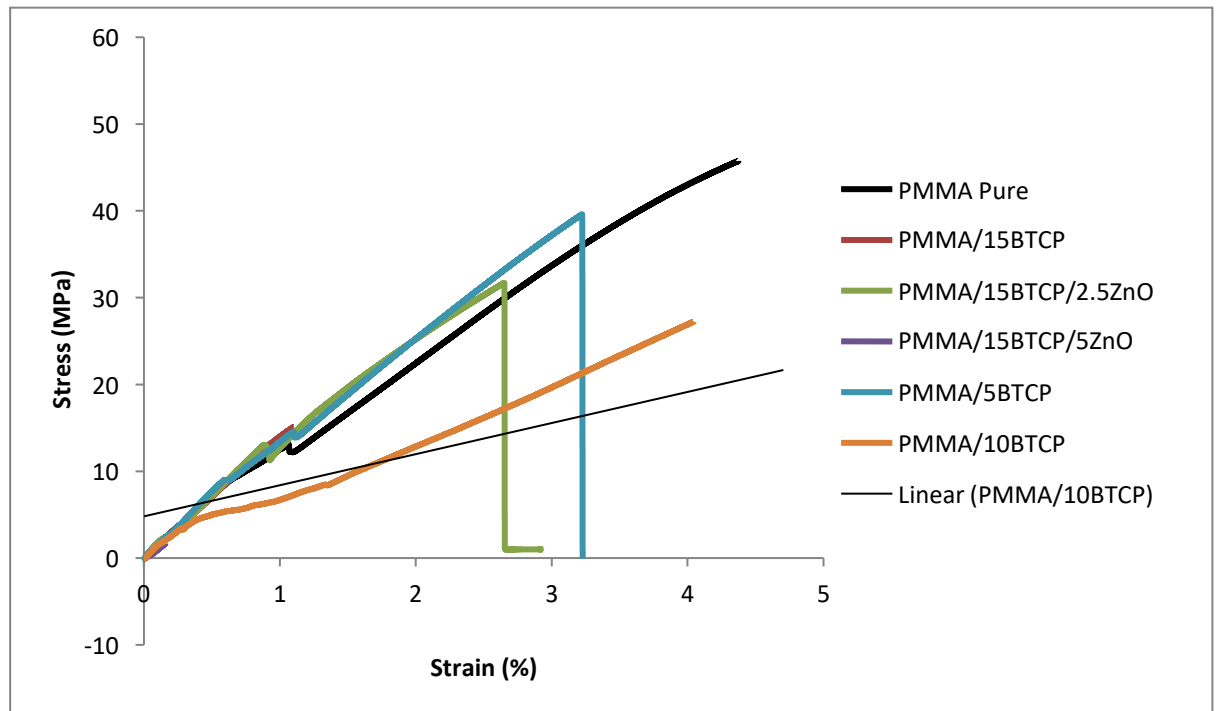


Figure 4.7 Stress strain curves of unfilled PMMA and developed composites

Figure 4.7 demonstrated the behavior of the pure PMMA and developed composites. The additional forces caused the PMMA pure to elongate close to 5% before it broke. With the increment of filler loading, the strain decreased below than 4%. The lowest elongation was detected for PMMA composites with incorporation of 2.5% ZnO. It showed a higher gradient than PMMA pure which play a part to the increment of highest modulus. PMMA/15% $\beta$ -TCP/5%ZnO presented a significant increase in tensile modulus (~1300MPa) as compared to pure PMMA (~900MPa). It could be expected that the addition of higher stiffness of filler loading will resulted to higher value in tensile modulus.

The tensile strength value was reduced with incorporation of fillers. Significant differences were detected between pure PMMA and developed composites. While, tensile modulus showed significantly increased between pure PMMA and 15% $\beta$ -TCP/5%ZnO filled PMMA. The morphology fractured of pure PMMA and developed composites is shown in Figure 4.8. The pure PMMA seems a rough surface as in Figure 4.8(a), the particles indicated the well distribution in polymer matrix as shown in Figure 4.8(b). Filler pull out could be observed in Figure 4.8(c) of porous structure.  $\beta$ -TCP represented in bulky particles whereas ZnO seem look as tiny particles.

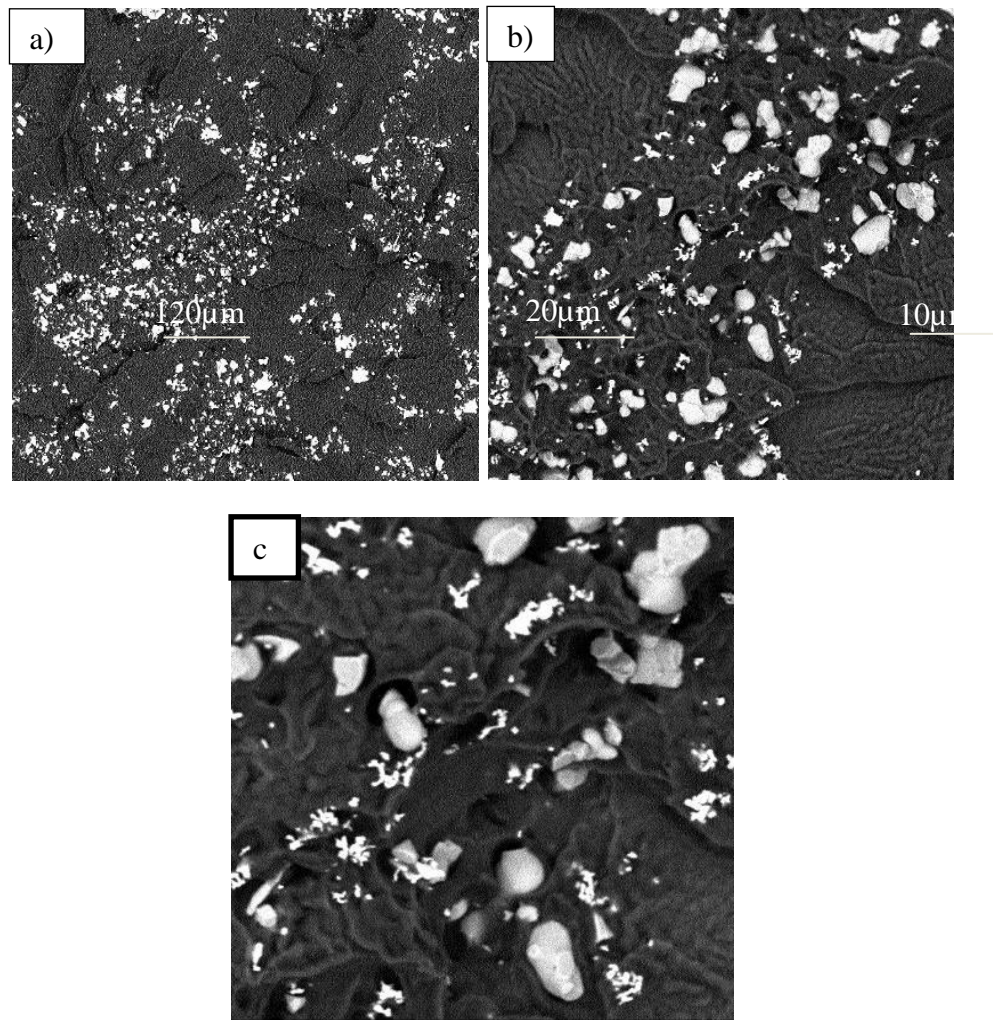


Figure 4.8 SEM microstructure of fractured PMMA/15 $\beta$ -TCP/2.5ZnO at a)1000x b)5000x and c)10000x magnification.

Radha *et al.*, (2017) mentioned that tensile properties are very crucial for bone cement due to the effect of stabilisation of the implant in the bone bed. The increment of tensile strength value for addition of 2.5% ZnO is due to the better uniform dispersion of ZnO particle and strong interfacial interaction in the polymer matrix. For the higher loading of 5% ZnO, the value of tensile strength could reduce due to the agglomeration of ZnO particles and non-uniform distribution consequence as shown in Fig 4.9(a). This will form weak spot there and hence affect the lower tensile strength (Poddar *et al.*, 2016). When there is no interfacial contact in the polymer matrix, a defect will form because the larger the loading of no particle, the lower the tensile strength value. Besides that, cracks will propagate due to the stress field around the aggregation of ZnO, which will cause failure and reveal to lower value of tensile strength. The void of PMMA/15% $\beta$ -TCP/5%ZnO represented in Figure 4.9(b) was effect to the crack and hence reduced tensile strength.

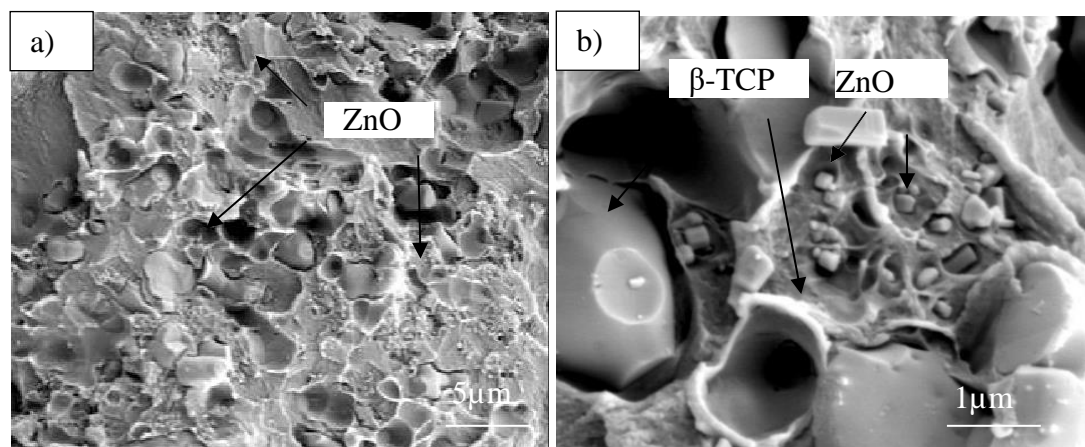


Figure 4.9 FESEM microstructure of fractured/15% $\beta$ TCP/5%ZnO at a) 10,000x and b) 50 000x magnification.



#### 4.7 Fracture toughness

Fracture toughness is a parameter to evaluate and compare material quality, also important to assure the performance of composites as well as influence the possibility of failure (Ayre *et al.*, 2014). Typically, the material undergo high stress which crack propagation is faster through the matrix in fracture toughness (Varela-rizo *et al.*, 2010). Simulated Body Fluid (SBF) test, a method that is well known to characterise the in vitro bioactivity of ceramic materials, lies in their immersion in an aqueous SBF solution which mimics the properties of human plasma for definite age and confirms the formation of the HA layer on the surface of the samples (Tham *et al.*, 2010). PMMA known as a glassy and fragile material which performed low fracture toughness (Tjong, 2006).

From the Figure 4.10, PMMA at 0 days has a  $K_{IC}$  value of 2.35 for sample pure PMMA. Then, once adding the days immersed the value was drop. PMMA composite filled 5%  $\beta$ -TCP revealed the highest value of  $K_{IC}$  compared to 10 % and 15% filled. Similar trend with study of (Chow *et al.*, 2008) reported that the fracture toughness value for HA content about 5% was the highest. Once the HA content increased, there was decreased in  $K_{IC}$  value (Chow *et al.*, 2008). However, in this study the value increased once adding 15%  $\beta$ -TCP to the composite.

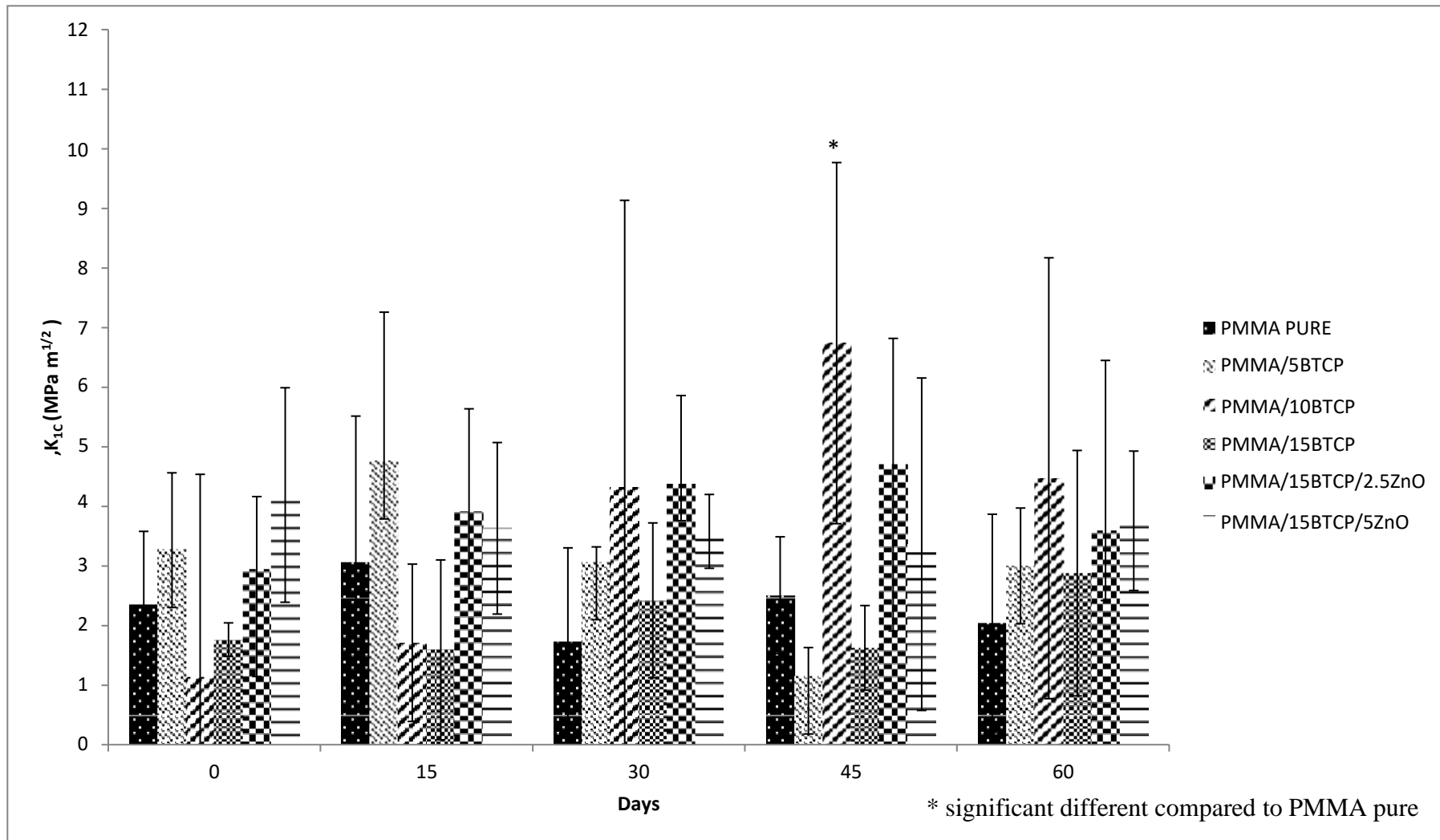


Figure 4.10 Fracture toughness value for PMMA composites at different immersion time (0,15,30,45,60) days

Table 4.6 Fracture toughness value for all sample PMMA/ $\beta$ -TCP/ZnO composites.

Samples	Fracture toughness, $K_{Ic}$ (MPa m <sup>1/2</sup> ),std				
	0 day	15 days	30 days	45 days	60 days
PMMA PURE	2.35(1.23) <sup>a</sup>	3.05(2.47) <sup>a</sup>	1.73(1.57) <sup>a</sup>	2.51(0.98) <sup>a</sup>	2.03(1.83) <sup>a</sup>
PMMA/5 $\beta$ TCP	3.27(1.29) <sup>a</sup>	4.76(2.5) <sup>a</sup>	3.07(0.25) <sup>a</sup>	1.15(0.48) <sup>a</sup>	2.99(0.97) <sup>a</sup>
PMMA/10 $\beta$ TCP	1.14(3.4) <sup>a</sup>	1.71(1.32) <sup>a</sup>	4.31(4.82) <sup>a</sup>	6.74(3.03) <sup>b</sup>	4.47(3.7) <sup>a</sup>
PMMA/15 $\beta$ TCP	1.76(0.28) <sup>a</sup>	1.59(1.51) <sup>a</sup>	2.42(1.3) <sup>a</sup>	1.62(0.71) <sup>a</sup>	2.88(2.06) <sup>a</sup>
PMMA/15 $\beta$ TCP/2.5ZnO	2.94(1.22) <sup>a</sup>	3.90(1.74) <sup>a</sup>	4.38(1.48) <sup>a</sup>	4.70(2.12) <sup>a</sup>	3.59(2.86) <sup>a</sup>
PMMA/15 $\beta$ TCP/5ZnO	4.19(1.8) <sup>a</sup>	3.63(1.44) <sup>a</sup>	3.58(0.62) <sup>a</sup>	3.36(2.79) <sup>a</sup>	3.76(1.17) <sup>a</sup>

Statistical analysis using non parametric test, Kruskalwalis within a column, values with the difference superscript letter are significant ( $p < 0.05$ )

Kenny & Buggy, (2003) mentioned that chemical reaction of the calcium and silicate ions that dissolved from the phosphate ion and glass ceramics in the surrounding body fluid was believed to form apatite layer (Figure 4.11). Apatite layer formation underwritten to lessen the strength loss in soaking (Chuan *et al.*, 2020). Generally,  $K_{IC}$  was changed after the immersion in SBF as mentioned by Elshereksi *et al.* (2009). The bond failure between filler and polymer matrix achieved once the sample provided to aqueous solution. The liquid condition will decrease the hoop stress due to swelling phenomenon around the filler and pull out of filler mechanism will be easier.

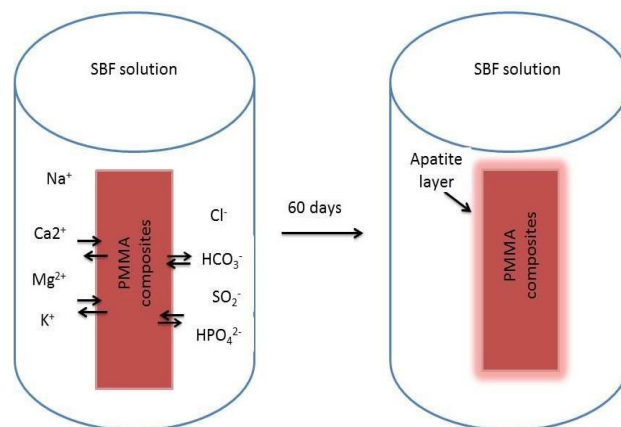


Figure 4.11 Schematic representation of apatite growth at surface of composite

As in the Figure 4.12 (a), PMMA surface fracture seems like rough and stripes pattern at 0 days. It indicated that the crack fracture was stable in propagating. From the site fracture, it can be observed that there is a stable crack propagation appeared with striped pattern. However, when times up to 60 days, the surface look like smooth and appeared some voids as could be seen in the Figure 4.12 (b), indicating that it was easy to crack due to rapid crack growth hence influencing in lower  $K_{IC}$  value rather than

before immerse (Elshereksi *et al.*, 2009). Hence the value of  $K_{IC}$  was slightly lower than PMMA pure which exposed to air. Similar documented with study from Elshereksi *et al.*, 2009 after immersion for 28 days the area fracture looks like in smooth phase. The attribute of hydrophobic PMMA will not attract the solution of SBF into the polymer matrix. However, hydrophobic PMMA could absorb up to 2% of its weight in water was found in literature (Kusy *et al.*, 2001). The fluid will enter the space vacancies from voids or pores created from entrapped air from mixing. The extent of moisture uptake contributed to structural change thereby reduces the value of  $K_{IC}$ .

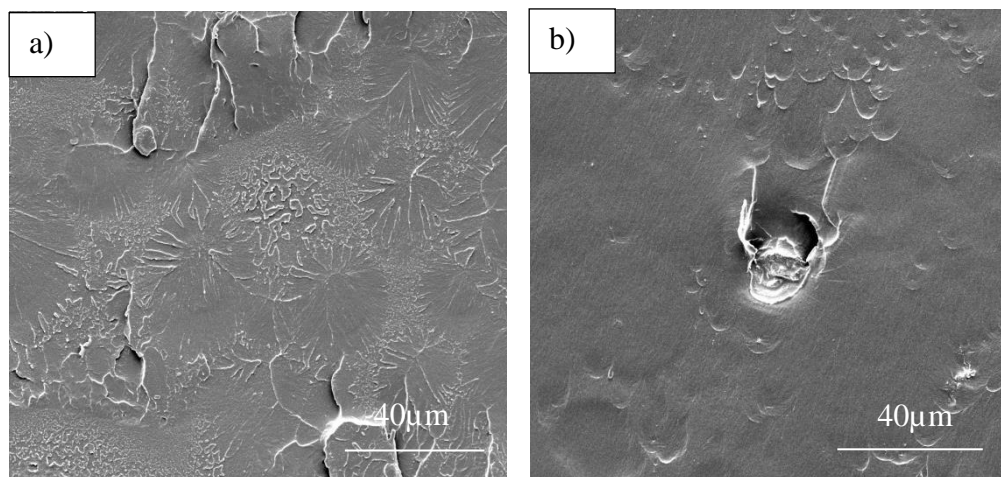


Figure 4.12 FESEM image for fractured surface of PMMA pure at a)0 day and b)60 days at 2000x magnification

For sample PMMA/5% $\beta$ -TCP, the value also drops after adding time. However, the tremendous increment was detected after 45 days treatment. (Ahmed & Ebrahim, 2014) found that  $ZrO_2$  with above 5 and 7 % reveal improvement to acrylic resin due to complete saturation of  $ZrO_2$  particle and polymer matrix. 3% value of  $ZrO_2$  will reveal the highest fracture toughness. Elshereksi *et al.* (2009) found that  $K_{IC}$  of PMMA is higher compared to PMMA composite. In this case, this is due to weak bonding between  $BaTiO_3$  with PMMA matrix. The weak adhesion of PMMA to the filler is correlated to

the partial embedding of filler to PMMA, similar finding with this study. All samples not significant except for PMMA/10% $\beta$ -TCP. For sample PMMA/10% $\beta$ -TCP, the value of 0 day was lowest compared to other composites and highest value was significantly detected at days of 45. Even though not significant, for sample PMMA/15% $\beta$ -TCP, the addition of days treatment affected the value to increased  $K_{IC}$ . It also clearly seen that sample PMMA/15% $\beta$ -TCP has the lowest fracture value for every treatment day. Similar with sample PMMA/15% $\beta$ -TCP, sample PMMA/15% $\beta$ -TCP/2.5%ZnO also has increased the  $K_{IC}$  after a few days immersed but reduced after 60 days. Contrast to PMMA/15% $\beta$ -TCP/5%ZnO, 0 day give the highest value compared to 15,30,45,60 days. The lowest value found at 45 days. After 60 days, it increased back but still below 0 day value's. Zakaria *et al.* (2017) found that the filler incorporation of HYB and MIX (CNT- $Al_2O_3$ ) in epoxy composites enhance the fracture toughness value about 26% and 9% respectively. Khandaker, Li and Morris, (2013) reported that with the incorporation of both micro (25.05 kPa m<sup>1/2</sup>) and nano (27.24kPa m<sup>1/2</sup>) to PMMA, the fracture toughness value could be enhanced compared to PMMA alone (9.71 kPa m<sup>1/2</sup>). Ahmed & Ebrahim, (2014) investigated that nanofiller of ZrO<sub>2</sub> and resin give high interfacial shear strength between them resulted from formation of crosslinks which present crack hence increase in fracture toughness as well as flexural and hardness. Dalby *et al.* (2001) found that with the addition of filler HA to the composite up to 40% the fractured toughness was increased.

Rahim *et al.*, (2012) in their study explained that molecules of water absorbed to the polymer matrix could induce the degradation of composites. The water molecules enter the polymer matrix and occupied the space between micro voids and polymer chain, leading to plasticization and swelling occurrence and elicit the chain scission hence monomer will be eluted. They also stated that the degradation and softening of resin composites would weaken physical and mechanical properties.

Alhaleb and Ahmad, (2011) from their studied showed that  $K_{IC}$  of PMMA/HA increasing until the loading of HA up to 5% as can see in Figure 4.10, PMMA with  $\beta$ -TCP 5% increased the value of  $K_{IC}$  from PMMA neat and reduced after PMMA incorporate with 10 and 15%  $\beta$ -TCP. The incorporation of  $Al_2O_3/ZrO_2$  (80:20) in their study reported that the addition of filler to PMMA increased  $K_{IC}$ . PMMA itself has the fracture toughness value of  $1.6 MPa^{-m/2}$ . The value increased to  $2.12 MPa^{-m/2}$  when added 5% of  $Al_2O_3/ZrO_2$ .

The advantages from sample immersion using SBF solution is the apatite layer produced from the solution which interact with  $\beta$ -TCP that could give advantages in cell proliferation as shown in Figure 4.13. The apatite layer promotes cell adhesion to the bone cement. As stated by Sa *et al.*, 2016, the evaluation of potential mineral abilities of HA-loaded cement confirmed when immersed into SBF compared to HA-free cements observed through SEM.

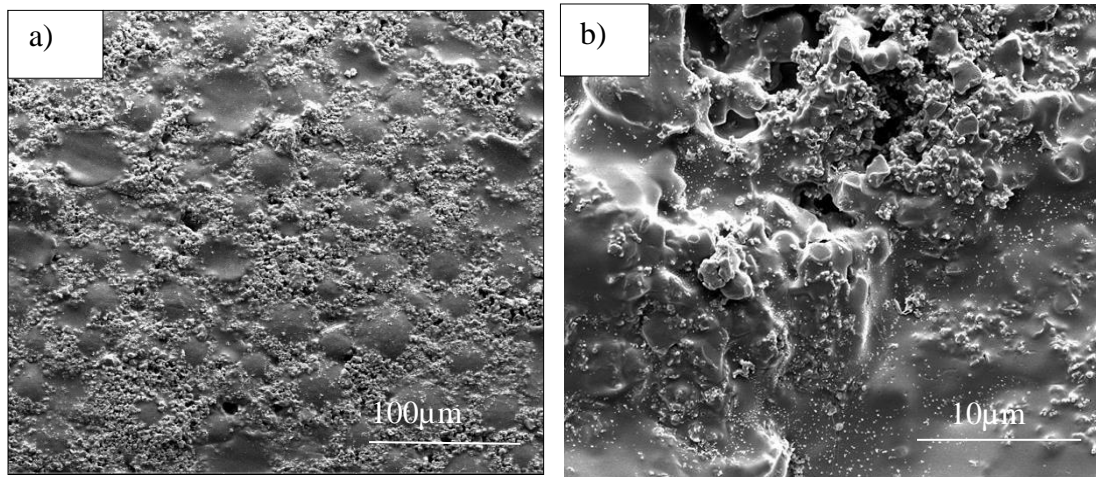


Figure 4.13 PMMA/15%β-TCP/2.5%ZnO apatite form at a) 1000x and b)10000x magnification

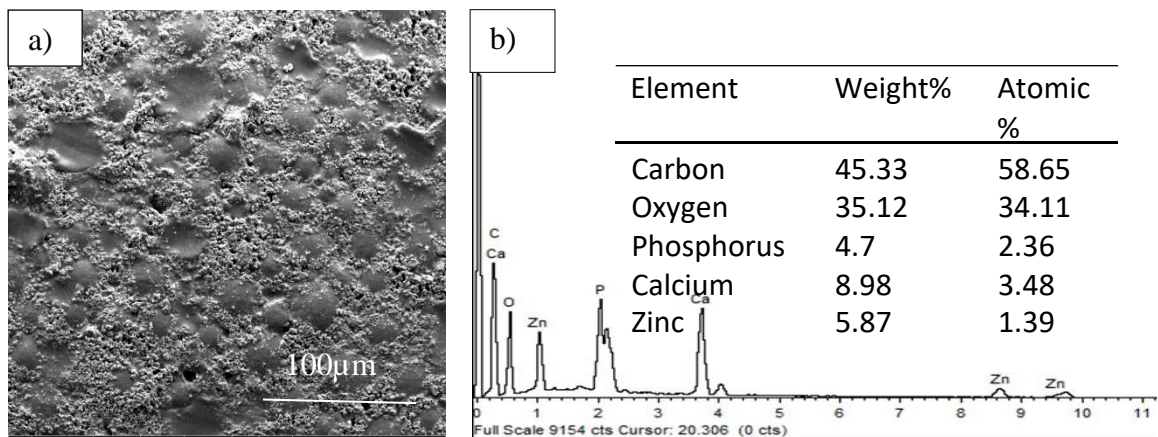


Figure 4.14 SEM micrograph of PMMA/15β-TCP/2.5ZnO after incubating in SBF  
 b) EDX spectrum of PMMA/15β-TCP/ZnO after 60 days incubation in SBF

Figure 4.14 a) showed that the accumulation of apatite form from reaction of SBF solution with component in PMMA composites. Ito *et al.*, (2002) also proved in their study that combination of Zn into calcium phosphate support the bonding to the bone directly. However, the presence of β-TCP required as a carrier of Zn since Zn release slowly from the implant. At high level it attempts hostile reactions. Ions concentration that presence in SBF consist of  $\text{Na}^+$ ,  $\text{K}^+$ ,  $\text{Mg}^{2+}$ ,  $\text{Ca}^{2+}$ ,  $\text{Cl}^-$ ,  $\text{HCO}_3^-$ ,  $\text{HPO}_4^{2-}$  and  $\text{SO}_4^{2-}$ . In human blood plasma the amount of ion concentrations same with SBF solution except for  $\text{Cl}^-$  and  $\text{HCO}_3^-$  (Kokubo, 1996).



There are number of reasons influenced the reduction of fracture toughness in PMMA/ZrO<sub>2</sub> since the increment of filler content including particle distribution in the polymer matrix, the type and size of the particles, the concentration of the added particles, and chemical reactions between the particles and polymer. High filler content contributes to the more filler to filler interaction rather than filler to matrix interaction, yield to agglomeration as a point of stress concentration thus reveal to non- uniform stress distribution. When introduce to the load or force, the agglomeration hinders the movement of molecular deformation hence decrease the fracture toughness (Zaidan *et al.*, 2019). Figure 4.14 b) showed the EDX spectra from SEM micrograph of PMMA/15%β-TCP/2.5%ZnO. There were shown the amount of existence component existed in the composites as well as confirmed the apatite layer formed.

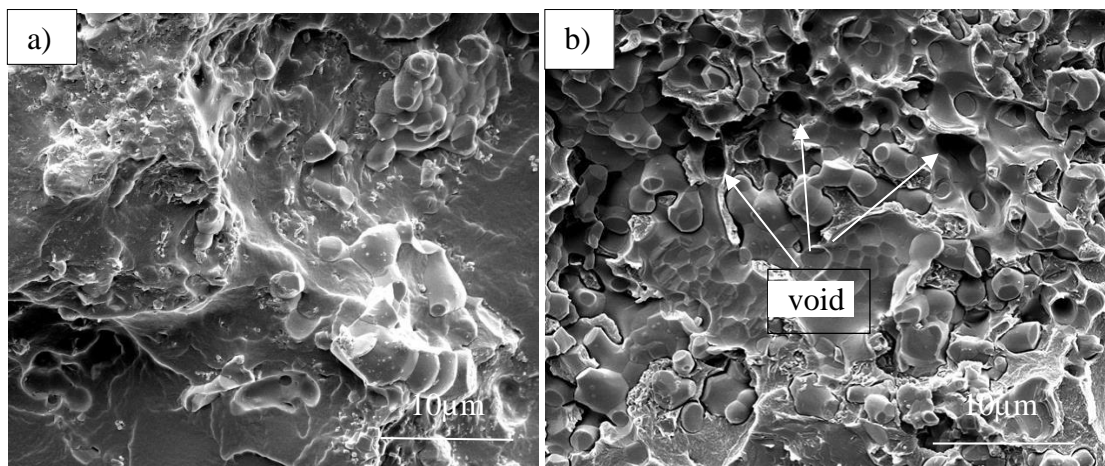


Figure 4.15 PMMA/15%β-TCP/2.5% ZnO a) 0 days b) after 60 days SBF soaked at 10000x magnification.

Figure 4.15 showed the fractures surface for PMMA/15%β-TCP/2.5% ZnO a) before immersion with SBF b) after SBF immersion. Before treated with SBF, no void presence due to fill of fillers and the fillers was non-uniformly distribute. The fillers were embedded in the resin matrix. After 60 days SBF immersion and fractured, Figure 4.15 b) shown there were voids presence in PMMA matrix, due to the fillers detached

from matrix. However, The  $K_{IC}$  for all specimen was insignificantly increased after being treated with SBF for 60 days. Hence, the tested composites achieved durability and suit to be applied as implant material in craniofacial field as meet standard ASTM International value range from 0.7-1.6 MPa.m<sup>1/2</sup> (Callister & Rethwisch, 2018).

#### 4.8 Cytotoxicity evaluation

In this study, the cell viability of hFOB treated with PMMA composites was analysed using MTT assay. It was done by measuring hFOB cells growth after exposure to tested materials with several extract concentration from 100, 50, 25, 12.5 and 6.25 mg/ml. Based on the Figure 4.16, PMMA filled 15% $\beta$ -TCP has shown the highest value of cell viability (131.39%) at concentration of 25 mg/ml. For hFOB with 100 mg/ml PMMA composites, the highest percentage of cell viability was 97.65% (filled 10%  $\beta$ -TCP) and the lowest was 65.19% (filled 15%  $\beta$ -TCP/2.5% ZnO). For composite filled ZnO, the cell viability was highest revealed from PMMA/15% $\beta$ -TCP/2.5%ZnO (112.04%) at concentration 50 mg/ml. The percentages of cell viability of samples with 50 mg/ml and below showed no cytotoxicity effect due to their value of cell viability is more than 70% (ISO, 2009a), ISO10993-5. The results showed that tested materials are nontoxic to the hFOB exclude for the highest concentration of 100mg/ml of PMMA filled 15%  $\beta$ -TCP/2.5%ZnO. No significant difference ( $p>0.05$ ) observed only for all sample at 12.5mg/ml. The rest shown significant differences among the concentrations group.

For concentration of 6.25 mg/ml, there are significant difference between PMMA and composite filled 15%  $\beta$ -TCP and 15% $\beta$ -TCP/2.5%ZnO and 15% $\beta$ -TCP/5%ZnO. Significant difference also revealed at concentration 25mg/ml between PMMA pure and 10% $\beta$ -TCP, 15% $\beta$ -TCP and 15% $\beta$ -TCP/5%ZnO. For 50 mg/ml,

PMMA filled 10% $\beta$ -TCP, 15% $\beta$ -TCP,2.5%ZnO and 5%ZnO showed significant different. At concentration 100mg/ml, only composite filled 15% $\beta$ -TCP/2.5%ZnO presented significant difference ( $p=0.009$ ) with pure PMMA as shown in Table 4.7.

Table 4.7 Cell viability of PMMA composite treated with hFOB at different concentration

Samples	Cell viability (%), (std)				
	Concentration (mg/ml)				
	6.25	12.5	25	50	100
PMMA PURE	93.21(5.21) <sup>a</sup>	96.04(13.71) <sup>a</sup>	102.59(13.1) <sup>a</sup>	88.55(11.7) <sup>a</sup>	84.88(13.16) <sup>a</sup>
PMMA /5 $\beta$ -TCP	94.15(7.92) <sup>a</sup>	98.70(5.7) <sup>a</sup>	94.71(12.72) <sup>b</sup>	83.99(3.44) <sup>a</sup>	81.16(9.79) <sup>a</sup>
PMMA/10 $\beta$ -TCP	92.54(9.92) <sup>a</sup>	104.76(7.52) <sup>a</sup>	123.08(13.24) <sup>b</sup>	109.86(7.27) <sup>b</sup>	97.65(6.81) <sup>a</sup>
PMMA/15 $\beta$ -TCP	118.13(1.49) <sup>b</sup>	109.39(7.37) <sup>a</sup>	131.39(17.6) <sup>b</sup>	101.30(3.94) <sup>b</sup>	90.77(11.08) <sup>a</sup>
PMMA/15 $\beta$ -TCP/2.5ZnO	111.54(6.92) <sup>b</sup>	101.51(4.77) <sup>a</sup>	107.39(7.42) <sup>a</sup>	112.04(7.43) <sup>b</sup>	65.19(2.84) <sup>b</sup>
PMMA/15 $\beta$ -TCP/5ZnO	112.54(4.04) <sup>b</sup>	97.07(5.74) <sup>a</sup>	127.80(9.82) <sup>b</sup>	111.47(9.97) <sup>b</sup>	76.94(14.29) <sup>a</sup>

Statistical analysis using One-way Anova, post hoc Tukey test within a column, values with the difference superscript letter are significant ( $p < 0.05$ )

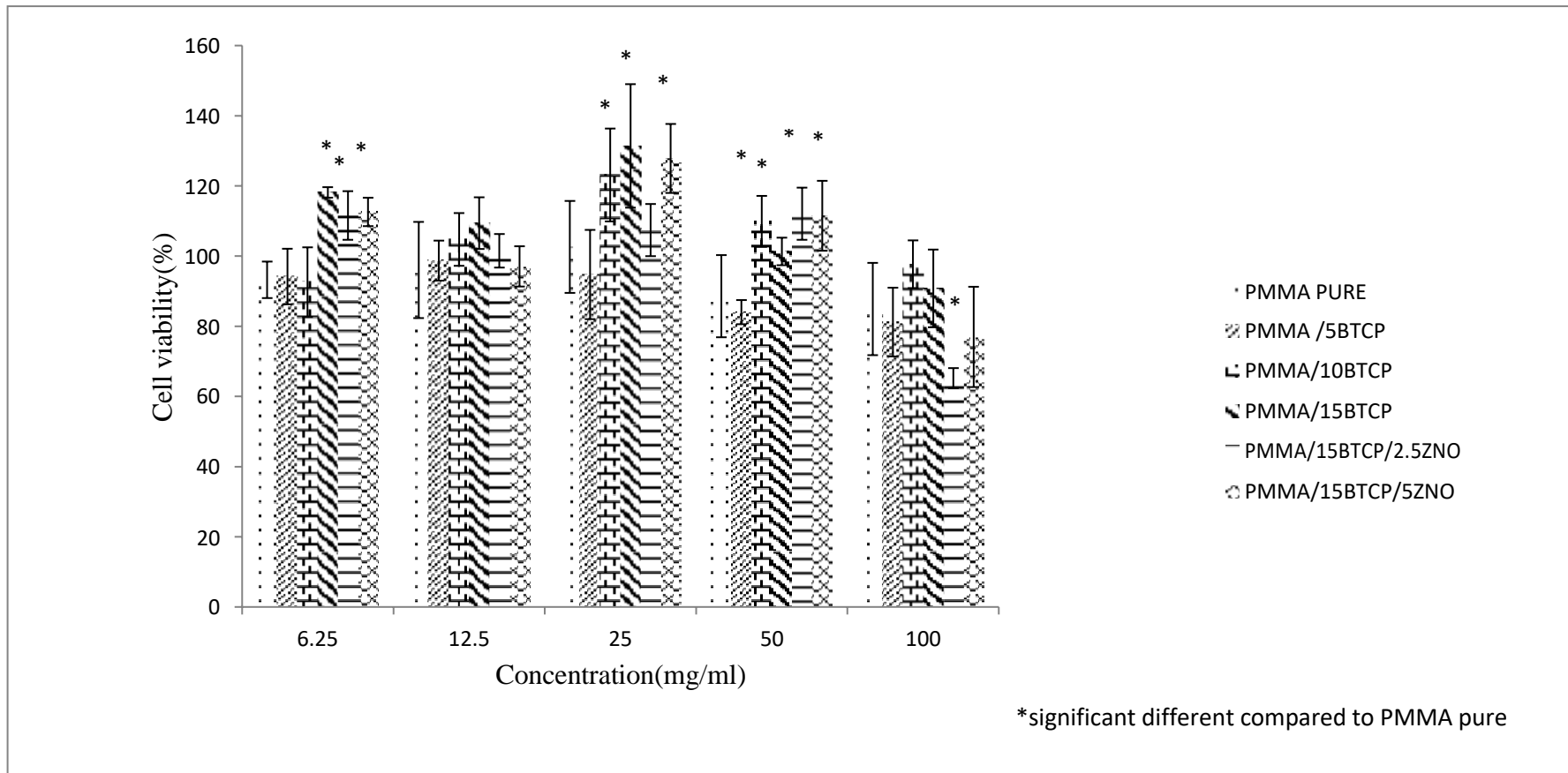


Figure 4.16 Cell viability of human fetal osteoblast (hFOB) cells treated with PMMA composites using MTT.

Based on the result, all pure PMMA revealed lower viability percentages in all concentration compared to PMMA composites. Probably this is due to pure PMMA has poor integration to the surrounding bone tissues and poor osteoconductive which does not allow bone cell adhesion and growth as mentioned by (García-Merino *et al.*, 2009). By adding  $\beta$ -TCP to PMMA resin, it could reduce its cytotoxicity effect as indicated by increasing cell viability percentage (Figure 4.16). However, the concentration of  $\beta$ -TCP added into PMMA resin should not exceed 15% because it might compromise the mechanical and physical properties of PMMA resin (Jiao *et al.*, 2015).

In this study, hFOB cells treated with PMMA-based materials at the concentration ranging from 6.25 to 100 mg/ml, exhibited proliferative activity especially by the PMMA filled  $\beta$ -TCP materials. Due to its similar chemical properties to bone, high biocompatibility, and excellent osteoconductivity, which can improve osteoblast adhesion and proliferation, hydroxyapatite and -tricalcium phosphate have been widely applied in bone tissue engineering. Stefanic *et al.*, (2013) found that  $\beta$ -TCP possessed osteoconductive, bioresorbability and bone bonding ability.

Osteoblast proliferation and differentiation are stimulated by cytokines, growth factor and calcium as chemical. The calcium phosphate additives bind serum proteins and growth factors efficiently, promoting cell attachment and spreading (Harb *et al.*, 2020). The presence of calcium in  $\beta$ -TCP has been reported to induce osteogenic differentiation and proliferation (Moursi *et al.*, 2002). The presence of  $\beta$ -TCP induces proliferation due to the combination of calcium and phosphate ion which could governs cell signalling (Park *et al.*, 2014).

In agreement with Moursi *et al.*, (2002), they found that PMMA reinforced HA enhanced the cell proliferation rather than pure PMMA as indicated by the presence of confluent multi layered cell culture with highly organized cellular matrix. (Dalby *et al.*, 2002) had found that the addition of HA was not improved the mechanical performance but contributed well to the bioactivity properties. The presence of HA in the material's hydrophilic character, resulting in good cell growth, proliferation and viability on these materials (Tihan, 2009). Besides, the addition of HA to PMMA reinforced the bone-cement interface by forming chemical bonds, resulting in direct contact with bone. The formation of secondary hydroxy-carbonate apatite (HCA) with a composition similar to bone-like apatite is linked to the bioactivity of calcium phosphates. The release of phosphate ions alone assisted in inducing proliferations against osteoblast cells (Abdullah *et al.*, 2018).

The results showed in the Figure 4.16 was in accordance to Fuiser (2016), which they found the addition of  $\beta$ -TCP to PMMA resin resulted in increment of cell viability except for incorporation of 5%  $\beta$ -TCP to PMMA matrix. However, the results were in contrast to (Petrovic *et al.*, 2006), in which incorporation of  $\beta$ -TCP to PEEK resulted in the inhibitory effect to the growth of osteoblast due to inhibition of cell proliferation.

It is interesting to note that HA and  $\beta$ -TCP did not demonstrate any cytotoxic effect as shown by (Monchau *et al.*, 2013). However, Jiao *et al.*, (2015), highlighted that the cytotoxicity of PMMA was related to the release of unpolymerized MMA monomer. As also mentioned by Arakawa, (2010), factors that influence the poor interaction between tissue and cement are high polymerisation exotherm, leaching of toxic unreacted MMA monomer and polymerization shrinkage. Leaching of free monomers prior to polymerization, residual monomers after polymerization, and residual initiators and activators have all been linked to inhibition of cell function and

growth/differentiation, increased release of inflammatory cytokines, and promoted cell death/necrosis (Meretoja *et al.*, 2010). MMA, like other methacrylate monomers, can disrupt intracellular redox balance, resulting in negative effects on cell function and viability (Jiao, 2015, Itthichaisri *et al.*, 2006). A recent study by Chuan *et al.* (2020) demonstrated that MC3T3-E1 cells experienced cytotoxicity effect when the residual MMA was released from the cement, which made difficult for cells in the extract to proliferate.

In addition, micro and macro size of surface characteristics and the interconnecting system could influence the cell growth. The topography and chemical reactivity of an implantable material's surface play an important role in the adhesion and proliferation of osteoblast cells, and thus in tissue development (Harb *et al.*, 2020).

The incorporation of  $\beta$ -TCP and ZnO were proven biocompatible even at the concentration of 100mg/ml since PMMA/15% $\beta$ -TCP/5%ZnO revealed insignificantly reduced of cell viability as shown in Figure 4.15. All PMMA composite possessed good cytocompatibility and promoted proliferation of hFOB cells except for PMMA/15% $\beta$ -TCP/2.5%ZnO at 100mg/ml which shown the viability less than 70%. Material is considered cytotoxic when it exhibited cell viability below 70%. Interestingly, when the ZnO was added by 5%, it improved the viability effect by increasing the viability percentage to more than 70%. With these reasons, the concentration of 50mg/ml was chosen for the antibacterial properties' evaluation.



## 4.9 Antibacterial study of *S.aureus* and *P.aureus*

### 4.9.1 Agar diffusion method

Agar diffusion method was used to evaluate antibacterial activity of PMMA/ $\beta$ -TCP/ZnO composites prior to bacteria growth study. Chlorhexidine (0.2 %) was chosen as a positive control since it has a broad bacterial spectrum activity. Figure 4.17 illustrates the inhibition zone observed for different composition of composites against *S. aureus*.

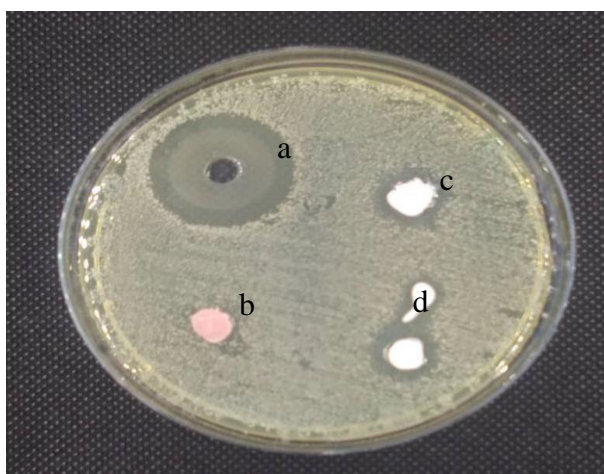


Figure 4.17 Inhibition zone for a) Chlorhexidine b) pure PMMA c) PMMA/15% $\beta$ -TCP/2.5% ZnO d)PMMA/15% $\beta$ -TCP/5% ZnO against *S.aureus*

No antibacterial activity was observed for pure PMMA. PMMA composites with 5% ZnO (4mm) exhibited better antibacterial properties compared to PMMA/2.5%ZnO (3mm). The zone of inhibition was increased as the filler content of zinc oxide increased, as shown in Figure 4.17. In this study, PMMA/15% $\beta$ -TCP/5%ZnO showed the highest antibacterial activity against *S. aureus*. The smaller size of ZnO will allow good penetration into the bacterial cell membrane and nucleus.

ZnO displays major antimicrobial activities when particle size is reduced to the nano sized. ZnO can interact with bacterial surface enable it to enter inside the cell, and consequently bring distinct bactericidal mechanisms. The wet condition in agar plate

will support zinc ion to leach out and interact with the negative charges species of bacteria cell membrane leading the inhibition of respiratory process and prone to bacterial cell death (Siddique, 2004). Besides, metal oxide elements are vital to inhibit bacteria growth due to the performance structure of their cell. As mentioned by Zahran *et al.* (2019), negatively charge from gram negative outer membrane and fine layer peptidoglycan could penetrate positive charge of silver nanoparticles. Silver nanoparticles difficult to attack *S.aureus* due to a dense layer of peptidoglycan and no outer membrane of positive gram strain. It is assumed the same for zinc oxide particles that could bring to bacteria death. Similar findings documented by Youssef *et al.* (2019) that the increment of ratio ZnO–NPs incorporated to PMMA matrix, the greater inhibition zone appeared indicating that the existence of antimicrobial activities.



Figure 4.18 Inhibition zone for a) Chlorhexidine b) pure PMMA c) PMMA/15% $\beta$ -TCP/2.5% ZnO and d) PMMA/15% $\beta$ -TCP/5% ZnO against *P. aeruginosa*.

Figure 4.18 shows the antimicrobial activity of all composites tested against *P. aeruginosa*. There was no inhibition against *P. aeruginosa*, indicating that there were no antibacterial activities. In their study, Sodagar *et al.* (2016) found that adding acrylic specimens reinforced with nanoparticles to the mix reduced bacterial growth and

population. The antibacterial activity increased as the concentration was increased. An antibacterial component in a composite containing cure monomer chemically bonded to the matrix resin (Imazato *et al.*, 1994).As a result, no inhibition zone was found in the agar diffusion with specimens containing MDPB (methacryloyloxydodecylpyridinium bromide), indicating that antibacterial components were not eluted or removed from the specimens. *E. coli* (Gram-negative bacteria) has an additional outer membrane made up of phospholipids, proteins, and lipopolysaccharides, which makes it more resistant to antibiotics than *S. aureus* (Gram-positive bacteria). Table 4.10 summarises the measurement of zone inhibition for both strains.

Table 4.8 Zone of Inhibition (mm) of *S.aureus* and *P.aeruginosa*

Samples	Diameter of inhibition(mm)	
	<i>S.aureus</i>	<i>P.aeruginosa</i>
Chlorohexidine	10	10
PMMA pure	0	0
PMMA/15%βTCP/2.5%ZnO	3	0
PMMA/15%βTCP/5%ZnO	4	0

#### 4.9.2 Bacteria growth study

Implantation of PMMA usually associated with bacterial infection caused by *S. aureus*, lead to destruction of bone and treatment failure (Mori *et al.*, 2019). Bacteria, existed in human living environment including drinking water, food and daily necessities, can cause diseases even death. Bacteria made up from polysaccharide, protein, lipid, nucleic acid and peptidoglycan, chemically. Nutrients for bacteria including oxygen and hydrogen. Hydrogen and oxygen are made up from water, hence water is essential nutrient for bacteria growth. Bacteria are conventionally divided into two main groups, Gram-positive and Gram-negative, according to their Gram stain retention property which depending on their cell wall properties. Antibacterial agents

that kill bacteria are considered bactericidal, whereas if they inhibit bacterial growth, they are considered bacteriostatic (Sirelkhatim *et al.*, 2015). Since Gram-positive and Gram-negative bacteria could react in different ways to antibacterial moieties, it is good practice to assess the antibacterial properties of any new device with both kinds of bacterial strain (Verné *et al.*, 2019).

Gram positive bacteria composed of one cytoplasmic membrane with multilayer of peptidoglycan polymer, and possess cell wall with thickness of (20–80 nm). Gram-negative bacteria wall is consisted of two cell membranes, an outer membrane and a plasma membrane with a thin layer of peptidoglycan (thickness of 7–8 nm) (Samarayanake, 2006). Nano particles size within such ranges could cross the peptidoglycan and subjected to damage (Sirelkhatim *et al.*, 2015).

The optical density of *S. aureus* bacterial strain is shown in Figure 4.19. Evaluation of bacterial growth was made by comparing the growth cured between untreated and treated bacteria. For control, the optical density of this PMMA composite was higher than that of other PMMA composites. The graph depicts the bacterial growth cycle throughout a 12-hour period, which contains four phases. The first cycle is the lag phase (which may last a few minutes or many hours because bacteria do not divide immediately but undergo a period of adaptation with vigorous metabolic activity), followed by the log phase (rapid cell division occurs, determined by the environmental conditions), the stationary phase (which occurs when nutrient depletion or toxic products cause growth to slow until the number of new cells produced equals the number of cells that die), and the decline or death phase (this is marked by a decline in the number of live bacteria) (Samaranayake, 2006).

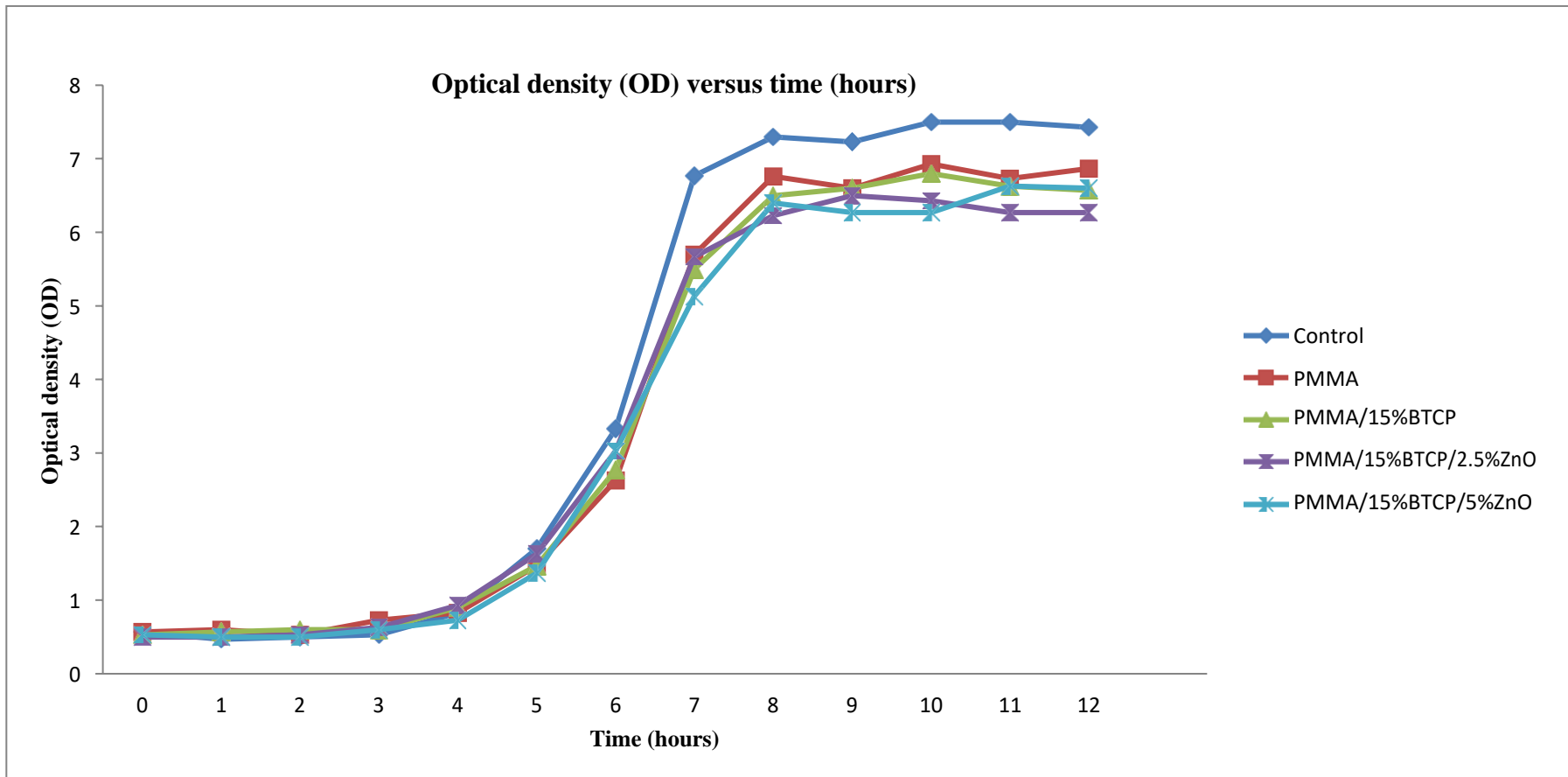


Figure 4.19 OD measurement of *S. aureus* growth on PMMA composites for 12 hours incubation period.

Table 4.9 Turbidity measurement of *S. aureus* treated with PMMA composites

Treated and untreated <i>S.aureus</i> with PMMA composites.	Mean of turbidity measurement, (std)		
	Lag phase (0 to 3hours)	Log phase (4 to 9 hours)	Stationary phase (10 to12 hours)
Untreated <i>S.aureus</i> (control)	0.517(0.06) <sup>a</sup>	3.95 (2.73) <sup>a</sup>	7.42 (0.17) <sup>a</sup>
Pure PMMA	0.608 (0.15) <sup>a</sup>	3.48 (2.44) <sup>a</sup>	6.78 (0.33) <sup>b</sup>
PMMA/15β-TCP	0.575 (0.08) <sup>a</sup>	3.42 (2.30) <sup>a</sup>	6.65 (0.49) <sup>a</sup>
PMMA/ 15β -TCP/2.5ZnO	0.542 (0.07) <sup>a</sup>	3.50 (2.20) <sup>a</sup>	6.37 (0.33) <sup>b</sup>
PMMA/ 15β -TCP/5ZnO	0.533 (0.05) <sup>a</sup>	3.33 (2.25) <sup>a</sup>	6.73 (0.50) <sup>a</sup>

Table 4.10 Turbidity measurement of *P. aeruginosa* treated with PMMA composites

Treated and untreated <i>P. aeruginosa</i> with PMMA composites.	Mean of turbidity measurement, (std)		
	Lag phase (0 to 4hours)	Log phase (5 to 9 hours)	Stationary phase (10 to 12 hours)
Untreated <i>P. aeruginosa</i> (control)	0.47 (0.05) <sup>a</sup>	2.21 (1.31) <sup>a</sup>	4.88 (0.18) <sup>b</sup>
Pure PMMA	0.51 (0.03) <sup>a</sup>	2.11 (1.22) <sup>a</sup>	4.60 (0.17) <sup>a</sup>
PMMA/15β -TCP	0.49 (0.07) <sup>a</sup>	2.22 (1.34) <sup>a</sup>	4.76 (0.25) <sup>a</sup>
PMMA/ 15β -TCP/2.5ZnO	0.44 (0.05) <sup>a</sup>	2.12 (1.22) <sup>a</sup>	4.43 (0.21) <sup>a</sup>
PMMA/ 15β -TCP/5ZnO	0.45 (0.05) <sup>a</sup>	2.11 (1.21) <sup>a</sup>	4.36 (0.18) <sup>a</sup>

Tables 4.9 and 4.10 shows a statistical analysis using nonparametric Kruskalwalis, within a column, value with a different superscript letter is significant ( $p<0.05$ )

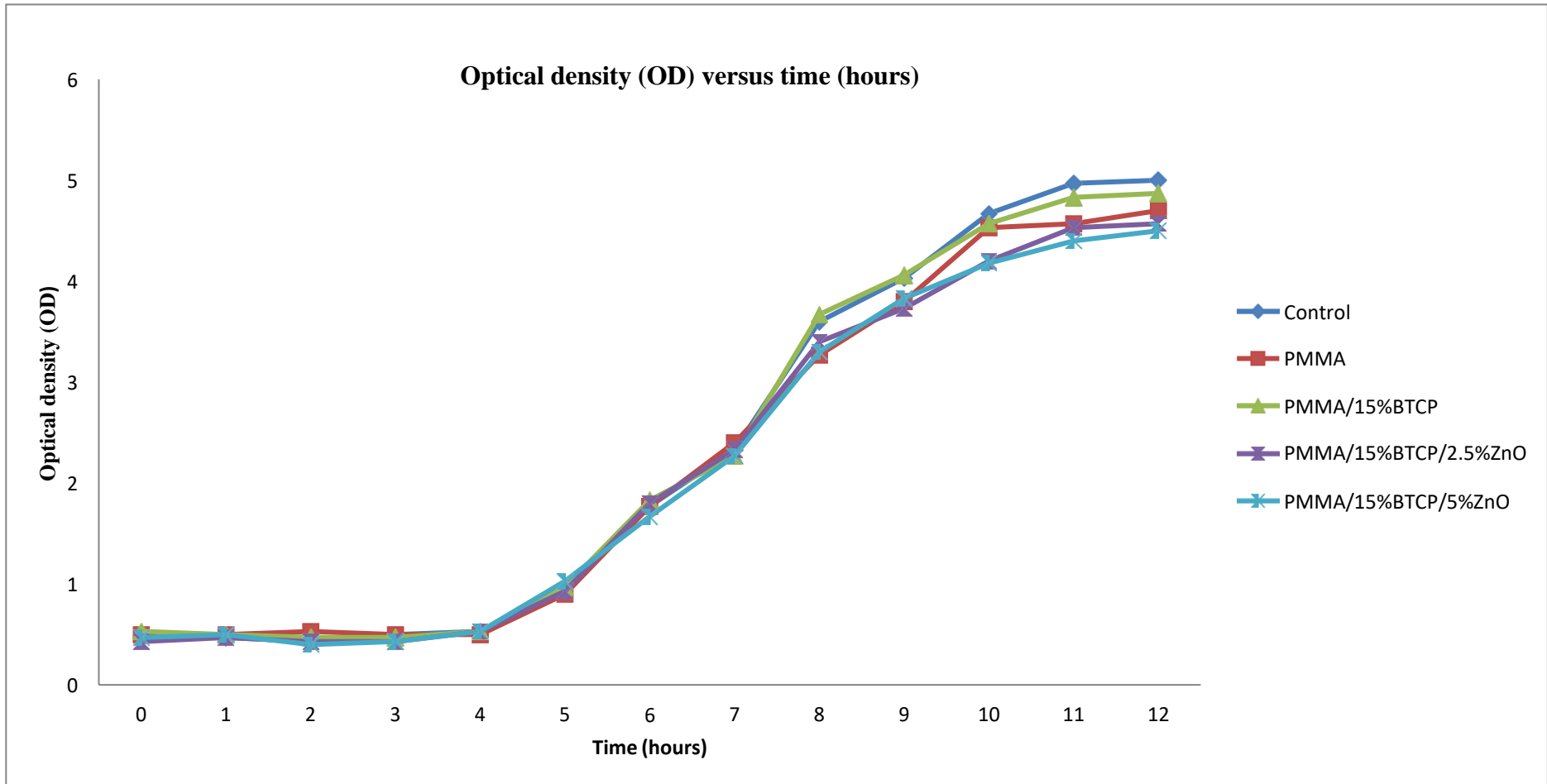
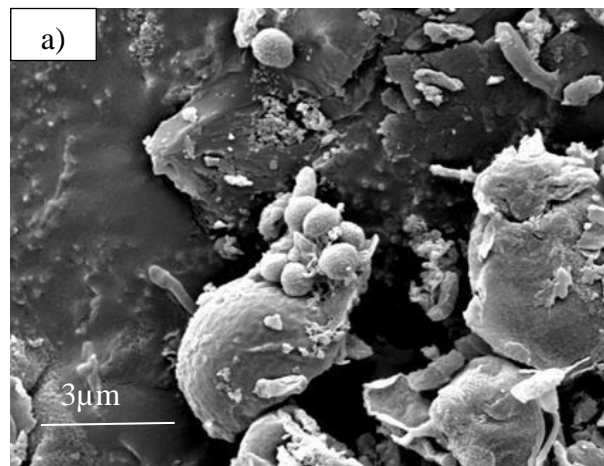


Figure 4.20 OD measurement of *P. aeruginosa* growth on PMMA composites for 12 hours incubation period.

Based on Figure 4.19, all composite samples appeared similar trend in the bacteria growth phases. Nevertheless, after 7 hours in stationary phase, a change was discovered. The lowest OD was revealed for PMMA /15% $\beta$ -TCP/2.5%ZnO indicating that bacterial growth slowly decreased when exposed to the composite having 2.5% ZnO. During stationary phase, extract PMMA/15% $\beta$ -TCP/2.5%ZnO showed significant antibacterial activities for *S.aureus* (Table 4.8).The treated *S.aureus* with 2.5%ZnO was observed to have lowest OD value in stationary phase (Figure 4.19). These values exhibit a significant different with control group  $p < 0.05$  as shown in Table 4.8. During log phase, bacteria reproduce by binary fission and bacteria are in their optimum growth and actively divide at a constant maximum rate. The result of antibacterial activities of treated bacteria for sample 2.5%ZnO marked potential values as antibacterial agent for *S.aureus*. The SEM images support the observation from the significant result toward bacteria in Figure 4.21 a) and b).





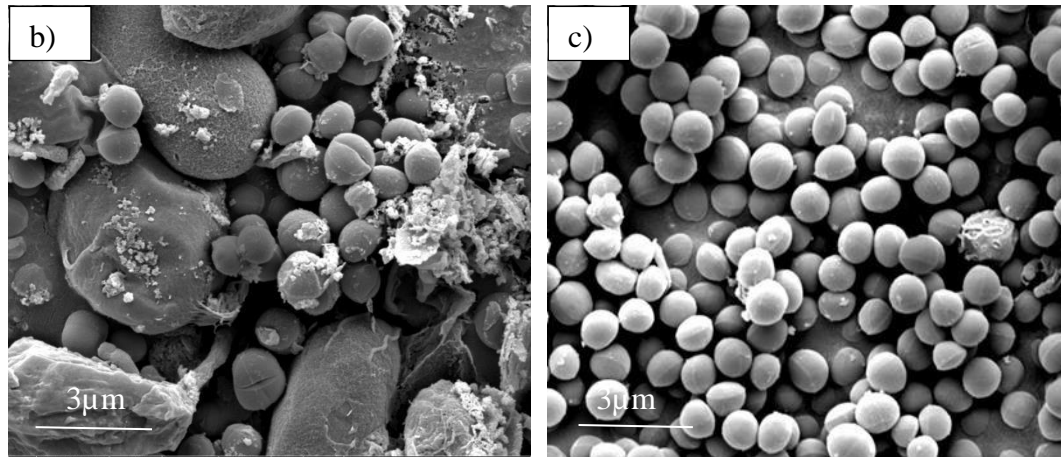


Figure 4.21 SEM photographs of structure of *S.aureus* treated with a)PMMA pure b)PMMA/15%β-TCP/2.5%ZnO and c) PMMA/15%β-TCP/5%ZnO at magnification 30 000x.

As shown in Figure 4.21(c), the morphology of the bacteria on the sample of PMMA/15%-TCP/5%ZnO did not change, indicating that the amount of ZnO at 5% did not significantly kill the bacteria. However, when *S. aureus* was treated with 2.5% ZnO or PMMA pure, its structure was significantly affected. The SEM image showed that PMMA pure treated with *S. aureus* significantly killed the bacteria. Even though there is no literature that PMMA alone has bactericidal effects, this finding suggests that PMMA pure has antibacterial effects on both strains. This is likely due to the monomer of PMMA pure still leaching out into the matrix, attacking the protein enzyme, resulting in cell death. Their cells were shrunken, elongated, and almost lost their normal spherical size. This occurs due to damage to the cell wall (Rahman et al., 2016). The hydrophobicity allowed diffusion process of PMMA through the double layer of membrane and mitochondrion, aggregate the membrane penetrability, leading to leach out of ions and other cells contents (Nazzaro *et al.*, 2013). The cell structure of the microorganism also affected probably due to the amount of ZnO is optimum for 2.5 % hence the action to destroy the cell structure was complete. ZnO itself has ability to

inhibit the growth of *S.aureus* through direct contact to membrane cell due to production of highly reactive species oxygen species released ( $\text{OH}^-$ ,  $\text{H}_2\text{O}_2$  and  $\text{O}_2^{2-}$ ) from ZnO. The antibacterial properties of zinc oxide revealed distorted and ruptured bacterial cell and subsequently damage membrane surface of bacteria as shown in Figure 4.21 (b). Bacterial treated with 5% ZnO seems to have no effect on the morphology of the bacterial *S. aureus*, as evidenced by SEM image shown in Figure 4.21 (c).

Figure 4.20 showed the optical density of bacterial strains *P.aeruginosa* growth. Among these sample groups, sample for PMMA/15% $\beta$ -TCP/5%ZnO revealed low OD values indicated that there was good sign of antibacterial activity.

Factor such as surface charge influence the adhesion of bacterial to any substrate. Katsikogianni *et al.*, (2015) mentioned in their study that bacterial adhesion increased on positive charge of PMMA/DMAEMA (dimethylamino ethyl methacrylate). Which is in agreement of our study of PMMA with positive charge of zinc ion. On the other hand, negatively charge of acrylic acid (PMMA/AA) would reduce the bacterial adhesion. However, Watterson *et al.* (2002), found that acrylic polymers not exhibited antimicrobial compound, because of that the combination of super hydrophobic surface play a role as a protection layer in reducing bacterial attachment instead of existence of antimicrobial compounds.

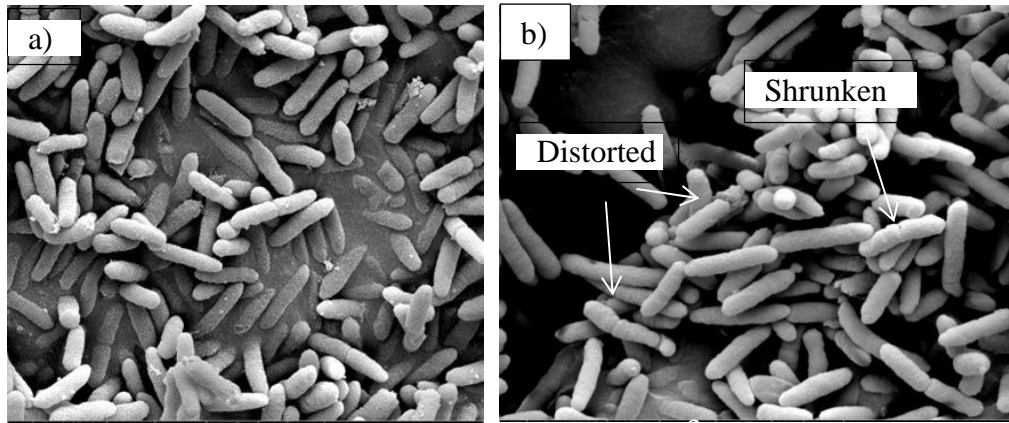


Figure 4.22 SEM photograph of a) untreated *P. aeruginosa* b) *P. aeruginosa* treated with PMMA pure under 30000x magnification.

All PMMA composites were shown to be significantly different compared to the untreated bacteria (Table 4.9). For PMMA/15% $\beta$ -TCP/5%ZnO, the optical density showed the lowest reading compared to other PMMA composites. As seen in Figure 4.22 (b), there was some rupture of the cell structure, indicating that pure PMMA significantly killed *P. aeruginosa* bacterial cells compared to untreated cells (Figure 4.22 (a)). Incorporation of 5% ZnO into PMMA composites is the highest composition that showed the highest antibacterial activity. Thus, in agreement with the study by Ann *et al.*(2014a), higher percentages of ZnO will induce higher toxicity to the bacteria. Production of reactive oxygen species (ROS) contributes to the toxicity level because ROS species like hydrogen peroxide H<sub>2</sub>O<sub>2</sub>, superoxide ion O<sub>2</sub><sup>-</sup> and hydroxyl radicals OH could damage cellular constituents like DNA, lipids, and protein. A number of oxygen atoms play a role in the contribution of ROS. ROS is usually produced by activity in the presence of UV light, but other researchers (Jones *et al.*, 2008; Hirota *et al.*, 2010) found that ROS can also be produced in darkness.

Structure of ZnO also affected to the antibacterial activity. ZnO in the form of rod structure has more O<sub>2</sub> atom while ZnO of plate's structure has deficient number of O<sub>2</sub> atom resulting to the oxidative stress towards bacteria. Rods and wires shape of ZnO-

NPs are easily penetrate into bacteria cell compared to spherical shape (Sirelkhatim *et al.*, 2015, Ann *et al.* (2015). Hence, the effect of toxicity also different (Ann *et al.*, 2014a).

Furthermore, decreasing particle size will enhancing antibacterial activity, the smaller particles size will yield to a higher number of ZnO nanopowder particles per unit volume for H<sub>2</sub>O<sub>2</sub> generation since hydrogen peroxide (H<sub>2</sub>O<sub>2</sub>) generated from ZnO surface is effective for inhibiting bacterial growth (Mohd Bakhori *et al.*, 2017).

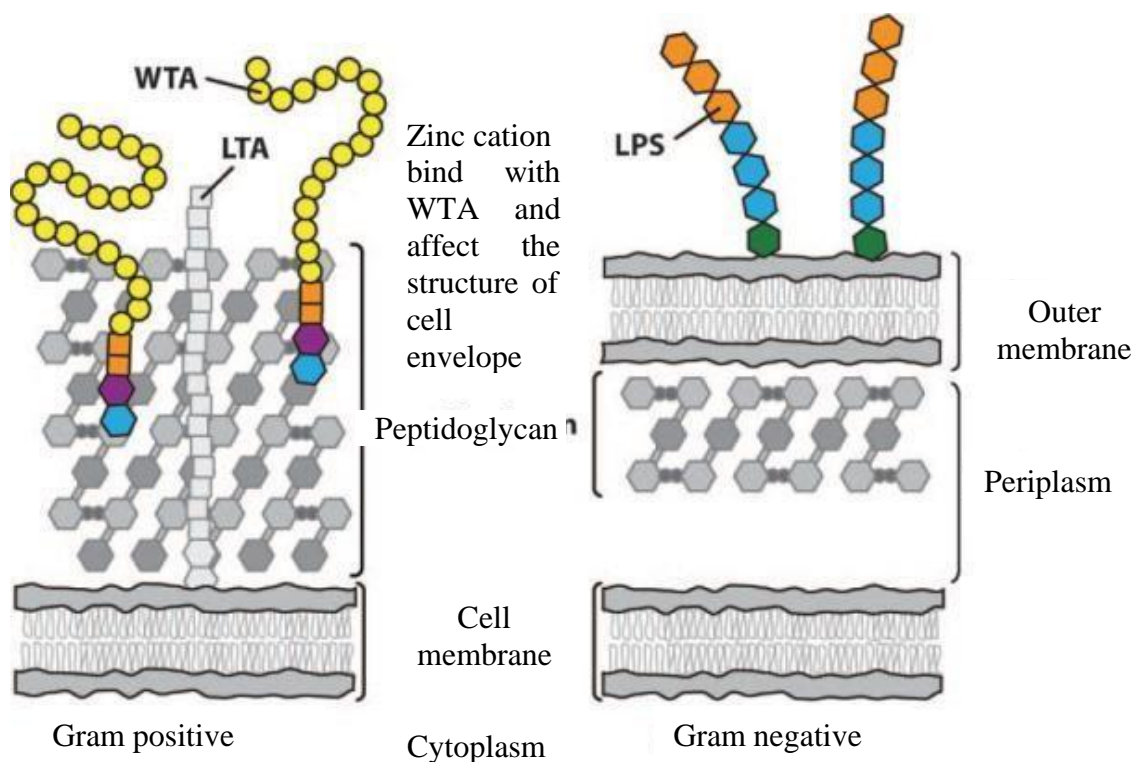


Figure 4.23 Possible mechanism of zinc oxide on both Gram-positive and negative bacteria.

Other possible mechanism of inhibition in antibacterial activities was the presence of cationic substance. The cation substance of ZnO presumably bonded with wall teichoic acids (WTA), then reacted to elongated or shrunken bacterial cell thereby

damage the cell as shown in Figure 4.23. WTAs is involved since the functions is related to protection of bacteria itself from any distribution from threats and adverse condition, also it acts to maintain the bacteria surface characteristics .The changes of bacterial after treatment of antibacterial agent such as abnormalities in morphological like cell size increase, non-uniform of peptidoglycan thickening cell wall and defects also due to the disruption of teichoic acid in bacterial cell (Rahman, 2018).

## CHAPTER 5

### CONCLUSION, LIMITATIONS AND RECOMMENDATIONS

#### 5.1 Conclusion

In this study,

- i. The fabricated PMMA composite was successfully developed.
- ii. Surface roughness and shrinkage of PMMA composite was significantly reduced with addition of fillers as compared to pure PMMA. There was a significant difference in surface roughness between pure PMMA and all PMMA composites, whereas, for shrinkage, a significant difference was only detected between pure and developed composites of PMMA/15% $\beta$ -TCP/5%ZnO.
- iii. As compared to pure PMMA, all PMMA composites showed a significant reduction in flexural strength. The tensile strength of PMMA/15% $\beta$ -TCP/5%ZnO was significantly reduced. The modulus, on the other hand, was unaffected. Within 0, 15, 45, and 60 days of immersion in SBF, there were no significant detected for all composites for fracture toughness value, with the exception of PMMA/10% $\beta$ -TCP, which showed a significant increase at 45 days. Hence, it promised that the implant would last longer.
- iv. All PMMA composites were found to be non-toxic at all concentrations ranging from 6.25 to 100mg/ml except for PMMA composite with 2.5%ZnO for concentration 100 mg/ml. As a result, the patient will be fitted with a PMMA composite suit.
- v. In agar diffusion, ZnO-filled PMMA has shown its antibacterial activity on *S. aureus* only, whereas for *P. aeruginosa* there was no inhibition zone detected. Optical density showed the lowest percentages for PMMA/15% $\beta$ -TCP/2.5%ZnO, indicating that the antibacterial activity was efficient for

PMMA/ $\beta$ -TCP/2.5%ZnO compared to the other composites. Incorporation of ZnO at 2.5% and 5% showed a promising antibacterial which effectively inhibited both bacteria strains compared to other composites without ZnO.

## **5.2 Recommendations**

- i. Incorporation of coupling agent should be introduced for better bonding, hence give the impact to increase mechanical properties of PMMA composites.
- ii. Other type of antibacterial agents such as natural-based chitosan should be introduced to enhance antibacterial activity.
- iii. Further investigation needs to perform for in vivo analysis in order to evaluate overall biocompatibility of material.

## REFERENCES

- Abdullah, A. M., Rahim, T. N. A. T., Hamad, W. N. F. W., Mohamad, D., Akil, H. M., & Rajion, Z. A. (2018). Mechanical and cytotoxicity properties of hybrid ceramics filled polyamide 12 filament feedstock for craniofacial bone reconstruction via fused deposition modelling. *Dental Materials*, **34(11)**, e309–e316. doi:10.1016/j.dental.2018.09.006
- Abdullah, Z. S. (2015). The effect of addition of hydroxyapatite microscopic fillers on surface roughness and some mechanical properties of heat cured acrylic resin, **27(September)**, 50–54.
- Actis, L., Gaviria, L., Guda, T., & Ong, J. L. (2013). Antimicrobial surfaces for craniofacial implants: state of the art. *Journal of the Korean Association of Oral and Maxillofacial Surgeons*, **39(2)**, 43–54. doi:10.5125/jkaoms.2013.39.2.43
- Ahmed, M. A., & Ebrahim, M. I. (2014). Effect of Zirconium Oxide Nano-Fillers Addition on the Flexural Strength , Fracture Toughness , and Hardness of Heat-Polymerized Acrylic Resin. *World Journal of Nano Science and Engineering*, **4(June)**, 50–57.
- Al-sanabani, J. S., Madfa, A. A., & Al-sanabani, F. A. (2013). Application of Calcium Phosphate Materials in Dentistry. *International Journal of Biomaterials*.
- Alharez, A. O., & Ahmad, Z. A. (2011). Effect of Al<sub>2</sub>O<sub>3</sub>/ZrO<sub>2</sub> reinforcement on the mechanical properties of PMMA denture base. *Journal of Reinforced Plastics and Composites*, **30(1)**, 86–93. doi:10.1177/0731684410379511
- Alp, G., Murat, S., & Yilmaz, B. (2019). Comparison of Flexural Strength of Different CAD/CAM PMMA-Based Polymers. *Journal of Prosthodontics*, **28(2)**, e491–e495. doi:10.1111/jopr.12755
- Alshemary, A. Z., Goh, Y.-F., Shakir, I., & Hussain, R. (2015). Synthesis, characterization and optical properties of chromium doped β-Tricalcium phosphate. *International Ceramics*, **41(1, Part B)**, 1663–1669. doi:http://dx.doi.org/10.1016/j.ceramint.2014.09.107
- Ann, L. C., Mahmud, S., Bakhori, S. K. M., Sirelkhatim, A., Mohamad, D., Hasan, H., ... Rahman, R. A. (2014a). Antibacterial responses of zinc oxide structures against *Staphylococcus aureus*, *Pseudomonas aeruginosa* and *Streptococcus pyogenes*. *Ceramics International*, **40(2)**, 2993–3001. doi:10.1016/j.ceramint.2013.10.008
- Ann, L. C., Mahmud, S., Bakhori, S. K. M., Sirelkhatim, A., Mohamad, D., Hasan, H., ... Rahman, R. A. (2014b). Effect of surface modification and UVA photoactivation on antibacterial bioactivity of zinc oxide powder. *Applied Surface Science*, **292**, 405–412. doi:10.1016/j.apsusc.2013.11.152
- Ann, L. C., Mahmud, S., Seeni, A., Bakhori, S. K. M., Sirelkhatim, A., Mohamad, D., & Hasan, H. (2015). Structural morphology and in vitro toxicity studies of nano- and micro-sized zinc oxide structures. *Journal of Environmental Chemical Engineering*, **3(1)**, 436–444. doi:10.1016/j.jece.2014.12.015



- Arakawa, K. (2010). Shrinkage forces due to polymerization of light-cured dental composite resin in cavities. *Polymer Testing*, **29**(8), 1052–1056. doi:10.1016/j.polymertesting.2010.09.008
- Ayre, W. N., Denyer, S. P., & Evans, S. L. (2014). Ageing and moisture uptake in polymethyl methacrylate (PMMA) bone cements. *Journal of the Mechanical Behavior of Biomedical Materials*, **32**, 76–88. doi:10.1016/j.jmbbm.2013.12.010
- Baino, F., & Vitale-Brovarone, C. (2015). Ceramics for oculo-orbital surgery. *Ceramics International*, **41**(4), 5213–5231. doi:10.1016/j.ceramint.2014.12.086
- Barba, T., Fort, R., Cottin, V., Provencher, S., & Durieu, I. (2019). Autoimmunity Reviews Treatment of idiopathic inflammatory myositis associated interstitial lung disease: A systematic review and meta-analysis. *Autoimmunity Reviews*, **18**(2), 113–122. doi:10.1016/j.autrev.2018.07.013
- Baroudi, K., Saleh, A. M., Silikas, N., & Watts, D. C. (2007). Shrinkage behaviour of flowable resin-composites related to conversion and filler-fraction. *Journal of Dentistry*, **35**(8), 651–655. doi:10.1016/j.jdent.2007.05.001
- Bauer, S., Schmuki, P., Mark, K. Von Der, & Park, J. (2013). Progress in Materials Science Engineering biocompatible implant surfaces Part I: Materials and surfaces. *Progress in Materials Science*, **58**(3), 261–326. doi:10.1016/j.pmatsci.2012.09.001
- Blyth, C. C., Gomes, L., Sorrell, T. C., Da Cruz, M., Sud, A., & Chen, S. C. A. (2011). Skull-base osteomyelitis: Fungal vs. bacterial infection. *Clinical Microbiology and Infection*, **17**(2), 306–311. doi:10.1111/j.1469-0691.2010.03231.x
- Bodey, G. P., Bolivar, R., Fainstein, V., & Jadeja, L. (1983). Infections Caused by *Pseudomonas aeruginosa*. *Reviews of Infectious Diseases*, **5**(2), 279–313.
- Botsi, S., Tsamis, C., Chatzichristidi, M., Papageorgiou, G., & Makarona, E. (2019). Facile and cost-efficient development of PMMA-based nanocomposites with custom-made hydrothermally-synthesized ZnO nanofillers. *Nano-Structures and Nano-Objects*, **17**, 7–20. doi:10.1016/j.nanoso.2018.10.003
- Breitbart, A. S., & Ablaza, V. J. (2007). Chapter 7 ■ Implant Materials. *Grabb and Smith's Plastic Surgery*, 58–65.
- Busscher, H. J., Weerkamp, A. H., van Der Mei, H. C., van Pelt, A. W., de Jong, H. P., & Arends, J. (1984). Measurement of the surface free energy of bacterial cell surfaces and its relevance for adhesion. *Applied and Environmental Microbiology*, **48**(5), 980–983. doi:10.1128/aem.48.5.980-983.1984
- Cai, R., Wang, H., Cao, M., Hao, L., Zhai, L., Jiang, S., & Li, X. (2015). Synthesis and antimicrobial activity of mesoporous hydroxylapatite/zinc oxide nanofibers. *Materials and Design*, **87**, 17–24. doi:10.1016/j.matdes.2015.08.004
- Carrodeguas, R. G., & De Aza, S. (2011).  $\alpha$ -Tricalcium phosphate: Synthesis, properties and biomedical applications. *Acta Biomaterialia*, **7**(10), 3536–3546. doi:10.1016/j.actbio.2011.06.019
- Chair, K., Bedoui, A., Bensalah, N., Sáez, C., Fernández-Morales, F. J., Cotillas, S., ... Rodrigo, M. A. (2017). Treatment of Soil-Washing Effluents Polluted with Herbicide

- Oxyfluorfen by Combined Biosorption-Electrolysis. *Industrial and Engineering Chemistry Research*, **56(8)**, 1903–1910. doi:10.1021/acs.iecr.6b04977
- Chakraborty, H., Sinha, A., Mukherjee, N., Ray, D., & Protim Chattopadhyay, P. (2013). A study on nanoindentation and tribological behaviour of multifunctional ZnO/PMMA nanocomposite. *Materials Letters*, **93**, 137–140. doi:10.1016/j.matlet.2012.11.075
- Chang, P. in. (1981). Polymer implant materials with improved X-ray opacity and biocompatibility. *Biomaterials*, **2(3)**, 151–155. doi:10.1016/0142-9612(81)90041-7
- Characterization, M. (2004). Key Words :, **3(1)**, 23–31.
- Chatterjee, A. (2010). Properties Improvement of PMMA Using Nano TiO<sub>2</sub>. *Journal Of Applied Polymer Science*, **118**, 2890–2897. doi:10.1002/app
- Chatterjee, D. K., Gnanasammandhan, M. K., & Zhang, Y. (2010). Small Upconverting Fluorescent Nanoparticles for Biomedical Applications. *Www.Small-Journal.Com*, **6(24)**, 2781–2795. doi:10.1002/sml.201000418
- Chatzistavrou, X., Fenno, J. C., Faulk, D., Badylak, S., Kasuga, T., Boccaccini, A. R., & Papagerakis, P. (2014). Fabrication and characterization of bioactive and antibacterial composites for dental applications. *Acta Biomaterialia*, **10(8)**, 3723–3732. doi:10.1016/j.actbio.2014.04.030
- Chew, K. W., & Tan, K. W. (2011). The effects of ceramic fillers on PMMA-based polymer electrolyte salted with lithium triflate, LiCF<sub>3</sub>SO<sub>3</sub>. *International Journal of Electrochemical Science*, **6(11)**, 5792–5801.
- Choi, J. J. E., Uy, C. E., Ramani, R. S., & Waddell, J. N. (2020). Evaluation of surface roughness, hardness and elastic modulus of nanoparticle containing light-polymerized denture glaze materials. *Journal of the Mechanical Behavior of Biomedical Materials*, **103(October 2019)**, 103601. doi:10.1016/j.jmbbm.2019.103601
- Chou, P. M., Mariatti, M., Chou, P. M., & Mariatti, M. (2010). The Properties of Polymethyl Methacrylate ( PMMA ) Bone Cement Filled with Titania and Hydroxyapatite Fillers The Properties of Polymethyl Methacrylate ( PMMA ) Bone Cement Filled with Titania and Hydroxyapatite Fillers, **2559**. doi:10.1080/03602559.2010.496403
- Chow, W. S., Tay, H. K., Azlan, A., & Ishak, Z. A. M. (2008). Mechanical and Thermal Properties of Hydroxyapatite Filled Poly ( Methyl Methacrylate ) Composites. *Proceedings of the Polymer Processing Society 24th Annual Meeting*, 1–3.
- Chuan, D., Zhang, L., Leng, C., Chen, Q., Miyazaki, T., & Liu, J. (2020). Setting behavior, apatite-forming ability, mechanical strength of polymethylmethacrylate bone cement through bioactivity modification of phosphate functional groups combined with Ca<sup>2+</sup> ions. *Journal of Biomaterials Science, Polymer Edition*, **31(16)**, 2128–2151. doi:10.1080/09205063.2020.1795459
- Cierech, M., Wojnarowicz, J., Kolenda, A., & Krawczyk-balska, A. (2019). Zinc Oxide Nanoparticles Cytotoxicity and Release from Newly Formed PMMA – ZnO Nanocomposites Designed for Denture Bases. *Nanomaterials*, **9**, 1318.

- Colombini, M. (2004). VDAC : The channel at the interface between mitochondria and the cytosol. *Molecular and Cellular Biochemistry*, **(256)**, 107–115.
- Combes, C., & Rey, C. (2010). Amorphous calcium phosphates: Synthesis, properties and uses in biomaterials. *Acta Biomaterialia*, **6(9)**, 3362–3378. doi:10.1016/j.actbio.2010.02.017
- Cross, M., Douglas, W. H., & Fields, R. P. (1983). The Relationship Between Filler Loading and Particle Size Distribution in Composite Resin Technology. *J Dental Restorative*, **62(7)**, 3–5.
- Daglilar, S., & Erkan, M. E. (2007). A study on bioceramic reinforced bone cements. *Materials Letters*, **61(7)**, 1456–1459. doi:10.1016/j.matlet.2006.07.068
- Dalby, M. J., Silvio, L. Di, Harper, E. J., & Bon, W. (2001). Initial interaction of osteoblasts with the surface of a hydroxyapatite-poly ( methylmethacrylate ) cement. *Biomaterial*, **22**, 1739–1747.
- Dalby, M. J., Silvio, L. Di, Harper, E. J., & Bonfield, W. (2002). Increasing hydroxyapatite incorporation into poly ( methylmethacrylate ) cement increases osteoblast adhesion and response. *Biomaterials*, **23**, 569–576.
- Daniels, A. U., Chang, M. K., & Andriano, K. P. (1990). Mechanical properties of biodegradable polymers and composites proposed for internal fixation of bone. *Journal of Applied Biomaterials : An Official Journal of the Society for Biomaterials*, **1(1)**, 57–78. doi:10.1002/jab.770010109
- Ding, M., Sahebgharani, N., Musharavati, F., Jaber, F., Zalnezhad, E., & Yoon, G. H. (2018). Synthesis and properties of HA / ZnO / CNT nanocomposite. *Ceramics International*, **44(7)**, 7746–7753. doi:10.1016/j.ceramint.2018.01.203
- Elshereksi, N. W., Mohamed, S. H., Arifin, A., & Ishak, Z. A. M. (2009a). Effect of Filler Incorporation on the Fracture Toughness Properties of Denture Base Poly(Methyl Methacrylate). *Journal of Physical Science*, **20(2)**, 1–12.
- Elshereksi, N. W., Mohamed, S. H., Arifin, A., & Ishak, Z. A. M. (2009b). Effect of Filler Incorporation on the Fracture Toughness Properties of Denture Base Poly (Methyl Methacrylate). *Journal of Physical Science*, **20(2)**, 1–12.
- Friedrich, K., Zhang, Z., & Schlarb, A. K. (2005). Effects of various fillers on the sliding wear of polymer composites. *Composites Science and Technology*, **65(15-16 Spec. Iss.)**, 2329–2343. doi:10.1016/j.compscitech.2005.05.028
- Fu, S., Feng, X., Lauke, B., & Mai, Y. (2008). Effects of particle size , particle / matrix interface adhesion and particle loading on mechanical properties of particulate – polymer composites, **39**, 933–961. doi:10.1016/j.compositesb.2008.01.002
- Gad, M. M., Fouda, S. M., Al-harbi, F. A., Napankangas, R., & Raustia, A. (2017). PMMA denture base material enhancement : a review of fiber , filler , and nanofiller addition. *International Journal of Nanomedicine*, **12**, 3801–3812.
- Gao, S., Lv, Y., Yuan, L., Ren, H., Wu, T., Liu, B., ... Zhou, F. (2019). Improved bone ingrowth of tricalcium phosphate filled Poly(methyl methacrylate) (PMMA) bone cements in vivo. *Polymer Testing*. doi:10.1016/j.polymertesting.2019.02.015

- García-Merino, I., de las Cuevas, N., Jiménez, J., Gallego, J., Gómez, C., Prieto, C., ... Serramía, M. J. (2009). The Spanish HIV BioBank: A model of cooperative HIV research. *Retrovirology*, **6**. doi:10.1186/1742-4690-6-27
- Gilbert, J. L., Hasenwinkel, J. M., Wixson, R. L., & Lautenschlager, E. P. (2000). A theoretical and experimental analysis of polymerization shrinkage of bone cement: A potential major source of porosity. *Journal of Biomedical Materials Research*, **52**(1), 210–218. doi:10.1002/1097-4636(200010)52:1<210::AID-JBM27>3.0.CO;2-R
- Gordon, T., Perlstein, B., Houbara, O., Felner, I., Banin, E., & Margel, S. (2011). Synthesis and characterization of zinc/iron oxide composite nanoparticles and their antibacterial properties. *Colloids and Surfaces A: Physicochemical and Engineering Aspects*, **374**(1–3), 1–8. doi:10.1016/j.colsurfa.2010.10.015
- Gottenbos, B., Van Der Mei, H. C., & Busscher, H. J. (2000). Initial adhesion and surface growth of *Staphylococcus epidermidis* and *Pseudomonas aeruginosa* on biomedical polymers. *Journal of Biomedical Materials Research*, **50**(2), 208–214. doi:10.1002/(SICI)1097-4636(200005)50:2<208::AID-JBM16>3.0.CO;2-D
- Grandi, G., Heitz, C., Santos, L. A. Dos, Silva, M. L., Sant’Ana Filho, M., Pagnocelli, R. M., & Silva, D. N. (2011). Comparative histomorphometric analysis between  $\alpha$ -Tcp cement and  $\beta$ -Tcp/Ha granules in the bone repair of rat calvaria. *Materials Research*, **14**(1), 11–16. doi:10.1590/S1516-14392011005000020
- Hajipour, M. J., Fromm, K. M., Ashkarran, A. A., Aberasturi, D. J. De, Larramendi, I. R. De, & Rojo, T. (2012). Antibacterial properties of nanoparticles. *Trends in Biotechnology*, **30**(10), 499–511. doi:10.1016/j.tibtech.2012.06.004
- Harb, S. V., Bassous, N. J., de Souza, T. A. C., Trentin, A., Pulcinelli, S. H., Santilli, C. V., ... Hammer, P. (2020). Hydroxyapatite and  $\beta$ -TCP modified PMMA-TiO<sub>2</sub> and PMMA-ZrO<sub>2</sub> coatings for bioactive corrosion protection of Ti6Al4V implants. *Materials Science and Engineering C*, **116**(April), 111149. doi:10.1016/j.msec.2020.111149
- Hassan, M., Asghar, M., & Din, S. U. (2019). Chapter 8. Thermoset polymethacrylate-based materials for dental applications. *Materials for Biomedical Engineering: Thermoset and Thermoplastic Polymers*. Elsevier Inc. doi:10.1016/B978-0-12-816874-5.00008-6
- Hazra, C., Kundu, D., Chatterjee, A., Chaudhari, A., & Mishra, S. (2014). Poly(methyl methacrylate) (core)-biosurfactant (shell) nanoparticles: Size controlled sub-100nm synthesis, characterization, antibacterial activity, cytotoxicity and sustained drug release behavior. *Colloids and Surfaces A: Physicochemical and Engineering Aspects*, **449**(1), 96–113. doi:10.1016/j.colsurfa.2014.02.051
- Heimann, R. B. (2013). Structure, properties, and biomedical performance of osteoconductive bioceramic coatings. *Surface and Coatings Technology*, **233**, 27–38. doi:10.1016/j.surfcoat.2012.11.013
- Hench, L. L., Splinter, R. J., Allen, W. C., & Greenlee, T. K. (1971). Bonding mechanisms at the interface of ceramic prosthetic materials. *Journal of Biomedical Materials Research*, **5**(6), 117–141. doi:10.1002/jbm.820050611

- Hong, R. Y., Qian, J. Z., & Cao, J. X. (2006). Synthesis and characterization of PMMA grafted ZnO nanoparticles. *Powder Technology*, **163**(3), 160–168. doi:10.1016/j.powtec.2006.01.015
- Horch, H. H., Sader, R., Pautke, C., Neff, A., Deppe, H., & Kolk, A. (2006). Synthetic, pure-phase beta-tricalcium phosphate ceramic granules (Cerasorb®) for bone regeneration in the reconstructive surgery of the jaws. *International Journal of Oral and Maxillofacial Surgery*, **35**(8), 708–713. doi:10.1016/j.ijom.2006.03.017
- Horowitz, M. P., & Greenamyre, J. T. (2010). Mitochondrial Iron Metabolism and Its Role in Neurodegeneration. *Journal of Alzheimer's Disease*, **20**, 551–568. doi:10.3233/JAD-2010-100354
- Hossain, U. H., Lima, V., Baake, O., Severin, D., Bender, M., & Ensinger, W. (2014). Nuclear Instruments and Methods in Physics Research B On-line and post irradiation analysis of swift heavy ion induced modification of PMMA ( polymethyl-methacrylate ). *Nuclear Inst. and Methods in Physics Research, B*, **326**, 135–139. doi:10.1016/j.nimb.2013.10.074
- Hua, X., Bao, Y., Zeng, J., & Wu, F. (2019). Nucleolus-Targeted Red Emissive Carbon Dots with Polarity-Sensitive and Excitation-Independent Fluorescence Emission: High-Resolution Cell Imaging and in Vivo Tracking. *ACS Applied Materials & Interfaces*, **11**, 32647–32658. research-article. doi:10.1021/acsami.9b09590
- Huang, G. J., Zhong, S., Susarla, S. M., Swanson, E. W., Huang, J., & Gordon, C. R. (2015). Craniofacial reconstruction with poly(methyl methacrylate) customized cranial implants. *Journal of Craniofacial Surgery*, **26**(1), 64–70. doi:10.1097/SCS.0000000000001315
- Imazato, S., Toriil, M., Tsuchitani, Y., McCabe, J. E., & Russell, R. R. B. (1994). Incorporation of Bacterial Inhibitor into Resin Composite. *Journal of Dental Research*, **73**(8), 1437–1443. doi:10.1177/00220345940730080701
- Ito, A., Kawamura, H., Otsuka, M., Ikeuchi, M., Ohgushi, H., Ishikawa, K., ... Ichinose, N. (2002). Zinc-releasing calcium phosphate for stimulating bone formation. *Materials Science and Engineering C*, **22**(1), 21–25. doi:10.1016/S0928-4931(02)00108-X
- Itthichaisri, C., Huebner, U., Schoen, R., Schmelzeisen, R., & Gellrich, N. (2007). Comparative in vitro study of the proliferation and growth of human osteoblast-like cells on various biomaterials. *Wiley Interscience*. doi:10.1002/jbm.a
- Jiao, Y., Ma, S., Li, J., Shan, L., Yang, Y., Li, M., & Chen, J. (2015). The influences of N-acetyl cysteine (NAC) on the cytotoxicity and mechanical properties of Poly-methylmethacrylate (PMMA)-based dental resin. *PeerJ*, **2015**(3), 1–16. doi:10.7717/peerj.868
- Johnson, A. J. W., & Herschler, B. A. (2011). Acta Biomaterialia A review of the mechanical behavior of CaP and CaP / polymer composites for applications in bone replacement and repair. *Acta Biomaterialia*, **7**(1), 16–30. doi:10.1016/j.actbio.2010.07.012
- Jones, D. W., & Rizkalla, A. S. (1996). Characterization of Experimental Composite Biomaterials. *Journal of Biomedical Materials Research (Applied Biomaterials)*, **33**,

89–100.

Karthick, R., Sirisha, P., & Sankar, M. R. (2014). Mechanical and Tribological Properties of PMMA-Sea Shell based Biocomposite for Dental application. *Procedia Materials Science*, **6(Icmpc)**, 1989–2000. doi:10.1016/j.mspro.2014.07.234

Kasraei, S., Sami, L., Hendi, S., Alikhani, M.-Y., Rezaei-Soufi, L., & Khamverdi, Z. (2014). Antibacterial properties of composite resins incorporating silver and zinc oxide nanoparticles on Streptococcus mutans and Lactobacillus. *Restorative Dentistry & Endodontics*, **39**, 109–14. doi:10.5395/rde.2014.39.2.109

Katsikogianni, M. G., Wood, D. J., & Missirlis, Y. F. (2015). Biomaterial Functionalized Surfaces for Reducing Bacterial Adhesion and Infection. *Handbook of Bioceramics and Biocomposites*, 1–28. doi:10.1007/978-3-319-09230-0

Katti, K. S. (2004). Biomaterials in total joint replacement. *Colloids and Surfaces B: Biointerfaces*, **39(3)**, 133–142. doi:10.1016/j.colsurfb.2003.12.002

Kenny, S. M., & Buggy, M. (2003). Bone cements and fillers: A review. *Journal of Materials Science: Materials in Medicine*, **14(11)**, 923–938. doi:10.1023/A:1026394530192

Khandaker, M., Li, Y., & Morris, T. (2013). Micro and nano MgO particles for the improvement of fracture toughness of bone – cement interfaces. *Journal of Biomechanics*, **46(5)**, 1035–1039. doi:10.1016/j.jbiomech.2012.12.006

Khullar, S., Chandra, P. S., Doddamani, R. S., Kapil, A., & Dhawan, B. (2016). Chronic osteomyelitis of skull due to Pseudomonas aeruginosa: A delayed uncommon complication following craniotomy. *Journal of Clinical and Diagnostic Research*, **10(12)**, DL01–DL02. doi:10.7860/JCDR/2016/23335.9022

Kim, S. B., Kim, Y. J., Yoon, T. L., Park, S. A., Cho, I. H., Kim, E. J., ... Shin, J. W. (2004). The characteristics of a hydroxyapatite-chitosan-PMMA bone cement. *Biomaterials*, **25(26)**, 5715–5723. doi:10.1016/j.biomaterials.2004.01.022

Kokubo, T. (1996). Formation of biologically active bone-like apatite on metals and polymers by a biomimetic process I. *Thermochimica Acta*, **281**, 479–490.

Kong, W., Yang, H., He, L., Zhao, J., Coppola, D., Dalton, W. S., ... Iol, M. O. L. C. E. L. L. B. (2008). MicroRNA-155 Is Regulated by the Transforming Growth Factor B/Smad Pathway and Contributes to Epithelial Cell Plasticity by Targeting RhoA. *Molecular and Cellular Biology*, **28(22)**, 6773–6784. doi:10.1128/MCB.00941-08

Kuemmerle, J. M., Oberle, A., Oechslin, C., Bohner, M., Frei, C., Boecken, I., & von Rechenberg, B. (2005). Assessment of the suitability of a new brushite calcium phosphate cement for cranioplasty - An experimental study in sheep. *Journal of Cranio-Maxillofacial Surgery*, **33(1)**, 37–44. doi:10.1016/j.jcms.2004.09.002

Kuete, V., Karaosmanoğlu, O., & Sivas, H. (2017). Anticancer Activities of African Medicinal Spices and Vegetables. *Medicinal Spices and Vegetables from Africa: Therapeutic Potential Against Metabolic, Inflammatory, Infectious and Systemic Diseases*, 271–297. doi:10.1016/B978-0-12-809286-6.00010-8

Kul, E., Aladağ, L. İ., & Yesildal, R. (2016). Evaluation of thermal conductivity and

- flexural strength properties of poly(methyl methacrylate) denture base material reinforced with different fillers. *Journal of Prosthetic Dentistry*, **116(5)**, 803–810. doi:10.1016/j.prosdent.2016.03.006
- Kumari, P. (2016). Osteomyelitis: Identification and Management. *MOJ Orthopedics & Rheumatology*, **5(5)**, 322–325. doi:10.15406/mojor.2016.05.00195
- Kusy, R. P., Whitley, J. Q., & Kalachandra, S. (2001). Mechanical properties and interrelationships of poly(methyl methacrylate) following hydration over saturated salts. *Polymer*, **42(6)**, 2585–2595. doi:10.1016/S0032-3861(00)00613-3
- Kwarcinski, J., Boughton, P., Ruys, A., Doolan, A., & Gelder, J. Van. (2006). applied sciences Cranioplasty and Craniofacial Reconstruction : A Review of Implant Material , Manufacturing Method and Infection Risk. *J Applied Science*, 1–17. doi:10.3390/app7030276
- Labres, Xavier, R., Camps, A. R., & Enric Jane Salas, Rui Albuquerque, E. V. O. and J. L.-L. (2014). Graft Materials in Oral Surgery: Revision. *Journal of Biomimetics Biomaterials and Tissue Engineering*, **2014(1)**, 1–7. doi:10.4172/1662-100X.1000124
- Ladha, K., & Shah, D. (2011). An in-vitro evaluation of the flexural strength of heat-polymerized poly (methyl methacrylate) denture resin reinforced with fibers. *Journal of Indian Prosthodontist Society*, **11(4)**, 215–220. doi:10.1007/s13191-011-0086-5
- Lee, S., Wu, C., Lee, S., & Chen, P. (2009). Cranioplasty using polymethyl methacrylate prostheses. *Journal of Clinical Neuroscience*, **16(1)**, 56–63. doi:10.1016/j.jocn.2008.04.001
- Liang, J. (2013). Composites : Part B Reinforcement and quantitative description of inorganic particulate-filled polymer composites. *Composites Part B*, **51**, 224–232. doi:10.1016/j.compositesb.2013.03.019
- Lin, O. H., & Mahmud, S. (2009). Effect of Particle Morphology on the Properties of Polypropylene / Nanometric Zinc Oxide ( Pp / Nanozno ) Composites. *Advanced Composites Letters*, **18(3)**, 77–83.
- Lopez-heredia, M. A., Sa, Y., Salmon, P., Wijn, J. R. De, Wolke, J. G. C., & Jansen, J. A. (2012). Acta Biomaterialia Bulk properties and bioactivity assessment of porous polymethylmethacrylate cement loaded with calcium phosphates under simulated physiological conditions. *Acta Biomaterialia*, **8**, 3120–3127. doi:10.1016/j.actbio.2012.05.007
- Low, P. H., Abdullah, J. Y., Abdullah, A. M., Yahya, S., Idris, Z., & Mohamad, D. (2019). Patient-Specific Reconstruction Utilizing Computer Assisted Three-Dimensional Modelling for Partial Bone Flap Defect in Hybrid Cranioplasty. *The Journal of Craniofacial Surgery*, **30(8)**, e720–e723. doi:10.1097/SCS.00000000000005713
- Ma, Z., Sa, R., Li, Q., & Wu, K. (2015). of hybrid graphene quantum dot and graphitic efficiency for photocatalytic solar water splitting. *Physical Chemistry Chemical Physics*. doi:10.1039/C5CP05847C
- Mano, J. F., Sousa, R. A., Boesel, L. F., Neves, N. M., & Reis, R. L. (2004). Bioinert, biodegradable and injectable polymeric matrix composites for hard tissue replacement:

State of the art and recent developments. *Composites Science and Technology*. doi:10.1016/j.compscitech.2003.09.001

Marghalani, H. Y. (2010). Effect of filler particles on surface roughness of experimental composite series. *J Appl Oral Sci.*, **18**(1), 59–67.

Marra, A., Silvestre, C., Duraccio, D., & Cimmino, S. (2016). Polylactic acid/zinc oxide biocomposite films for food packaging application. *International Journal of Biological Macromolecules*, **88**, 254–262. doi:10.1016/j.ijbiomac.2016.03.039

Matteis, V. De, Cannavale, A., Martellotta, F., Rinaldi, R., Calcagnile, P., Ferrari, F., ... Fiorito, F. (2019). Energy & Buildings Nano-encapsulation of phase change materials: From design to thermal performance, simulations and toxicological assessment. *Energy & Buildings*, **188–189**, 1–11. doi:10.1016/j.enbuild.2019.02.004

Meretoja, V. V., Mattila, R. H., Hautama, M., Aho, A. J., & Vallittu, P. K. (2010). Osteoblast response to polymethyl methacrylate bioactive glass composite. *J Mater Sci: Mater Med*, 1685–1692. doi:10.1007/s10856-010-4018-4

Mickiewicz, R. A. (2001). Polymer-calcium phosphate composites for use as an injectable bone substitute. *Department of Materials Science and Engineering*, (June), 1–42.

Mohd Bakhori, S. K., Mahmud, S., Ling, C. A., Sirelkhatim, A. H., Hasan, H., Mohamad, D., ... Abd Rahman, R. (2017). In-vitro efficacy of different morphology zinc oxide nanopowders on *Streptococcus sobrinus* and *Streptococcus mutans*. *Materials Science and Engineering C*, **78**, 868–877. doi:10.1016/j.msec.2017.04.085

Mok, D., Lessard, L., Cordoba, C., Harris, P. G., & Nikolis, A. (2004). A review of materials currently used in orbital floor reconstruction. *The Canadian Journal of Plastic Surgery = Journal Canadien de Chirurgie Plastique*, **12**(3), 134–40. Retrieved from <http://www.pubmedcentral.nih.gov/articlerender.fcgi?artid=3792801&tool=pmcentrez&rendertype=abstract>

Monchau, F., Hivart, P., Genestie, B., Chai, F., Descamps, M., & Hildebrand, H. F. (2013). Calcite as a bone substitute. Comparison with hydroxyapatite and tricalcium phosphate with regard to the osteoblastic activity. *Materials Science and Engineering C*, **33**(1), 490–498. doi:10.1016/j.msec.2012.09.019

Mori, A. De, Gregorio, E. Di, Kao, A. P., Tozzi, G., Barbu, E., Sanghani-kerai, A., ... Roldo, M. (2019). Antibacterial PMMA Composite Cements with Tunable Thermal and Mechanical Properties. *ACS Omega*. doi:10.1021/acsomega.9b02290

Moszner, N., & Klapdohr, S. (2004). Nanotechnology for dental composites Norbert Moszner and Simone Klapdohr. *Polymer*, **1**, 130–156.

Moursi, A. M., Winnard, A. V., Winnard, P. L., Lannutti, J. J., & Seghi, R. R. (2002). Enhanced osteoblast response to a polymethylmethacrylate-hydroxyapatite composite. *Biomaterials*, **23**(1), 133–144. doi:10.1016/S0142-9612(01)00088-6

Murugavel, S., Ravikumar, C., Jaabil, G., & Alagusundaram, P. (2019). Synthesis, crystal structure analysis, spectral investigations (NMR, FT-IR, UV), DFT calculations, ADMET studies, molecular docking and anticancer activity of 2-(1-benzyl-5-methyl-1H-1,2,3-triazol-4-yl)-4-(2-chlorophenyl)-6-methoxypyridine – A novel poten. *Journal*



- of *Molecular Structure*, **1176**, 729–742. doi:10.1016/j.molstruc.2018.09.010
- Nam, K. (2014). Characterization and bacterial anti-adherent effect on modified PMMA denture acrylic resin containing platinum nanoparticles. *J Adv Prosthodont*, 207–214.
- Nazir, N. M., & Mohamad, D. (2012). Biocompatibility of in House  $\beta$ -Tricalcium Phosphate Ceramics with Normal Human Osteoblast Cell. *Journal of Engineering Science and Technology*, **7(2)**, 169–176.
- Nazzaro, F., Fratianni, F., & Martino, L. De. (2013). Effect of Essential Oils on Pathogenic Bacteria. *Pharmaceuticals*, 1451–1474. doi:10.3390/ph6121451
- Noushad, M., Ab Rahman, I., Che Zulkifli, N. S., Husein, A., & Mohamad, D. (2014). Low surface area nanosilica from an agricultural biomass for fabrication of dental nanocomposites. *Ceramics International*, **40(3)**, 4163–4171. doi:10.1016/j.ceramint.2013.08.073
- Olson, M. E., & Horswill, A. R. (2013). Staphylococcus aureus Osteomyelitis: Bad to the bone. *Cell Host and Microbe*, **13(6)**, 629–631. doi:10.1016/j.chom.2013.05.015
- Omar, M. F., Subli, M. H., Zulkepli, N. N., Abdullah, M. M. A. B., & Ting, S. S. (2014). Experimental Investigation on Mechanical and Morphology Properties of Ultra-High Molecular Zinc Oxide ( ZnO ) Hybrid Composites Experimental Investigation on Mechanical and Morphology Properties of Ultra-High Molecular Weight Polyethelene ( UHMWPE )/ Chit. *8th MUCET*, (March 2016), 10–11.
- Oshtory, R., Lindsey, D. P., Giori, N. J., & Mirza, F. M. (2010). Bioabsorbable tricalcium phosphate bone cement strengthens fixation of suture anchors. *Clinical Orthopaedics and Related Research*, **468(12)**, 3406–3412. doi:10.1007/s11999-010-1412-7
- Padmavathy, N., & Vijayaraghavan, R. (2008). Enhanced bioactivity of ZnO nanoparticles—an antimicrobial study. *Science and Technology of Advanced Materials*, **9(3)**, 035004. doi:10.1088/1468-6996/9/3/035004
- Pandiselvi, K., & Thambidurai, S. (2015). Synthesis, characterization, and antimicrobial activity of chitosan-zinc oxide/polyaniline composites. *Materials Science in Semiconductor Processing*, **31**, 573–581. doi:10.1016/j.mssp.2014.12.044
- Park, C. H., Kim, E. K., Tijing, L. D., Amarjargal, A., Pant, H. R., Kim, C. S., & Shon, H. K. (2014). Preparation and characterization of LA/PCL composite fibers containing beta tricalcium phosphate ( $\beta$ -TCP) particles. *Ceramics International*, **40(3)**, 5049–5054. doi:10.1016/j.ceramint.2013.10.016
- Park, J. H., Bae, J. Y., Shim, J., & Jeon, I. (2012). Evaluation of suitable porosity for sintered porous  $\beta$ -tricalcium phosphate as a bone substitute. *Materials Characterization*, **71**, 103–111. doi:10.1016/j.matchar.2012.06.012
- Pasquet, J., Chevalier, Y., Couval, E., Bouvier, D., & Bolzinger, M. A. (2015). Zinc oxide as a new antimicrobial preservative of topical products: Interactions with common formulation ingredients. *International Journal of Pharmaceutics*, **479(1)**, 88–95. doi:10.1016/j.ijpharm.2014.12.031
- Pasquet, J., Chevalier, Y., Pelletier, J., Couval, E., Bouvier, D., & Bolzinger, M. (2014).

Colloids and Surfaces A : Physicochemical and Engineering Aspects The contribution of zinc ions to the antimicrobial activity of zinc oxide. *Colloids and Surfaces A: Physicochemical and Engineering Aspects*, **457**, 263–274. doi:10.1016/j.colsurfa.2014.05.057

Pawar, R. R., Bajaj, H. C., & Lee, S. (2016). Journal of Industrial and Engineering Chemistry Activated bentonite as a low-cost adsorbent for the removal of Cu ( II ) and Pb ( II ) from aqueous solutions : Batch and column studies. *Journal of Industrial and Engineering Chemistry*, **34**, 213–223. doi:10.1016/j.jiec.2015.11.014

Pefferkorn, A. (2012). Shrinkage characteristics of experimental polymer containing composites under controlled light curing modes. *Polymers*, **4(1)**, 256–274. doi:10.3390/polym4010256

Peng, Z., Wang, L., Du, L., Guo, S., Wang, X., & Tang, T. (2010). Adjustment of the antibacterial activity and biocompatibility of hydroxypropyltrimethyl ammonium chloride chitosan by varying the degree of substitution of quaternary ammonium. *Carbohydrate Polymers*, **81(2)**, 275–283. doi:10.1016/j.carbpol.2010.02.008

Pereira, M. D. M., Oréface, R. L., Mansur, H. S., Lopes, M. T. P., Turchetti-Maia, R. M. D. M., & Vasconcelos, A. C. (2003). Preparation and biocompatibility of poly (methyl methacrylate) reinforced with bioactive particles. *Materials Research*, **6(3)**, 311–315. doi:10.1590/S1516-14392003000300002

Perni, S., Thenault, V., Abdo, P., Margulis, K., Magdassi, S., & Prokopovich, P. (2015). Antimicrobial activity of bone cements embedded with organic nanoparticles. *International Journal of Nanomedicine*, **10**, 6317–6329. doi:10.2147/IJN.S86440

Petrovic, L., Pohle, D., Mu, H., Rechtenwald, T., & Schlegel, K. A. (2006). Effect of b TCP filled polyetheretherketone on osteoblast cell proliferation in vitro, 41–46. doi:10.1007/s11373-005-9032-z

Philip, C. (2012). *Development of the Finite Volume Method for Hip Joint Stress Analysis*. University College Dublin.

Pikis, S., Goldstein, J., & Spektor, S. (2014). Potential neurotoxic effects of polymethylmethacrylate during cranioplasty. *Journal of Clinical Neuroscience*. doi:10.1016/j.jocn.2014.06.006

Poddar, M. K., Sharma, S., & Moholkar, V. S. (2016). Investigations in two-step ultrasonic synthesis of PMMA/ZnO nanocomposites by in-situ emulsion polymerization. *Polymer*, **99**, 453–469. doi:10.1016/j.polymer.2016.07.052

Pulit-Prociak, J., Chwastowski, J., Kucharski, A., & Banach, M. (2016). Functionalization of textiles with silver and zinc oxide nanoparticles. *Applied Surface Science*, **385**, 543–553. doi:10.1016/j.apsusc.2016.05.167

Puska, M., Moritz, N., Aho, A. J., & Vallittu, P. K. (2016). Morphological and mechanical characterization of composite bone cement containing polymethylmethacrylate matrix functionalized with trimethoxysilyl and bioactive glass. *Journal of the Mechanical Behavior of Biomedical Materials*, **59**, 11–20. doi:10.1016/j.jmbbm.2015.12.016

Qasim, S. Bin, Kheraif, A. A. Al, & Ramakrishaniah, R. (2012). An investigation into

- the impact and flexural strength of light cure denture resin reinforced with carbon nanotubes. *World Applied Sciences Journal*, **18(6)**, 808–812. doi:10.5829/idosi.wasj.2012.18.06.942
- Quirynen, M., Marechal, M., Busscher, H. J., Weerkamp, A. H., Darius, P. L., & van Steenberghe, D. (1990). The influence of surface free energy and surface roughness on early plaque formation: An in vivo study in man. *Journal of Clinical Periodontology*, **17(3)**, 138–144. doi:10.1111/j.1600-051X.1990.tb01077.x
- Radha, G., Balakumar, S., Venkatesan, B., & Vellaichamy, E. (2017). A novel nano-hydroxyapatite – PMMA hybrid scaffolds adopted by conjugated thermal induced phase separation (TIPS) and wet-chemical approach: Analysis of its mechanical and biological properties. *Materials Science and Engineering: C*, **73**, 164–172. doi:10.1016/j.msec.2016.11.098
- Radin, S. R., & Ducheyne, P. (1993). The effect of calcium phosphate ceramic composition and structure on in vitro behavior.II.Precipitation. *Journal of Biomedical Materials Research*, **27**, 35–45.
- Rahim, Tuan, Tuan, A., Mohamad, D., Akil, H., Ab, I., ... Ab Rahman, I. (2012). Water sorption characteristics of restorative dental composites immersed in acidic drinks. *Dental Materials*, **28(6)**, e63–e70. doi:10.1016/j.dental.2012.03.011
- Rahman, F. S. A. (2018). *Synthesis and cytotoxicity studies of coumarin derivatives as antibacterial agent for newly developed glass ionomer cements (GICS)*. Universiti Sains Malaysia.
- Rahman, F. S. A., Yusufzai, S. K., Osman, H., & Mohamad, D. (2016). Synthesis, characterisation and cytotoxicity activity of thiazole substitution of coumarin derivatives (characterisation of coumarin derivatives). *Journal of Physical Science*, **27(1)**, 77–87.
- Raj, I., Mozetic, M., Jayachandran, V. P., & Jose, J. (n.d.). Fracture resistant , antibio film adherent , self- assembled PMMA / ZnO nanoformulations for biomedical applications : physico-chemical and biological perspectives of nano reinforcement.
- Ramakrishna, S., Mayer, J., Wintermantel, E., & Leong, K. W. (2001). Biomedical applications of polymer-composite materials: A review. *Composites Science and Technology*, **61(9)**, 1189–1224. doi:10.1016/S0266-3538(00)00241-4
- Ramesh, S., Leen, K. H., Kumutha, K., & Arof, A. K. (2007). FTIR studies of PVC/PMMA blend based polymer electrolytes. *Spectrochimica Acta - Part A: Molecular and Biomolecular Spectroscopy*, **66(4–5)**, 1237–1242. doi:10.1016/j.saa.2006.06.012
- Ridwan-Pramana, A., Wolff, J., Raziei, A., Ashton-James, C. E., & Forouzanfar, T. (2015). Porous polyethylene implants in facial reconstruction: Outcome and complications. *Journal of Cranio-Maxillofacial Surgery*, **43(8)**, 1330–1334. doi:10.1016/j.jcms.2015.06.022
- Salem, W., Leitner, D. R., Zingl, F. G., Schratte, G., Prassl, R., Goessler, W., ... Schild, S. (2014). Antibacterial activity of silver and zinc nanoparticles against *Vibrio cholerae* and enterotoxigenic *Escherichia coli*. *International Journal of Medical Microbiology* :

IJMM. doi:10.1016/j.ijmm.2014.11.005

Samad, H. A., Jaafar, M., Othman, R., Kawashita, M., & Razak, N. H. A. (2011). New bioactive glass-ceramic : Synthesis and application in PMMA bone cement composites. *Bio-Medical Materials and Engineering*, **21**, 247–258. doi:10.3233/BME-2011-0673

Santos, M., Soo, S., & Petridis, H. (2013). The effect of Parylene coating on the surface roughness of PMMA after brushing. *Journal of Dentistry*, **41(9)**, 802–808. doi:10.1016/j.jdent.2013.06.011

Sawai, J. (2003). Quantitative evaluation of antibacterial activities of metallic oxide powders (ZnO, MgO and CaO) by conductimetric assay. *Journal of Microbiological Methods*, **54(2)**, 177–182. doi:10.1016/S0167-7012(03)00037-X

Shalabi, M. M., Gortemaker, A., & Hof, M. A. Van. (2006). Critical Reviews in Oral Biology & Medicine Implant Surface Roughness and Bone Healing : *International and American Associations for Dental Research*. doi:10.1177/154405910608500603

Sharma, D., Rajput, J., Kaith, B. S., Kaur, M., & Sharma, S. (2010). Synthesis of ZnO nanoparticles and study of their antibacterial and antifungal properties. *Thin Solid Films*, **519(3)**, 1224–1229. doi:10.1016/j.tsf.2010.08.073

Siddique, R. (2004). Performance characteristics of high-volume Class F fly ash concrete. *Cement and Concrete Research*, **CI(March 2003)**, 487–493. doi:10.1016/j.cemconres.2003.09.002

Silikas, N., Al-Kheraif, A., & Watts, D. C. (2005). Influence of P/L ratio and peroxide/amine concentrations on shrinkage-strain kinetics during setting of PMMA/MMA biomaterial formulations. *Biomaterials*, **26(2)**, 197–204. doi:10.1016/j.biomaterials.2004.02.028

Sirelkhatim, A. H., Mahmud, S., Azman, S., Dasmawati, M., Habsah, H., Sendi, R. K., ... Rahman, M. A. A. (2013). Structural, Optical and Antibacterial Properties of ZnO Commercial Powder Grades. *Advanced Materials Research*, **795(September)**, 19–23. doi:10.4028/www.scientific.net/AMR.795.19

Sirelkhatim, A., Mahmud, S., Seeni, A., Kaus, N. H. M., Ann, L. C., Bakhori, S. K. M., ... Mohamad, D. (2015). Review on zinc oxide nanoparticles: Antibacterial activity and toxicity mechanism. *Nano-Micro Letters*, **7(3)**, 219–242. doi:10.1007/s40820-015-0040-x

Sodagar, A., Khalil, S., Kassae, M. Z., & Shahroudi, A. S. (2016). Antimicrobial properties of poly (methyl methacrylate) acrylic resins incorporated with silicon dioxide and titanium dioxide nanoparticles on cariogenic bacteria. *Journal of Orthodontic Science*, 7–13. doi:10.4103/2278-0203.176652

Soumya, S., Mohamed, A. P., Paul, L., Mohan, K., & Ananthakumar, S. (2014). Solar Energy Materials & Solar Cells Near IR reflectance characteristics of PMMA / ZnO nanocomposites for solar thermal control interface films. *Solar Energy Materials & Solar Cells*, **125**, 102–112. doi:10.1016/j.solmat.2014.02.033

Sousa, R. A., Reis, R. L., Cunha, A. M., & Bevis, M. J. (2003). Processing and properties of bone-analogue biodegradable and bioinert polymeric composites. *Composites Science and Technology*. doi:10.1016/S0266-3538(02)00213-0

- Soygun, K., Bolayir, G., & Boztug, A. (2013). Mechanical and thermal properties of polyamide versus reinforced PMMA denture base materials. *Journal of Advanced Prosthodontics*, **5**(2), 153–160. doi:10.4047/jap.2013.5.2.153
- Stefanic, M., Krnel, K., & Kosmac, T. (2013). Novel method for the synthesis of a ??-tricalcium phosphate coating on a zirconia implant. *Journal of the European Ceramic Society*, **33**(15–16), 3455–3465. doi:10.1016/j.jeurceramsoc.2013.05.015
- Steflik, D. E., Sisk, A. L., & Gardr, G. R. P. L. K. (1993). Osteogenesis at the dental implant interface : High-voltage electron microscopic and conventional transmission electron microscopic observations. *Journal of Biomedical Materials Research*, **27**, 791–800.
- Tham, W. L., Chow, W. S., & Ishak, Z. A. M. (2010). Simulated body fluid and water absorption effects on poly (methyl methacrylate)/ hydroxyapatite denture base composites. *EXPRESS Polymer Letters*, **4**(9), 517–528. doi:10.3144/expresspolymlett.2010.66
- Tham, W. L., Chow, W. S., & Ishak, Z. A. M. (2011). Effects of titanate coupling agent on the mechanical , thermal , and morphological properties of poly (methyl methacrylate)/ hydroxyapatite denture base composites. *Journal of Composite Materials*. doi:10.1177/0021998311401085
- Tjong, S. C. (2006). Structural and mechanical properties of polymer nanocomposites, **53**(August), 73–197. doi:10.1016/j.msar.2006.06.001
- Varela-rizo, H., Weisenberger, M., Bortz, D. R., & Martin-gullon, I. (2010). Fracture toughness and creep performance of PMMA composites containing micro and nanosized carbon filaments. *Composites Science and Technology*, **70**(7), 1189–1195. doi:10.1016/j.compscitech.2010.03.005
- Velu, R., & Singamneni, S. (2015). Thermal Aspects of Selective Laser Sintering of PMMA+B-TCP Composites. *SFF Symposium Proceedings*, 1738–1749.
- Verné, E., Foroni, F., Lucchetta, G., & Miola, M. (2019). Antibacterial and Bioactive Composite Bone Cements. *Current Materials Science*, 144–153. doi:10.2174/1874464812666190819143740
- Vimbela, G. V, Ngo, S. M., Frazee, C., Yang, L., & Stout, D. A. (2017). Antibacterial properties and toxicity from metallic nanomaterials. *International Journal of Nanomedicine*, **12**, 3941–3965.
- Vojdani, M., Bagheri, R., & Khaledi, A. A. R. (2012). Effects of aluminum oxide addition on the flexural strength, surface hardness, and roughness of heat-polymerized acrylic resin. *Journal of Dental Sciences*, **7**(3), 238–244. doi:10.1016/j.jds.2012.05.008
- Wacharawichanant, S. (2010). Effect of Zinc Oxide on the Morphology and Mechanical Properties of Poly (Styrene-co-Acrylonitrile)/Poly (Methyl Methacrylate)/Zinc Oxide Composites. *Science Journal UBU*, **1**(2), 21–26. Retrieved from [http://scjubu.sci.ubu.ac.th/document/Eng/1\\_2\\_2010/3.pdf](http://scjubu.sci.ubu.ac.th/document/Eng/1_2_2010/3.pdf)
- Watterson, J. M., Watson, D. G., Meyer, E. M., & Lenox, R. H. (2002). A role for protein kinase C and its substrates in the action of valproic acid in the brain : implications for neural plasticity. *Brain Research*, **934**, 69–80.

- Woodruff, M. A., & Hutmacher, D. W. (2010). The return of a forgotten polymer - Polycaprolactone in the 21st century. *Progress in Polymer Science (Oxford)*, **35(10)**, 1217–1256. doi:10.1016/j.progpolymsci.2010.04.002
- Yadav, R., & Kumar, M. (2020). Investigation of the physical, mechanical and thermal properties of nano and micro-sized particulate-filled dental composite material. *Journal of Composite Materials*. doi:10.1177/0021998320902212
- Yadav, S. K., Ray, S., Ershad, M. D., Vyas, V. K., Prasad, S., Ali, A., ... Pyare, R. (2017). Development of zirconia substituted 1393 bioactive glass for orthopaedic application. *Oriental Journal of Chemistry*, **33(6)**, 2720–2730. doi:10.13005/ojc/330605
- Yamada, M., Kojima, N., Att, W., Hori, N., Suzuki, T., & Ogawa, T. (2009). N-Acetyl cysteine restores viability and function of rat odontoblast-like cells impaired by polymethylmethacrylate dental resin extract. *Redox Report*, **14(1)**, 13–22. doi:10.1179/135100009X392430
- Yamaguchi, M., Oishi, H., & Suketa, Y. (1987). Stimulatory effect of zinc on bone formation in tissue culture. *Biochemical Pharmacology*, **36(22)**, 4007–4012. doi:10.1016/0006-2952(87)90471-0
- Yamamoto, O. (2001). Influence of particle size on the antibacterial activity of zinc oxide. *International Journal of Inorganic Materials*, **3(7)**, 643–646. doi:10.1016/S1466-6049(01)00197-0
- Youssef, A., El-nagar, I., El-torky, A., & El-hakim, A. E. A. (2019). Preparation and Characterization of PMMA Nanocomposites Based on ZnO-NPs for Antibacterial Packaging Applications. *Proceedings of the 5th World Congress on New Technologies (NewTech'19)*, 1–13. doi:10.11159/icnfa19.105
- Zafar, M. S. (2020). Prosthodontic applications of polymethyl methacrylate (PMMA): An update. *Polymers*, **12(10)**, 1–35. doi:10.3390/polym12102299
- Zahran, S. A., Ali-tammam, M., Hashem, A. M., Aziz, R. K., & Ali, A. E. (2019). Azoreductase activity of dye-decolorizing bacteria isolated from the human gut microbiota. *Scientific Reports*, 1–14. doi:10.1038/s41598-019-41894-8
- Zakaria, M. R., Helmi, M., Kudus, A., & Zamri, M. H. (2017). Improvement of Fracture Toughness in Epoxy Nanocomposites through Chemical Hybridization of Carbon Nanotubes and Alumina. *Materials*, **10**, 301. doi:10.3390/ma10030301
- Zebarjad, S. M. (2011). A Study on Mechanical Properties of PMMA/Hydroxyapatite Nanocomposite. *Engineering*, **03(08)**, 795–801. doi:10.4236/eng.2011.38096
- Zivic, F., Babic, M., Grujovic, N., Mitrovic, S., Favaro, G., & Caunii, M. (2012). Effect of vacuum-treatment on deformation properties of PMMA bone cement. *Journal of the Mechanical Behavior of Biomedical Materials*, **5(1)**, 129–138. doi:10.1016/j.jmbbm.2011.08.015

## APPENDICES

### APPENDIX A      FLEXURAL STRENGTH

#### Test of Normality

	Shapiro-wilk		
	Statistic	df	<i>p</i> value
PMMA Pure	0.750	7	0.013
PMMA/5BTCP	0.948	7	0.713
PMMA/10BTCP	0.927	7	0.529
PMMA/15BTCP	0.945	7	0.680
PMMA/15BTCP/2.5ZnO	0.931	7	0.557
PMMA/15BTCP/5ZnO	0.899	7	0.325

#### ANOVA

	Sum of Square	df	Mean Square	F	Sig
Between group	2398.747	5	479.749	4.471	0.003
Within group	3863.047	36	107.307		
Total	6261.794	41			

#### Multiple comparison

Designation	Designation	Sig
PMMA Pure	PMMA/5BTCP	0.028
	PMMA/10BTCP	0.184
	PMMA/15BTCP	0.244
	PMMA/15BTCP/2.5ZnO	0.013
	PMMA/15BTCP/5ZnO	0.042
PMMA/10BTCP	PMMA Pure	0.028
	PMMA/10BTCP	0.968
	PMMA/15BTCP	0.935
	PMMA/15BTCP/2.5ZnO	1.000
	PMMA/15BTCP/5ZnO	1.000
PMMA/15BTCP	PMMA Pure	0.184
	PMMA/5BTCP	0.968
	PMMA/15BTCP	1.000
	PMMA/15BTCP/2.5ZnO	0.895
	PMMA/15BTCP/5Zno	0.987
PMMA/15BTCP/2.5ZnO	PMMA Pure	0.244
	PMMA/5BTCP	0.935
	PMMA/10BTCP	1.000
	PMMA/15BTCP/2.5ZnO	0.832
	PMMA/15BTCP/5ZnO	0.968
PMMA/15BTCP/5ZnO	PMMA Pure	0.013
	PMMA/5BTCP	1.000
	PMMA/10BTCP	0.895

	PMMA/15BTCP	0.832
	PMMA/15BTCP/5ZnO	0.998
	PMMA Pure	0.042
	PMMA/5BTCP	1.000
	PMMA/10BTCP	0.987
	PMMA/15BTCP	0.968
	PMMA/15BTCP/2.5ZnO	0.998



## APPENDIX B TENSILE STRENGTH

### Test of Normality

	Shapiro-wilk		
	statistic	df	<i>p</i> value
PMMA Pure	0.784	7	0.028
PMMA/5BTCP	0.877	7	0.214
PMMA/10BTCP	0.852	7	0.129
PMMA/15BTCP	0.963	7	0.840
PMMA/15BTCP/2.5ZnO	0.822	7	0.067
PMMA/15BTCP/5ZnO	0.904	7	0.355

### Anova

	Sum of Square	df	Mean Square	F	Sig
Between group	1261.513	5	252.303	3.351	0.014
Within group	2710.875	36	75.302		
Total	3972.388	41			

### Multiple comparison

Designation	Designation	Sig
PMMA Pure	PMMA/5BTCP	0.277
	PMMA/10BTCP	0.039
	PMMA/15BTCP	0.031
	PMMA/15BTCP/2.5ZnO	0.039
	PMMA/15BTCP/5ZnO	0.021
PMMA/5BTCP	PMMA Pure	0.277
	PMMA/10BTCP	0.931
	PMMA/15BTCP	0.903
	PMMA/15BTCP/2.5ZnO	0.931
	PMMA/15BTCP/5ZnO	0.833
PMMA/10BTCP	PMMA Pure	0.039
	PMMA/5BTCP	0.931
	PMMA/15BTCP	1.000
	PMMA/15BTCP/2.5ZnO	1.000
	PMMA/15BTCP/5Zno	1.000
PMMA/15BTCP	PMMA Pure	0.031
	PMMA/5BTCP	0.903
	PMMA/10BTCP	1.000
	PMMA/15BTCP/2.5ZnO	1.000
	PMMA/15BTCP/5ZnO	1.000
PMMA/15BTCP/2.5ZnO	PMMA Pure	0.039
	PMMA/5BTCP	0.931
	PMMA/10BTCP	1.000
	PMMA/15BTCP	1.000
	PMMA/15BTCP/5ZnO	1.000
PMMA/15BTCP/5ZnO	PMMA Pure	0.021
	PMMA/5BTCP	0.833
	PMMA/10BTCP	1.000

	PMMA/15BTCP	1.000
	PMMA/15BTCP/2.5ZnO	1.000

## APPENDIX C      TENSILE MODULUS

### Test of Normality

	Shapiro-wilk		
	statistic	df	<i>p</i> value
PMMA Pure	.952	7	.750
PMMA/5BTCP	.961	7	.825
PMMA/10BTCP	.910	7	.396
PMMA/15BTCP	.838	7	.096
PMMA/15BTCP/2.5ZnO	.957	7	.789
PMMA/15BTCP/5ZnO	.836	7	.091

### ANOVA

	Sum of Square	df	Mean Square	F	Sig
Between group	947766.237	5	189553.247	2.157	.081
Within group	3163625.111	36	87878.475		
Total	4111391.348	41			

## APPENDIX D      SHRINKAGE

### Test of Normality

	Shapiro-wilk		
	statistic	df	<i>p</i> value
PMMA Pure	0.907	7	0.376
PMMA/5BTCP	0.887	7	0.258
PMMA/10BTCP	0.892	7	0.284
PMMA/15BTCP	0.971	7	0.906
PMMA/15BTCP/2.5ZnO	0.887	7	0.259
PMMA/15BTCP/5ZnO	0.945	7	0.685

### ANOVA

	Sum of Square	df	Mean Square	F	Sig
Between group	58.329	5	11.666	3.089	.020
Within group	135.979	36	3.777		
Total	194.308	41			

### Multiple comparison

Designation	Designation	Sig
PMMA Pure	PMMA/5BTCP	0.979
	PMMA/10BTCP	0.603
	PMMA/15BTCP	0.105
	PMMA/15BTCP/2.5ZnO	0.305
	PMMA/15BTCP/5ZnO	0.021
	PMMA Pure	0.979
	PMMA/10BTCP	0.948
	PMMA/15BTCP	0.386
	PMMA/15BTCP/2.5ZnO	0.731
	PMMA/15BTCP/5ZnO	0.114
	PMMA Pure	0.603
	PMMA/5BTCP	0.948
	PMMA/15BTCP	0.889
	PMMA/15BTCP/2.5ZnO	0.995
	PMMA/15BTCP/5Zno	0.505
	PMMA Pure	0.105
	PMMA/5BTCP	0.386
	PMMA/10BTCP	0.889
	PMMA/15BTCP/2.5ZnO	0.993
	PMMA/15BTCP/5ZnO	0.983
	PMMA Pure	0.305
	PMMA/5BTCP	0.731
	PMMA/10BTCP	0.995
	PMMA/15BTCP	0.993
	PMMA/15BTCP/5ZnO	0.811
	PMMA Pure	0.021

	PMMA/5BTCP	0.114
	PMMA/10BTCP	0.505
	PMMA/15BTCP	0.983
	PMMA/15BTCP/2.5ZnO	0.811

## APPENDIX E SURFACE ROUGHNESS

### Test of Normality

	Shapiro-wilk		
	statistic	df	<i>p</i> value
PMMA Pure	0.937	7	0.612
PMMA/5BTCP	0.960	7	0.819
PMMA/10BTCP	0.835	7	0.090
PMMA/15BTCP	0.944	7	0.675
PMMA/15BTCP/2.5ZnO	0.942	7	0.658
PMMA/15BTCP/5ZnO	0.968	7	0.881

### ANOVA

	Sum of Square	df	Mean Square	F	Sig
Between group	4.419	5	0.884	8.654	.000
Within group	3.677	36	0.102		
Total	8.096	41			

### Multiple comparison

Designation	Designation	Sig
PMMA Pure	PMMA/5BTCP	0.009
	PMMA/10BTCP	0.050
	PMMA/15BTCP	0.000
	PMMA/15BTCP/2.5ZnO	0.000
	PMMA/15BTCP/5ZnO	0.000
PMMA/5BTCP	PMMA Pure	0.009
	PMMA/10BTCP	0.986
	PMMA/15BTCP	0.889
	PMMA/15BTCP/2.5ZnO	0.325
	PMMA/15BTCP/5ZnO	0.645
PMMA/10BTCP	PMMA Pure	0.050
	PMMA/5BTCP	0.986
	PMMA/15BTCP	0.524
	PMMA/15BTCP/2.5ZnO	0.095
	PMMA/15BTCP/5Zno	0.267
PMMA/15BTCP	PMMA Pure	0.000
	PMMA/5BTCP	0.889
	PMMA/10BTCP	0.524
	PMMA/15BTCP/2.5ZnO	0.915
	PMMA/15BTCP/5ZnO	0.997
PMMA/15BTCP/2.5ZnO	PMMA Pure	0.000
	PMMA/5BTCP	0.325
	PMMA/10BTCP	0.095
	PMMA/15BTCP	0.915
	PMMA/15BTCP/5ZnO	0.994
PMMA/15BTCP/5ZnO	PMMA Pure	0.000

	PMMA/5BTCP	0.645
	PMMA/10BTCP	0.267
	PMMA/15BTCP	0.997
	PMMA/15BTCP/2.5ZnO	0.994

## APPENDIX F FRACTURE TOUGHNESS O DAY

### Test of Normality

	Shapiro-wilk		
	Statistic	df	<i>p</i> value
PMMA Pure	0.823	3	0.171
PMMA/5BTCP	0.989	3	0.804
PMMA/10BTCP	0.854	3	0.252
PMMA/15BTCP	1.000	3	1.000
PMMA/15BTCP/2.5ZnO	0.984	3	0.761
PMMA/15BTCP/5ZnO	0.964	3	0.638

### ANOVA

	Sum of Square	df	Mean Square	F	Sig
Between group	17.998	5	3.600	1.104	0.408
Within group	39.122	12	3.260		
Total	57.120	17			



## APPENDIX G FRACTURE TOUGHNESS 15 DAYS

### Test of Normality

	Shapiro-wilk		
	statistic	df	<i>p</i> value
PMMA Pure	0.778	3	0.063
PMMA/5BTCP	1.000	3	0.980
PMMA/10BTCP	0.927	3	0.477
PMMA/15BTCP	0.956	3	0.596
PMMA/15BTCP/2.5ZnO	0.961	3	0.621
PMMA/15BTCP/5ZnO	0.980	3	0.730

### ANOVA

	Sum of Square	df	Mean Square	F	Sig
Between group	31.119	5	6.224	1.737	0.201
Within group	43.000	12	3.583		
Total	74.119	17			

## APPENDIX H FRACTURE TOUGHNESS 30 DAYS

### Test of Normality

	Shapiro-wilk		
	Statistic	df	<i>p</i> value
PMMA Pure	1.000	3	0.987
PMMA/5BTCP	0.925	3	0.470
PMMA/10BTCP	0.871	3	0.299
PMMA/15BTCP	0.986	3	0.770
PMMA/15BTCP/2.5ZnO	0.858	3	0.263
PMMA/15BTCP/5ZnO	0.842	3	0.219

### ANOVA

	Sum of Square	df	Mean Square	F	Sig
Between group	16.607	5	3.321	0.664	0.658
Within group	60.004	12	5.000		
Total	76.611	17			

**APPENDIX I FRACTURE TOUGHNESS 45 DAYS**

Test of Normality

	Shapiro-wilk		
	Statistic	df	<i>p</i> value
PMMA Pure	0.973	3	0.686
PMMA/5BTCP	0.947	3	0.556
PMMA/10BTCP	0.894	3	0.368
PMMA/15BTCP	0.971	3	0.674
PMMA/15BTCP/2.5ZnO	0.996	3	0.873
PMMA/15BTCP/5ZnO	0.811	3	0.141

ANOVA

	Sum of Square	df	Mean Square	F	Sig
Between group	106.713	5	21.343	5.528	0.007
Within group	46.327	12	3.861		
Total	153.040	17			

Multiple comparison

Designation	Designation	Sig
PMMA Pure	PMMA/5BTCP	0.952
	PMMA/10BTCP	0.029
	PMMA/15BTCP	0.993
	PMMA/15BTCP/2.5ZnO	0.746
	PMMA/15BTCP/5ZnO	0.994
PMMA/5BTCP	PMMA Pure	0.952
	PMMA/10BTCP	0.007
	PMMA/15BTCP	1.000
	PMMA/15BTCP/2.5ZnO	0.300
	PMMA/15BTCP/5ZnO	0.737
PMMA/10BTCP	PMMA Pure	0.029
	PMMA/5BTCP	0.007
	PMMA/15BTCP	0.011
	PMMA/15BTCP/2.5ZnO	0.258
	PMMA/15BTCP/5Zno	0.071
PMMA/15BTCP	PMMA Pure	0.993
	PMMA/5BTCP	1.000
	PMMA/10BTCP	0.011
	PMMA/15BTCP/2.5ZnO	0.438
	PMMA/15BTCP/5ZnO	0.878
PMMA/15BTCP/2.5ZnO	PMMA Pure	0.746
	PMMA/5BTCP	0.300
	PMMA/10BTCP	0.258
	PMMA/15BTCP	0.438
	PMMA/15BTCP/5ZnO	0.956
PMMA/15BTCP/5ZnO	PMMA Pure	0.994

	PMMA/5BTCP	0.737
	PMMA/10BTCP	0.071
	PMMA/15BTCP	0.878
	PMMA/15BTCP/2.5ZnO	0.956

**APPENDIX J                      FRACTURE TOUGHNESS 60 DAYS**

Test of Normality

	Shapiro-wilk		
	Statistic	df	<i>p</i> value
PMMA Pure	0.917	3	0.442
PMMA/5BTCP	0.891	3	0.358
PMMA/10BTCP	0.847	3	0.231
PMMA/15BTCP	0.855	3	0.254
PMMA/15BTCP/2.5ZnO	0.948	3	0.560
PMMA/15BTCP/5ZnO	0.902	3	0.393

ANOVA

	Sum of Square	df	Mean Square	F	Sig
Between group	10.578	5	2.116	0.400	0.840
Within group	63.534	12	5.295		
Total	74.112	17			

## APPENDIX K      CYTOTOXICITY 6.25mg/ml

### Test of Normality

	Shapiro-wilk		
	Statistic	df	<i>p</i> value
PMMA Pure	0.911	6	0.441
PMMA/5BTCP	0.870	6	0.228
PMMA/10BTCP	0.771	6	0.031
PMMA/15BTCP	0.866	6	0.211
PMMA/15BTCP/2.5ZnO	0.875	6	0.249
PMMA/15BTCP/5ZnO	0.892	6	0.331

### Rank

Group	N	Mean Rank
A	6	7.17
B	6	5.83
Total	12	

Kruskal walis H	0.410
df	1
Asymp.Sig.	0.522

### Rank

Group	N	Mean Rank
A	6	11.50
B	6	9.83
C	6	7.17
Total	18	

Kruskal walis H	2.012
df	2
Asymp.Sig.	0.366

### Rank

Group	N	Mean Rank
A	6	12.50
B	6	9.83
C	6	8.33
Total	6	19.33
	24	

Kruskal walis H	8.540
-----------------	-------

df	3
Asymp.Sig.	0.036

Rank

Group	N	Mean Rank
A	6	13.33
B	6	9.83
c	6	9.00
D	6	21.50
E	6	23.83
	30	

Kruskal walis H	14.290
df	4
Asymp.Sig.	0.006

Rank

Group	N	Mean Rank
A	6	14.33
B	6	9.83
C	6	9.83
D	6	23.67
E	6	26.75
F	6	26.58
Total	36	

Kruskal walis H	17.722
df	5
Asymp.Sig.	0.003

## APPENDIX L ANTIBACTERIAL STUDY OF *S. aureus*

### Kruskal Wallis Test

	reading
Chi-square	2.779
df	3
Asymp.Sig	0.427

	reading
Chi-square	0.995
df	1
Asymp.Sig	0.318

	reading
Chi-square	1.485
df	2
Asymp.Sig	0.476

### Test of Normality

	Shapiro-wilk		
	Statistic	df	<i>p</i> value
PMMA Pure	0.753	12	0.003
PMMA/5BTCP	0.715	12	0.001
PMMA/10BTCP	0.807	12	0.011
PMMA/15BTCP	0.674	12	0.000
PMMA/15BTCP/2.5ZnO	0.608	12	0.000
PMMA/15BTCP/5ZnO	0.902	3	0.393

	reading
Chi-square	6.412
df	4
Asymp.Sig	0.170

	reading
Chi-square	5.493
df	3
Asymp.Sig	0.139

### LAG PHASE

sample	mean	N	Standard deviation
Control	0.5167	12	0.05774
PMMA Pure	0.6083	12	0.15050
PMMA/15BTCP	0.5750	12	0.07538
PMMA/15BTCP/2.5ZnO	0.5417	12	0.06686
PMMA/15BTCP/5ZnO	0.5333	12	0.04924



Total	0.5550	60	0.09099
-------	--------	----	---------

#### LOG PHASE

sample	mean	N	Standard deviation
Control	3.9533	15	2.73283
PMMA Pure	3.4800	15	2.44166
PMMA/15BTCP	3.4200	15	2.30410
PMMA/15BTCP/2.5ZnO	3.5000	15	2.20681

#### STATIONARY PHASE

sample	mean	N	Standard deviation
Control	7.4167	12	0.16967
PMMA Pure	6.7750	12	0.32787
PMMA/15BTCP	6.6500	12	0.48711
PMMA/15BTCP/2.5ZnO	6.3667	12	0.32845
PMMA/15BTCP/5ZnO	6.4417	12	0.31754
Total	6.7300	60	0.49993

**APPENDIX M      ANTIBACTERIAL STUDY OF *P.aeruginosa***

**LAG PHASE 0-3**

sample	mean	N	Standard deviation
Control	0.4667	12	0.04924
PMMA Pure	0.5083	12	0.02887
PMMA/15BTCP	0.4917	12	0.06686
PMMA/15BTCP/2.5ZnO	0.4417	12	0.05149
PMMA/15BTCP/5ZnO	0.4500	12	0.05222
Total	0.4717	60	0.05552

**LAG PHASE 4-9**

sample	mean	N	Standard deviation
Control	2.2056	18	1.31796
PMMA Pure	2.1056	18	1.22449
PMMA/15BTCP	2.2222	18	1.34232
PMMA/15BTCP/2.5ZnO	2.1222	18	1.21585
PMMA/15BTCP/5ZnO	2.1056	18	1.21145
Total	2.1522	90	1.23600

**STATIONARY PHASE 10-12**

sample	mean	N	Standard deviation
Control	4.8778	9	0.17873
PMMA Pure	4.6000	9	0.16583
PMMA/15BTCP	4.7556	9	0.25055
PMMA/15BTCP/2.5ZnO	4.4333	9	0.20616
PMMA/15BTCP/5ZnO	4.3556	9	0.18105
Total	4.6044	45	0.27299

**APPENDIX N      CYTOTOXICITY 12.5mg/ml**

Test of Normality

	Shapiro-wilk		
	Statistic	df	<i>p</i> value
PMMA Pure	.912	6	.447
PMMA/5BTCP	.895	6	.345
PMMA/10BTCP	.923	6	.526
PMMA/15BTCP	.785	6	.043
PMMA/15BTCP/2.5ZnO	.754	6	.022
PMMA/15BTCP/5ZnO	.998	6	1.000

Rank

Group	N	Mean Rank
A	6	6.58
B	6	6.42
total	12	

Kruskal walis H	0.006
df	1
Asymp.Sig.	0.936

Group	N	Mean Rank
A	6	9.08
B	6	7.42
c	6	12.00
total	18	

Kruskal walis H	2.271
df	2
Asymp.Sig.	.321

Group	N	Mean Rank
A	6	10.92
B	6	8.25
C	6	14.00
D	6	16.83
Total	24	

Kruskal walis H	4.996
df	3
Asymp.Sig.	.172

Group	N	Mean Rank
A	6	13.08
B	6	9.75
C	6	17.33
D	6	21.33
E	6	16.00
Total	30	

Kruskal walis H	5.928
df	4
Asymp.Sig.	.205

Group	N	Mean Rank
A	6	15.92
B	6	11.58
C	6	21.00
D	6	25.92
E	6	19.17
F	6	17.42
Total	36	

Kruskal walis H	6.348
df	5
Asymp.Sig.	0.274

## APPENDIX O CYTOTOXICITY 25mg/ml

### Test of normality

	Shapiro-wilk		
	Statistic	df	<i>p</i> value
PMMA Pure	0.920	6	0.508
PMMA/5BTCP	0.876	6	0.251
PMMA/10BTCP	0.825	6	0.097
PMMA/15BTCP	0.851	6	0.160
PMMA/15BTCP/2.5ZnO	0.898	6	0.360

### ANOVA

	Sum of Square	df	Mean Square	F	Sig
Between group	9550.174	5	1910.035	12.883	0.000
Within group	4447.736	30	148.258		
Total	13997.911	35			

### Multiple comparison

Designation	Designation	Sig
PMMA Pure	PMMA/5BTCP	0.997
	PMMA/10BTCP	0.009
	PMMA/15BTCP	0.000
	PMMA/15BTCP/2.5ZnO	0.664
	PMMA/15BTCP/5ZnO	0.000
PMMA/5BTCP	PMMA Pure	0.997
	PMMA/10BTCP	0.027
	PMMA/15BTCP	0.000
	PMMA/15BTCP/2.5ZnO	0.901
	PMMA/15BTCP/5ZnO	0.000
PMMA/10BTCP	PMMA Pure	0.009
	PMMA/5BTCP	0.027
	PMMA/15BTCP	0.522
	PMMA/15BTCP/2.5ZnO	0.241
	PMMA/15BTCP/5Zno	0.346
PMMA/15BTCP	PMMA Pure	0.000
	PMMA/5BTCP	0.000
	PMMA/10BTCP	0.522
	PMMA/15BTCP/2.5ZnO	0.005
	PMMA/15BTCP/5ZnO	1.000
PMMA/15BTCP/2.5ZnO	PMMA Pure	0.664
	PMMA/5BTCP	0.901
	PMMA/10BTCP	0.241
	PMMA/15BTCP	0.005
	PMMA/15BTCP/5ZnO	0.002
PMMA/15BTCP/5ZnO	PMMA Pure	0.000
	PMMA/5BTCP	0.000
	PMMA/10BTCP	0.346
	PMMA/15BTCP	1.000

	PMMA/15BTCP/2.5ZnO	0.002
--	--------------------	-------

**APPENDIX P      CYTOTOXICITY 50mg/ml**

Test of normality

	Shapiro-wilk		
	Statistic	df	<i>p</i> value
PMMA Pure	0.807	6	0.068
PMMA/5BTCP	0.970	6	0.896
PMMA/10BTCP	0.952	6	0.755
PMMA/15BTCP	0.654	6	0.002
PMMA/15BTCP/2.5ZnO	0.818	6	0.085
PMMA/15BTCP/5ZnO	0.894	6	0.338

Group	N	Mean Rank
A	6	7.50
B	6	5.50
Total	12	

Kruskal walis H	0.930
df	1
Asymp.Sig.	0.335

Group	N	Mean Rank
A	6	7.50
B	6	5.50
C	6	15.50
Total	18	

Kruskal walis H	11.814
df	2
Asymp.Sig.	0.003

Group	N	Mean Rank
A	6	7.50
B	6	5.50
C	6	23.33
D	6	17.67
E	6	23.50
Total	30	

Kruskal walis H	22.776
df	4
Asymp.Sig.	0.000

Group	N	Mean Rank
A	6	7.50
B	6	5.50
C	6	25.67
D	6	19.33
E	6	25.75
F	6	27.25
Total	36	

Kruskal walis H	25.479
df	5
Asymp.Sig.	0.000



## APPENDIX Q CYTOTOXICITY 100mg/ml

### Test of normality

	Shapiro-wilk		
	Statistic	df	<i>p</i> value
PMMA Pure	0.891	6	0.326
PMMA/5BTCP	0.925	6	0.545
PMMA/10BTCP	0.904	6	0.397
PMMA/15BTCP	0.933	6	0.602
PMMA/15BTCP/2.5ZnO	0.917	6	0.484
	0.915	6	0.469

### ANOVA

	Sum of Square	df	Mean Square	F	Sig
Between group	4333.376	5	866.675	9.357	0.000
Within group	2778.812	30	92.627		
Total	7112.189	35			

### Multiple comparison

Designation	Designation	Sig
PMMA Pure	PMMA/5BTCP	1.000
	PMMA/10BTCP	0.372
	PMMA/15BTCP	0.957
	PMMA/15BTCP/2.5ZnO	0.009
	PMMA/15BTCP/5ZnO	0.138
PMMA/5BTCP	PMMA Pure	1.000
	PMMA/10BTCP	0.428
	PMMA/15BTCP	0.975
	PMMA/15BTCP/2.5ZnO	0.007
	PMMA/15BTCP/5ZnO	0.113
PMMA/10BTCP	PMMA Pure	0.372
	PMMA/5BTCP	0.428
	PMMA/15BTCP	0.857
	PMMA/15BTCP/2.5ZnO	0.000
	PMMA/15BTCP/5Zno	0.001
PMMA/15BTCP	PMMA Pure	0.957
	PMMA/5BTCP	0.975
	PMMA/10BTCP	0.857
	PMMA/15BTCP/2.5ZnO	0.001
	PMMA/15BTCP/5ZnO	0.021
PMMA/15BTCP/2.5ZnO	PMMA Pure	0.009
	PMMA/5BTCP	0.007
	PMMA/10BTCP	0.000
	PMMA/15BTCP	0.001
	PMMA/15BTCP/5ZnO	0.840
PMMA/15BTCP/5ZnO	PMMA Pure	0.138
	PMMA/5BTCP	0.113

	PMMA/10BTCP	0.001
	PMMA/15BTCP	0.021
	PMMA/15BTCP/2.5ZnO	0.840

## LIST OF PUBLICATIONS AND PRESENTATIONS

### Publications: Original articles

1. Wan Nur Fadilla Wan Hamad, Abdul Manaf Abdullah, Dasmawati Mohamad. Effect of zinc oxide on flexural and physical properties of PMMA composites", AIP Translational Craniofacial Conference (TCC), 020014-1-020014-4, 2016.
2. Wan Nur Fadilla Wan Hamad, Abdul Manaf Abdullah, Dasmawati Mohamad, Nurul Asma Abdullah, Tensile and Shrinkage Evaluation on newly developed  $\beta$ -TCP /ZnO filled PMMA for craniofacial reconstruction Journal of Microscopy, Vol. 16, No.1 ,2020, 141-149.

### Presentations :

1. Wan Nur Fadilla Wan Hamad, Abdul Manaf Abdullah, Dasmawati Mohamad, Effect of zinc oxide on flexural and physical properties of PMMA composites", AIP Translational Craniofacial Conference (TCC), AIP Conference Proceedings, 2016, USM Penang. (Oral presenter)
2. Wan Nur Fadilla Wan Hamad, Abdul Manaf Abdullah, Dasmawati Mohamad, Tensile and shrinkage of newly developed  $\beta$ -TCP/ZnO filled PMMA for craniofacial reconstruction, Postgraduate Research Day 2017, 27 April 2017, School of Dental Sciences, USM. (Poster presentation)
3. Wan Nur Fadilla Wan Hamad, Abdul Manaf Abdullah, Dasmawati Mohamad, Cytotoxicity Evaluation of PMMA Composite on Human Fetal Osteoblast Cell, 2<sup>nd</sup> Postgraduate Research Day 2018, 22 February 2018, School of Dental Sciences, USM. (Poster presentation)
4. Wan Nur Fadilla Wan Hamad, Abdul Manaf Abdullah, Dasmawati Mohamad, Nurul Asma Abdullah, A Cytotoxicity Evaluation of PMMA Composite on Human Fetal Osteoblast Cell, tissue engineering and regenerative medicine society of Malaysia, 17<sup>th</sup> International Conference of Asia Pacific Association of Surgical Tissue Bank (APASTB), 27-30 August 2018, Bangi Putrajaya Hotel Selangor Malaysia. (Oral presenter)
5. Wan Nur Fadilla Wan Hamad, Dasmawati Mohamad, Evaluation of Tensile Strength and Shrinkage of new Antibacterial PMMA composite, Malaysian Journal of Microscopy, 18<sup>th</sup>-20<sup>th</sup> December 2019, Swiss Garden Hotel, Kuantan, Pahang. (E poster presentation)

# Effect Of Zinc Oxide on Flexural and Physical Properties of PMMA Composites

Wan Nur Fadilla Wan Hamad<sup>1</sup>, Abdul Manaf Abdullah<sup>1</sup>, Dasmawati Mohamad<sup>1,2</sup>

<sup>1</sup>School of Dental Sciences, Health Campus, Universiti Sains Malaysia, 16150 Kubang Kerian, Kelantan, Malaysia

<sup>2</sup>Corresponding author: [dasmawati@usm.my](mailto:dasmawati@usm.my)

**Abstract.** Polymethylmethacrylate (PMMA) is the most widely accepted material in maxillofacial implants due to its superior advantages. The material used for craniofacial implant should have good mechanical and antibacterial properties to withstand forces and eliminate infection. A study was conducted to prepare PMMA incorporated with  $\beta$ -tricalcium phosphate ( $\beta$ -TCP) filler and zinc oxide as an antibacterial agent at different compositions and investigate the flexural properties of the produced PMMA/ $\beta$ -TCP/ZnO composites. Pure PMMA as control, 15%  $\beta$ -TCP filled, 15%  $\beta$ -TCP with 2.5% ZnO filled as well as 15%  $\beta$ -TCP with 5% ZnO filled PMMA were prepared. PMMA were mixed together with  $\beta$ -TCP and zinc oxide manually according to the percentages specified until it has reached the homogeneous state. Flexural specimens were prepared by casting the paste in silicone mould which has been fabricated using 3D printed flexural template. The number of samples was  $n=7$  for each composition. Statistical analysis of One Way ANOVA was employed to compare the flexural properties of each samples. Flexural strength of pure PMMA, 15%  $\beta$ -TCP filled, 15%  $\beta$ -TCP with 2.5% ZnO filled as well as 15%  $\beta$ -TCP with 5% ZnO filled PMMA were 60.79, 46.75, 38.72 and 41.49 MPa respectively. The addition of either  $\beta$ -TCP or  $\beta$ -TCP with ZnO decreased the flexural properties and it showed significant differences as compared to pure PMMA ( $p<0.05$ ). 5% ZnO filled PMMA showed higher flexural properties as compared to 2.5% ZnO filled PMMA, however the differences were found not significant ( $p>0.05$ ).

## INTRODUCTION

Polymethylmethacrylate (PMMA) is one of the most widely accepted thermoplastic material in orthopedic as well as maxillofacial implants due to its superior advantages such as excellent toughness, stiffness, transparent to visible light, and low thermal conductivity [1]. It acts as a bone cement to achieve implant fixation. However, bone cement has drawbacks such as high shrinkage, the stiffness mismatch between the bone and the cement [2].

Therefore, the properties of PMMA need to be altered in order to overcome the limitation of the polymer itself. In this study,  $\beta$ -TCP which acts as a filler, and zinc oxide as an antibacterial agent were incorporated into PMMA.  $\beta$ -TCP is well known as one of biomaterial that is widely used in dentistry and orthopedic to repair the mammalian hard tissue defects. It possess unique properties including good osteoconductivity, direct bond formation with the connective tissue and rapid bone repair within a few weeks of implantation [3]. It is suitable to be used due to a nontoxic, antigenic and noncarcinogenic biomaterial.

Other than that, ZnO is introduced in this study in order to reduce infections problem which is a common problem occurred after the implantation has been applied to the patient. ZnO is well known to possess antibacterial properties as well as low in cost, nontoxic and chemically stable in presence of air and moisture. ZnO can be efficient antimicrobial agent via several mechanism including the production of reactive oxygen species (ROS) because of the semiconductive properties of ZnO, the destabilization of microbial membrane upon direct contact of ZnO particles to the cell walls, and the intrinsic antimicrobial properties of  $Zn^{2+}$  ions [4]. Incorporation of antibacterial agents do not affect the structure of the bulk materials hence preserve the good mechanical properties.

Implantation materials need to have good mechanical and antibacterial properties. Hence, there is a need to investigate the incorporation of  $\beta$ -TCP and zinc oxide towards the polymer matrix on flexural properties of PMMA composites.



## Cytotoxicity Evaluation of PMMA Composite on Human Fetal Osteoblast Cell

Wau Nur Fadilla Wau Hamad<sup>1</sup>, Abdul Manaf Abdullah<sup>1</sup>, Dasmawati Mohamad<sup>2</sup>, Nurul Asma Abdullah<sup>2\*</sup><sup>1</sup>School of Dental Sciences, USM Campus, Universiti Sains Malaysia, 16150 Kubang Kerian, Kelantan<sup>2</sup>School of Health Sciences, USM Campus, Universiti Sains Malaysia, 16150 Kubang Kerian, Kelantan

## ARTICLE INFO

Published: xxxxxxxx

\*Corresponding author  
email:  
dilla.hamad@yahoo.com**Keywords:**  
antibacterial, human  
fetal osteoblast cell,  
PMMA composites

## SUMMARY

Traumatic injuries in the craniofacial areas may result in disfiguring defects and compromise the protection of the underlying brain. Reconstruction is necessary for the functional and aesthetic reasons. In this study, Polymethyl methacrylate (PMMA) was used due to the excellent properties where there are biocompatible, biologically inert and rigid for cranial bone reconstruction. However, many patients these days were exposed to infection after craniofacial reconstruction using PMMA. Therefore, incorporation of antibacterial agents to the PMMA are desirable to eliminate infection. However, cytotoxicity test needs to be conducted first before accomplish the antibacterial activity of PMMA composites. Hence, the study is aimed for the evaluation of cytotoxicity of the PMMA composites filled with  $\beta$ -TCP and ZnO in different composition on Human Fetal Osteoblast Cell (HFOB).

A study was conducted to prepare antibacterial PMMA composites incorporated with fillers  $\beta$ -TCP and ZnO with different composition and to investigate the biocompatibility of the PMMA composites.

$\beta$ -TCP and Zinc Oxide were purchased from Sigma-Aldrich and Nacalai Tesque respectively. Pure PMMA as control, 5%, 10%, and 15%  $\beta$ -TCP filled, 15%  $\beta$ -TCP with 2.5% ZnO filled as well as 15%  $\beta$ -TCP with 5% ZnO filled PMMA were prepared. PMMA were mixed together with  $\beta$ -TCP and ZnO manually according to the percentages specified until it has reached the homogeneous state. Specimens were prepared by casting the paste in silicone mould which has been fabricated using 3D printed flexural template. Next, cytotoxicity evaluation was carried out on human fetal osteoblast cells (HFOB). HFOB were incubated at different concentrations (100, 50, 25, 12.5, 6.25 mg/ml) (n=3) of PMMA composites extracts for three days. Then, MTT solution (3-(4, 5-dimethylthiazolyl)-2,5-diphenyl-tetrazolium bromide) was added to each well at 37°C and after 4 hours. The culture medium with the MTT solution was removed. Formazan crystals of viable cells were dissolved in DMSO (dimethyl sulfoxide). Lastly, ELISA reader was utilized to obtain the data and then, cell viability of HFOB was calculated.

At 100 mg/ml, PMMA filled 10% $\beta$ TCP showed the highest percentages (96.53%) of cell viability and the lowest value reveal to PMMA filled 15% $\beta$ TCP (64.47%) with 2.5%ZnO. Overall, PMMA filled 15% $\beta$ TCP filled 5%ZnO (132.73%) reveal the highest cell viability at 25 mg/ml. It can be concluded that there was no toxicity effect of PMMA composites on human fetal osteoblast cell.

**Acknowledgement:** The study was funded by bridging grant (304.PPSPG.6316131).

## **Tensile and Shrinkage Evaluation on newly developed $\beta$ -TCP /ZnO filled PMMA for craniofacial reconstruction**

Wan Nur Fadilla Wan Hamad, Abdul Manaf Abdullah, Dasmawati Mohamad\*

School of Dental Sciences, Health Campus, Universiti Sains Malaysia, 16150 Kubang Kerian, Kelantan, Malaysia.

---

### **Abstract**

Unfilled PMMA suffers from its moderate mechanical properties and high shrinkage. This study aimed to evaluate tensile and shrinkage of newly developed  $\beta$ -TCP/ZnO filled PMMA for craniofacial reconstruction.  $\beta$ -TCP was fixed at 15 wt%, whereas ZnO was varied between 0, 2.5 and 5 wt%. Unfilled PMMA was also prepared as control ( $n=7$ /composition).  $\beta$ -TCP particles were in 1-5  $\mu\text{m}$  sizes whereas ZnO particles were in nanosize of less than 260nm. The effect of filler incorporation on the tensile and morphological were determined using Universal Testing Machine (AGX 2 plus, Shimadzu, Japan), field emission scanning electron microscope (FESEM) and scanning electron microscope (SEM). Shrinkage was calculated using volumetric shrinkage formula. Statistical analysis of One-Way ANOVA ( $p<0.05$ ) was employed to assess the differences in the mean of tensile and shrinkage properties between the developed composites and unfilled PMMA. Shrinkage percentages reduced from 8.29 % (unfilled PMMA) to 4.8% with incorporation of 5%ZnO. The tensile strength of the composites was significantly reduced with incorporation of  $\beta$ -TCP/ZnO fillers. Tensile modulus and shrinkage properties of the composites were significantly improved. Thus, this newly developed  $\beta$ -TCP/ZnO filled PMMA is a promising biomaterial for craniofacial reconstruction.

**Keywords:**  $\beta$ -TCP/ZnO filled PMMA, tensile, shrinkage, craniofacial reconstruction

---

### **Article Info**

Received 17<sup>th</sup> October 2019

Accepted 17<sup>th</sup> March 2020

Published 1<sup>st</sup> April 2020

\*Corresponding author: Dasmawati Mohamad; e-mail: [dasmawati@usm.my](mailto:dasmawati@usm.my)

Copyright Malaysian Journal of Microscopy (2020). All rights reserved.

ISSN: 1823-7010, eISSN: 2600-7444



Available online at [www.elsevier.com/locate/dental](http://www.elsevier.com/locate/dental)

ScienceDirect

journal homepage: [www.elsevier.com/locate/dental](http://www.elsevier.com/locate/dental)

## Mechanical and cytotoxicity properties of hybrid ceramics filled polyamide 12 filament feedstock for craniofacial bone reconstruction via fused deposition modelling

Abdul Manaf Abdullah<sup>a</sup>, Tuan Noraihan Azila Tuan Rahim<sup>b</sup>,  
Wan Nur Fadilla Wan Hamad<sup>a</sup>, Dasmawati Mohamad<sup>a,\*</sup>,  
Hazizan Md Akil<sup>b</sup>, Zainul Ahmad Rajion<sup>a</sup>

<sup>a</sup> School of Dental Science, Health Campus, Universiti Sains Malaysia, 16150 Kubang Kerian, Kelantan, Malaysia

<sup>b</sup> School of Materials and Mineral Resources Engineering, Engineering Campus, Universiti Sains Malaysia, 14300 Nilong Tegal, Pulau Pinang, Malaysia

### ARTICLE INFO

#### Article history:

Received 5 March 2018

Received in revised form

21 June 2018

Accepted 12 September 2018

#### Keywords:

Fused deposition modelling

Polyamide 12

Hybrid ceramics

Craniofacial bone

Mechanical

Cytotoxicity

Filament feedstock

 $\beta$ -TCPZrO<sub>2</sub>

### ABSTRACT

**Objective:** To compare the mechanical and biological properties of newly developed hybrid ceramics filled and unfilled polyamide 12 (PA 12) for craniofacial reconstruction via a fused deposition modelling (FDM) framework.

**Methods:** 15 wt% of zirconia (ZrO<sub>2</sub>) as well as 20, 35, and 40 wt% of beta-tricalcium phosphate ( $\beta$ -TCP) were compounded with PA 12, followed by the fabrication of filament feedstocks using a single screw extruder. The fabricated filament feedstocks were used to print the impact specimens. The melt flow rate, tensile properties of fabricated filament feedstocks, and 3D printed impact properties of the specimens were assessed using melt flow indexer, universal testing machine, and Inod pendulum tester, respectively. The microstructure of selected filament feedstocks and broken impact specimens were analysed using a field emission scanning electron microscope and universal testing machine. Human periodontal ligament fibroblast cells (HPDLF) were used to evaluate the cytotoxicity of the materials by [3-(4,5-dimethylthiazol-2-yl)-2,5-diphenyltetrazolium bromide] (MTT) assay.

**Results:** Hybrid ceramics filled PA 12 indicated sufficient flowability for FDM 3D printing. The tensile strength of hybrid ceramics filled PA 12 filament feedstocks slightly reduced as compared to unfilled PA 12. However, the tensile modulus and impact strength of hybrid ceramics filled PA 12 increased by 8%–11% and 88%–181%, respectively. A significant increase was also detected in the cell viability of the developed composite at concentrations of 12.5, 25, 50 and 100 mg/ml.

**Significance:** The newly developed hybrid ceramics filled PA 12 filament feedstock with improved properties is suitable for an FDM-based 3D printer, which enables the creation of patient-specific craniofacial implant at a lower cost to serve low-income patients.

© 2018 The Academy of Dental Materials. Published by Elsevier Inc. All rights reserved.

\* Corresponding author.

E-mail address: [dasmawati@usm.my](mailto:dasmawati@usm.my) (D. Mohamad).

<https://doi.org/10.1016/j.dental.2018.09.006>

0306-4641/© 2018 The Academy of Dental Materials. Published by Elsevier Inc. All rights reserved.

# Certificate of Appreciation

is hereby awarded to

Wan Nur Fadilla Wan Hamad  
Universiti Sains Malaysia

in recognition of his/her participation as

ORAL SYIS

2018  
**APASTB**

17<sup>th</sup> International Conference of Asia Pacific  
Association of Surgical Tissue Banks (APASTB)

27 - 30 August 2018  
Bangi-Putrajaya Hotel Selangor, Malaysia

Jointly organized by:

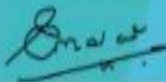
Tissue Engineering and Regenerative Medicine Society  
of Malaysia (TESMA)

Malaysian Biomaterials Society (MBS)

Malaysian Association of Cell and Tissue Banking (MACTB)



Prof. Dr. Suzina Sheikh  
Abdul Hamid  
Chairperson, APASTB2018



Dr Chandramalar T  
Santhirathelagan  
President of Malaysia Association  
of Cell and Tissue Banking (MACTB)



Dr Thamil Selvee Ramasamy  
President of Tissue Engineering and  
Regenerative Medicine Society  
of Malaysia (TESMA)



Assoc. Prof Dr Dasmawati  
Mohamad  
President of Malaysian Biomaterials  
Society (MBS)

Next



# Certificate of Appreciation

is hereby awarded to

**WAN NUR FADILLA WAN HAMAD**

in recognition of his/her participation as

**ORGANISING COMMITTEE**

**2018**  
**APASTB**

**17<sup>th</sup> International Conference of Asia Pacific  
Association of Surgical Tissue Banks (APASTB)**

**27 - 30 August 2018**

**Bangi-Putrajaya Hotel Selangor, Malaysia**

**Jointly organized by:**

Tissue Engineering and Regenerative Medicine Society  
of Malaysia (TESMA)

Malaysian Biomaterials Society (MBS)

Malaysian Association of Cell and Tissue Banking (MACTB)



**Prof. Dr. Suzina Sheikh  
Abdul Hamid**  
Chairperson, APASTB2018



**Dr Chandramalar T  
Santhirathelagan**  
President of Malaysia Association  
of Cell and Tissue Banking (MACTB)



**Dr Thamil Selvee Ramasamy**  
President of Tissue Engineering and  
Regenerative Medicine Society  
of Malaysia (TESMA)



**Assoc. Prof Dr Dasmawati  
Mohamad**  
President of Malaysian Biomaterials  
Society (MBS)



CERTIFICATE OF  
**APPRECIATION**

*This is to certify that*

**WAN NUR FADILLA WAN HAMAD**

*has presented a paper at the*

**2<sup>nd</sup> POSTGRADUATE RESEARCH DAY**  
*in conjunction with*  
**15<sup>th</sup> STUDENT SCIENTIFIC CONFERENCE**  
*"Deciphering the Intricacies in Science"*

*Date*  
22 February 2018

*Venue*  
School of Dental Sciences  
Health Campus, Universiti Sains Malaysia



  
**DR. KHAIROL BARIAH AHMAD AMIN NOORDIN**  
Chairperson  
2<sup>nd</sup> Postgraduate Research Day  
in conjunction with  
15<sup>th</sup> Student Scientific Conference

  
**PROFESSOR DR. ADAM HUSEIN**  
Dean  
School of Dental Sciences  
Health Campus, Universiti Sains Malaysia



# Certificate of Participation

is hereby granted to  
**WAN NUR FADELLA BINTI WAN HAMAD**

For Successfully Participating in

**28<sup>TH</sup> SCIENTIFIC CONFERENCE OF  
MICROSCOPY SOCIETY MALAYSIA**

held on

18<sup>th</sup>-20<sup>th</sup> December 2019  
Swiss Garden Hotel, Kuantan

A handwritten signature in black ink, appearing to read "Fauzi".

Professor Dr. Azekah Fauzi Mohd Noor  
Chairman of 28<sup>th</sup> SCMSM  
and  
President of Microscopy Society Malaysia

A handwritten signature in black ink, appearing to read "Ghazali".

Associate Professor Dr. Mohd Ghazali Bin Yusoff  
Co-Chairman of 28<sup>th</sup> SCMSM